Strength Analysis of Bolted Shear Connections Under Fire Conditions Using the Finite Element Approach

by

Andrea K. Arakelian

A Thesis
Submitted to the Faculty
of the

WORCESTER POLYTECHNIC INSTITUTE

In partial fulfillment of the requirements for the

Degree of Master of Science
in
Civil Engineering

Andrea K. Arakelian

December, 2008

Approved:

Leonard D. Albano

Dr. Leonard D. Albano, Major Advisor
Civil and Environmental Engineering Department

Robert W. Fitzgerald

Dr. Robert W. Fitzgerald, Advisor
Civil and Environmental Engineering Department

Tahar El-Korchi

Professor Tahar El-Korchi, Head of Department
Civil and Environmental Engineering Department

Abstract

The fire resistance of structural building elements has become an increasing concern after the terrorist attacks on September 11th, 2001. This concern has pushed for changes in the building codes and standards to incorporate a performance-based approach to design. Performance-based design is a process where fire safety solutions are determined using a representation of the actual fire stages that may occur in a structure during a fire event.

The American Institute of Steel Construction (AISC) has added Appendix 4 in the Specification for Structural Steel Buildings to the current edition of the Steel Construction Manual to provide engineers with guidance in designing steel structures and components for fire conditions. The performance-based approach outlined in Appendix 4 is designed to prevent loss of life, structural collapse, and the outbreak of fires through elimination of ignition sources. Adopting this approach, requires structural engineers to have a better understanding of the behavior of steel connections under fire conditions as well as the tools, techniques and judgment for analysis.

The focus of this thesis is to study the strength behavior of steel connections under fire conditions with the assistance of the finite element software, ALGOR. Connections of varying thickness and bolt patterns are constructed using the ALGOR pre-processing software. A time-temperature fire curve is combined with external loads, applied to the models and then analyzed in the program. Stress-strain diagrams are created using the results and yield loads are determined for the various connections at normal and elevated temperatures. These yield loads are compared to values found from a mathematical

analysis of the limit state equations in Chapter J of the Specifications. The elevated models are created with temperature-dependent material properties, therefore the yield loads are associated with critical temperatures within the connection models.

It is found that the capacity and governing temperature of the connections is determined by the limit state of bearing at the bolt hole. At elevated temperatures, the finite element analysis produces capacities significantly lower than the analysis at normal temperatures.

Acknowledgements

I would like to thank my advisor, Professor Leonard D. Albano, for his patience, support and guidance throughout the process of this research. His contributions proved to be invaluable to the development of this work.

I would also like to thank Professor Robert W. Fitzgerald for his advice and especially for his expertise in the area of fire engineering.

Many thanks to my family, friends and co-workers who have been there for me throughout the process of this work and provided assistance when I needed it.

Most importantly, I thank my husband, Lars, for his unyielding support and understanding over the past years.

Table of Contents

List of Figures

List of Tables

1.0 INTRODUCTION

1.1 Problem Statement

In the aftermath of the terror attacks on September 11th, 2001, the loss of life and property damage due to thermal exposure have become increasing concerns among engineers. As a result, structural engineers have become more involved in designing structures to withstand thermal forces. Until recently, prescriptive design, where quantitative steps are identified to achieve an end goal, has been the design method used in building codes and standards. Prescriptive design provides measures on methods of curbing fires after a fire event has occurred in a structure. However, performance-based design is a developing design process used to supplement prescriptive fire design. The performance-based design process is a representation of the actual stages and developments that may occur in a structure during a fire event.

Due to the increasing awareness of performance-based design, several codes have incorporated guidelines for this new design method. In steel design, Appendix 4 has been added to the Specification for Structural Steel Buildings [20] to provide structural engineers with guidance in designing steel framed building systems and components for fire conditions. These guidelines are designed to extend beyond the structural performance of the steel assembly or component to the life safety of the individuals occupying the area.

Applying the performance-based concept, this research will provide insight into the behavior and strength of steel connections when exposed to fire conditions. Limited

research has been done regarding the strength performance of steel assemblies or components. The previous research of steel connections has been focused on the rotational rigidity of the connections under fire conditions. The specific goals of this research are to provide insight into the load carrying capacity of the connections at elevated temperatures and the temperatures at which yielding begins to occur. Connection models will be created using the finite element program, ALGOR [13]. A nonlinear mechanical analysis will be combined with a heat transfer analysis to study the strength behavior of the connections through stress-strain analyses.

1.2 Research Objectives

The primary objective of this research is to determine the capacities of various steel connections and the temperatures at which yielding begins to occur. Two nonlinear models are created, one at normal temperatures and the other at elevated temperatures, and analyzed using finite element software. The resulting capacities are compared to capacities obtained at various limit states determined using guidelines in the Specification for Structural Steel Buildings.

A secondary objective is to gain familiarity creating and analyzing models with the available finite element software. The computer program, ALGOR, is used as a tool for assessing structures according to the guidelines set forth in the Specifications for performance-based design. This software is used to study stresses and displacements in complex models due to static and dynamic loading applied constantly or varying over time. Other program capabilities include the modeling of thermal conditions to monitor temperatures or heat flow through a model, as well as fluid flow and electrostatic

problems. In order to create and analyze a finite element model using ALGOR, the type of analysis, model geometry, element and material specifications, boundary conditions and applied external loads are defined. There are several trial-and-error processes encountered when defining these criteria and these will be touched on throughout this research.

1.3 Methodology and Scope of Work

Background Research

Research on the elevated temperature effects of connections is conducted. Several papers were found in engineering journals and from conference proceedings at the American Institute of Steel Construction website [15]. Much of the previous research was conducted beginning in the late 1960's by individual researchers and included the development of programs to analyze the behavior of structures subjected to fire. The most relevant programs and previous studies of others are summarized in Chapter 2.0.

Currently, the AISC has incorporated guidelines for the design of structures and components under fire conditions in the Specification for Structural Steel Buildings [20]. These guidelines are a first step toward the usage of performance-based building codes, and they provide access to practicing engineers to this new design approach. Rather than relying on prescriptive codes where fixed values are provided, the performance based approach provides designers the steps to achieve specific performance objectives such that the performance of a structure can be reliably predicted. This approach relies on designers to have the tools and techniques to predict performance reliability and to design for fire safety. Finite element programs, such as ALGOR, are one of the tools to assist

engineers in predicting the behavior of structures and elements when exposed to fire conditions.

Connection Criteria

Once the background research is complete, the connection layouts are determined. The connections analyzed in this thesis are limited to single-plate, simple shear connections. Chapter J, Section J3 in the Specifications is used as a guide to determine the nominal bolt hole dimensions, minimum edge distances, minimum spacing of the bolts and the type of bearing. The bolt pattern and thickness of the connection plate are varied to compare the temperature effects in each connection.

Mathematical Analysis

A mathematical analysis is done to determine the design strength of each connection based on the varying connection plate thicknesses and number of bolts. The provisions in Chapter J, Section J3 in the Specifications are used to evaluate the strength limit states of the connection. The limit states include the fracture in the net section, yielding in the gross section and the bolt bearing capacity, which determine the failure mode of the connection. There are two design approaches, Load and Resistance Factored Design (LRFD) and Allowable Stress Design (ASD), found in the Specifications. Values for the limit states of each connection are determined for both design methods.

Finite Element Models and Analysis Procedure

The finite element software package, ALGOR [12][13], is used to create models and to analyze each connection. A nonlinear mechanical event simulation (MES) analysis is performed first to determine the behavior of the connections for an external ramp load under normal temperature conditions. Stress-strain diagrams are created from this output which correlate to failure loads for each connection. The resulting failure load from the computer analyses are then compared to the failure loads determined for each limit state from Chapter J of the Specifications.

Performance evaluations at elevated temperatures are performed using a heat transfer analysis combined with a nonlinear MES analysis. Similar stress-strain diagrams are constructed and the yield load results are compared to the normal temperature results. The temperatures at which yielding occurs are also determined from the output of the finite element analysis.

Methods of Comparison

Due to the large amount of output information available from the program, specific nodes are chosen to monitor and compare throughout the finite element analyses. These nodes are selected in the vicinity of the bolt holes and in the free fields, away from the bolts. At these selected nodes, the stress-strain diagrams are created for the normal and elevated temperature analyses. Since the stress-strain curves do not provide definitive yield points, the offset method is used to determine the yield strain in each model. These yield strains are then used to determine specific loads at which yielding occurs. The yield

loads for the normal and elevated temperature models are compared against each other and against the limit state values obtained from using Chapter J in the Specifications [20].

Anticipated Results

According to Appendix 4 in the Specifications, one of the primary structural responses of steel to elevated temperatures is the progressive decrease in strength and stiffness. Therefore, the results of this analysis will most likely indicate a reduction in the strength of the connection when the temperatures are increased in the model. The amount of strength lost and the temperature at which yielding begins to occur are two unknowns yet to be determined.

2.0 LITERATURE REVIEW

This literature review serves the purpose of providing the reader with background knowledge regarding connections under fire conditions. Objectives of the research include:

- Identify the characteristics of performance-based design and the differences versus prescriptive design procedures.
- Identify how performance-based design applies to the Specification for Structural Steel Buildings.
- Provide an overview of available finite element software programs.
- Discuss the previous findings of other researchers on steel connections at elevated temperatures.

2.1 Standard Fire Test

In the United States, the standard time-temperature relation typically used is the ASTM E-119 [17] fire curve developed by the American Society of Testing and Materials. This test involves subjecting the structural component to a heated furnace environment for a desired duration. If the endpoint criteria are not obtained prior to the end of the test, the assembly passes the test and is rated. The endpoint criteria are grouped into three categories [9]:

- Structural Integrity – This criterion addresses the need for members to continuously support its self-weight and any applied loads.
- Temperature – The temperature criterion addresses the maximum temperatures that structural members can be exposed. These temperatures are conservative estimates of the maximum allowable reduction in load-bearing capacity of the

assembly, based on an average reduction in strength due to elevated temperatures.

- Ignition of Cotton Waste – The ignition of cotton waste endpoint addresses the ability of the structural assembly to prevent the transmission of flame and hot gases to the side not exposed to the furnace fire.

Depending on the intended use of the member or assembly, samples may be tested under loaded or unloaded conditions. Floor and roof assemblies and bearing walls are always tested under fully loaded conditions to induce maximum design stress levels. However, columns, beams and girders may be tested under various loading conditions including the unloaded option. In addition, structural assemblies may be restrained or unrestrained against thermal expansion. The degree of restraint is dependent on the geometry, connection method and framing system of the assembly [9].

Once the loading conditions are determined, the furnace is heated to follow the ASTM E-119 time-temperature curve shown in Figure 2.1-1 to simulate conditions in a fully developed room fire.

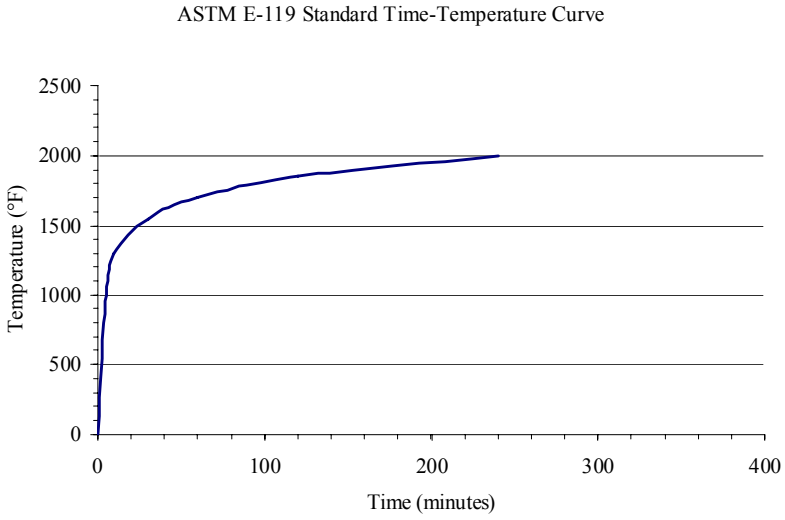

Figure 2.1-1: ASTM E-119 Standard Time-Temperature Curve

Values for this curve are based on the standard time-temperature relation adopted by the International Standard, ISO 834, provided in Table 2.1-1 per the SFPE Handbook of Fire Protection Engineering [9].

Table 2.1-1: Standard Time-Temperature Relationship According to ISO 834

Time (Minutes)	Temperature (°F)
0	68 (Room Temperature at Start of Test)
5	1000
10	1300
30	1550
60	1700
120	1850
240	2000

2.2 Performance-Based Design Approach

The traditional approach of prescriptive fire design is defined quantitatively in terms of the materials used, the shape and size of structural elements, the thicknesses of fire

protection materials and construction details. Most building codes are based on prescriptive design, which have proven over several years to provide sufficient protection against substantial loss of life. Some structures, however, require a higher level of protection against manmade events and natural disasters. The performance-based design approach was developed to supplement traditional prescriptive design. A performance-based method for structural fire design investigates a structural element using a set of objective tests to evaluate its fire performance in relation to key function criteria such as sustainability of a working load during a thermal event, length of time prior to collapse or the cause of collapse. A performance-based approach may be used to address a particular aspect of the design while the rest of the design follows a prescriptive design approach.

The following outlines the steps in a performance-based design approach according the SFPE Handbook of Fire Protection Engineering [9]:

- Establish fire safety goals. Fire safety goals may include life safety, property protection, mission continuity, environmental consequences, or heritage preservation.
- Evaluate the condition of the occupants, building contents, process equipment or facility and identify potential hazards.
- Define the appropriate fire scenarios and select the suitable calculation method and fire models.
- Develop and assess the proposed solution.
- Document the proposed solution and obtain approval of the solution.

One of the most significant aspects of the performance-based approach is the ability to predict an appropriate fire scenario. The SFPE Handbook of Fire Protection Engineering provides algebraic equations to estimate temperatures in enclosed, compartment fires during the four characteristic stages of a fire: ignition, growth, flashover, full development, and decay. Although all fires do not follow this idealization, it does provide a framework for describing compartment fires. All fires include the ignition stage, however, they may fail to grow or they may be affected by manual or automatic suppression systems such as automatic sprinkler systems and automatic smoke and heat vents [9].

2.3 AISC Guidelines for Structural Design for Fire Conditions

The American Institute of Steel Construction (AISC) has developed Appendix 4 in the Specification for Structural Steel Buildings [19] to provide guidance in the design of steel-framed structures for fire conditions. When elements are analyzed with this performance-based approach, a more robust structural design is expected to evolve. The primary structural responses of steel to elevated temperatures are thermal expansion and progressive decrease in strength and stiffness. The performance objective underlying the guidelines in Appendix 4 is that of life safety. The fire safety of a structure or assembly is aimed at three levels:

- To prevent the outbreak of fires through elimination of ignition sources
- To prevent uncontrolled fire development through early detection and suppression
- To prevent loss of life or structural collapse

Structural design provisions to check the integrity of the structure or assembly and the risk of progressive failure due to fire conditions can be developed according to these levels. Three limit states are used to predict failure due to fire by: (1) estimating the probability of ignition, (2) predicting the probability of the development of a structurally significant fire and (3) predicting the probability of failure if these conditions occur [19].

According to Appendix 4, the analysis of a structure for fire conditions using the performance-based approach involves application of a time-temperature fire curve to the steel structure or element. Ventilation, the length of exposure to the fire, localization of the fire and the reliability of fire protection systems are factors which may influence the structural response of the assembly or structure. Therefore, various fire scenarios may produce different structural responses and demonstrate the capability of the structure to withstand high thermal exposures [19].

Once the steel is subjected to a fire condition, the temperature rise in the steel must be predicted using a heat transfer analysis. The heat transfer analysis may range from a one-dimensional analysis where the steel is assumed to be uniformly heated to a three-dimensional analysis. A lumped heat capacity analysis is a first-order, one-dimensional analysis to predict the temperature rise in the steel using algebraic equations. In this analysis, the material properties of the steel can be estimated at a temperature near the mid-point of the temperature range for the duration of the exposure. An advanced, three-dimensional analysis would use a computer model to analyze the response of the steel members and include temperature variations within the steel members. In either case, the

material properties for all members in the assembly will change due to increases in temperature [19].

The calculation of the thermal response of the steel assembly or structure is best performed with the use of finite element computer software. This is due to the varying exposure conditions of the design fire, the temperature-dependent material properties and the temperature variation within the steel member. The following section describes some of the available finite element programs and their capabilities.

2.4 Finite Element Analysis Programs

The use of finite element software has become a reliable method to predict the behavior of structures exposed to fires. Computer modeling serves as a cost effective and less time consuming alternative to the actual preparation and fire testing of structural assemblies. Development of programs for fire modeling began in the 1960's which lead to the finite element software available today.

There are several programs, summarized in the following section, that were specifically written for modeling the behavior of structures subjected to fires. Most of the early programs were developed by individual researchers in order to model one specific element, such as steel beams or concrete columns, which were subjected to fire. In general, these programs are limited because analysis of any other element is not permitted and development has stopped on many of the programs.

Currently, many commercially available software programs are used to model structures exposed to fires. These programs have not been developed specifically for this task, however, they offer numerous possibilities and have the pre- and post-processing capabilities necessary to perform a thermal analysis combined with a mechanical event. Software packages such as ABAQUS [14], ALGOR [13], ANSYS [15], and Nastran [16] are used in numerous engineering fields for their powerful pre-processing and post-processing capabilities. These programs allow the engineer to spend more time developing the model and interpreting the results since the formation of the element and global stiffness matrices are automatically performed by the finite element software.

2.4.1 FASBUS II

FASBUS II is the second version of a program FASBUS, that originated at the Illinois Institute of Technology Research Institute (IITRI). The American Iron and Steel Institute sponsored research in 1968 at the IITRI to develop a nonlinear structural finite element computer program for assessing the performance of steel deck and concrete floors supported by steel framing under uncontrolled fires. The resulting program, called FASBUS (Fire Analysis of Steel Building Systems), was completed in 1972. However, the initial software was continuously refined under sponsorship by Wiss, Janney, Elstner Associates, Inc. until 1981 when a second version, FASBUS II, was completed. This program uses the node and element definition of a structural system, time-temperature history, and temperature dependent material stress-strain curves to calculate deflections, stresses, and the failure mode of a given floor assembly. In 1981, a large scale fire test was conducted in a real building environment to prove that FASBUS II could accurately duplicate the interaction of a floor assembly under a thermal condition [2].

2.4.2 FIRES-T3

In October 1977, Iding, Bresler, and Nizamuddin [3] developed the program FIRES-T3 (Fire Response of Structures – Thermal Three Dimensional Version) to evaluate the temperature distribution history of structures in fire environments. The program permits the use of three-dimensional, two-dimensional or one-dimensional elements together in the same model. The solution technique in FIRES-T3 is a nonlinear finite element method, due to the temperature-dependent properties of the structural material, combined with time step integration. Consideration of the layout of the finite element mesh and the time step intervals are key factors that determine the effectiveness of the application. On one hand, both must be fine enough to ensure proper modeling of the thermal behavior of the structure, and on the other, as few elements should be used since computational effort increases with the number of nodes.

A few problems in the nonlinear modeling of a fire were encountered using the FIRES-T3 program. The first issue arises since the fire boundary condition, including conduction and radiation, is highly nonlinear. In order to ensure convergence of an iterative solution, the time step must be kept quite small since numeric instability in the fire region may result at high temperatures. Therefore, a higher order nonlinear technique would improve the stability and convergence rate of the solution. An attempt was made to improve the instability of the nonlinear iteration by incorporating convergence factors into the program, however, this did not prove to be entirely successful. Another issue is the difficulty in modeling the heat transfer of the turbulent

environment within an actual fire. One solution is to subdivide the fire compartment into zones with different characteristics and detailed temperature and flow fields [3].

2.4.3 SAFIR

The program SAFIR was developed at the University of Leige in Belgium by Jean-Marc Franssen [4] during the late 1980's. It was written to specifically model the behavior of structures subjected to fires with the hopes that other options, either in the library of finite elements or in the modeling capabilities of the program, could be later developed to adapt to different situations and structures.

The SAFIR program employs beam elements, shell elements, or truss elements to compose the finite element model. The different element types can be mixed in a single mechanical analysis. The thermal and mechanical analyses are performed separately using the same program, and there is automatic transmission of information from one analysis to the other. The mechanical analysis is influenced by the thermal analysis which is required to study the behavior of the structure under fire conditions.

Limitations are apparent regarding the thermal capabilities of the program. The pre-processor function is limited to the preparation of input files for two-dimensional thermal analysis only. A three-dimensional analysis would need to be created with a text editor and imported into the program. The numerical size of the structure to be analyzed is also limited, which often results in the creation of substructures to breakdown the model size [4].

2.5 Previous Research of Steel Connections Under Fire Conditions

The following is an overview of some of the previous research done in the area of structural steel connections under fire conditions. Previous researchers studied the effects of elevated temperatures on the rotational restraint of connections as well as the effect of the connections as part of the continuity of the steel frame.

2.5.1 Rotational Restraint of Shear Connections

Bletzacker, R.W.

Early research on the topic of restraints was conducted for the American Iron and Steel Institute (AISI) by Bletzacker [5] at the Ohio State University in 1965-1966. The experiments were based on physical tests performed on twelve assemblies using separate steel beams and having different restraining conditions and various composite or non-composite floor slab compositions. The models were subjected to the standard ASTM E-119 fire tests and restraining criteria. Loading and moments were applied through use of hydraulic jacks and other mechanical means.

Bletzacker's research concluded that realistic levels of restraint, such as those provided by simple beam-to-column shear connections in steel framed construction, will provide fire endurance equal to or greater than that measured when testing very highly restrained specimens. It was observed that even typical shear connections provide rotational and axial restraint for the beam due to interaction with the concrete floor slab and the stiffness of the columns [5].

Iding, R.H. and Bresler, B.F.

Robert Iding and Boris Bresler collaborated on numerous papers and conducted extensive research on the behavior of steel structures when exposed to fire conditions beginning in 1977. Their literature includes: "Effect of Restraint Conditions on Fire Endurance of Steel-Framed Construction" [2], "Prediction of Fire Response of Buildings Using Finite Element Methods" [6] and "Effect of Fire Exposure on Steel Frame Buildings" [7]. Much of their research focused on various floor-beam assemblies and the response to the standard ASTM E-119 fire exposure.

In particular, the paper entitled, "Effect of Restraint Conditions on Fire Endurance of Steel-Framed Construction" [2] studied the degrees of restraint provided by various types of connections. The basic approach to the study was to compare the calculated fire response of a beam-slab assembly having similar restraint conditions as a typical steel-framed building to experimentally recorded fire responses of the same assembly. The test data used was based on experimental data published by R.W. Bletzacker [5] and included a restrained specimen, three simply supported unrestrained specimens, and several partially restrained specimens. A finite element computer model was developed to simulate the experimental fire tests. The computer program FASBUS II, described in Section 2.4.1, was used as the nonlinear analysis program in this study.

The research of Iding and Bresler determined that the rotational restraint offered by the simply supported, shear tab connectors resulted in the same fire endurance as fully restrained test specimens. Both the simply supported and the fully restrained end

conditions indicated an increase in the fire endurance due to a reduction of the midspan moment and flexural stresses caused by the negative bending moments induced at the ends of the beam. Therefore, the introduction of high levels of rotational restraint within the design does not seem to result in higher fire endurance. The studies also suggest that axial restraint does not increase the fire endurance of assemblies since these forces are relieved through local buckling.

2.5.2 Continuity Effects In Steel Frames

Khan, F.R. and Nassetta, A.F.

Kahn and Nassetta [8] researched the effect of high temperatures on tall, steel-framed buildings due to new trends in architecture and changes in technology of steel and glass. They studied various types of column exposures including partial exposure beyond the exterior glass line, fully exposed columns using curtain wall construction, and exposure due to set back elevation. Their research determined that two types of differential movement occurred: movement between the exterior columns and interior columns, and movement between adjacent exterior columns. These observations identified beam-to-column connections as an area of study because of the rotational capabilities under fire conditions.

The research by Kahn and Nassetta determined that when designing a steel-framed building for thermal conditions, the type of construction plays an important role in predicting the movement between framing members. Consideration of the anticipated relative movement of the beam-to-column connections will affect the structure as a whole if a thermal event occurs. If a relative movement between the exterior and interior

columns is expected to be more than ¾-inches, a connection that allows free rotation and no appreciable moments should be used. This is achieved by designing beam-to-column shear connections with unrestrained rotation.

Khan and Nassetta suggested that welded shear connections be avoided since this type of joint restrains rotation. Bolted type shear connections with horizontally slotted bolt holes should be used; however, high strength friction bolts which provide greater fixity than non-high strength bolts, should be avoided. Since the beams connected to the columns must also provide lateral stability for the structural frame, it is suggested that the connections be designed to slip and rotate at higher forces, but develop the necessary restraining axial force for the stability of the columns under normal loads [8].

2.6 Summary of Research

The following is a summary of the significant points of interest found from the literature review.

- The American Institute of Steel Construction has added guidelines in the current edition of the Specification for Structural Steel Buildings for the design of steel structures under fire conditions indicating the importance of structural fire design. The guidelines use a performance-based design approach where a time-temperature relationship is calculated and a realistic time to failure for unprotected structural members can be determined. Based on this time to failure, methods to calculate required protection are summarized using prescriptive design.

- The development of computer programs has proved to be a reliable, cost effective and less time consuming method to simulate fire conditions on structural assemblies. In many early cases, the results of the mathematical models were tested against actual fire scenarios and the results were found to be reasonably accurate. Observed weaknesses with the early programs, such as FASBUS, SAFIR and FIRES-T3, included the difficulty modeling the nonlinear properties and the convergence to a solution. Current software packages, such as ALGOR, ABAQUS, Nastran and ANSYS, have powerful computing processors, due to advancements in technology, which provide upgrades in modeling, simulation and results evaluation and presentation.

- Research by others regarding steel connections indicates that steel shear connection assemblies have proven to exhibit as much rotational restraint under fire conditions as fully restrained moment connections. Connections with less stiffness, typically a three-bolt, single plate connection, are adequate to develop restrained characteristics when exposed to fire conditions.

Rather than focus on the rotational restraint of connections like other researchers, this thesis focuses on the strength capabilities of the connections under fire conditions. The strength analysis will be done by comparing the stress-strain results of connection models constructed in ALGOR against capacities developed using the AISC guidelines for the

limit states of bolted connections. The following chapter will begin the development of the connections in accordance with criteria in the Steel Construction Manual.

3.0 CONNECTION DEVELOPMENT USING AISC GUIDELINES

Steel connection design begins with an understanding of the types of connections as described in the American Institute of Steel Construction's (AISC) Steel Construction Manual [1]. Connections have the ability to transfer moment through the resistance to rotation. Therefore, the type of connection is contingent on the amount of rotation allowed. There are three types of connections: rigid, simple shear and partially restrained connections.

A connection that prevents any rotation from occurring is categorized as a moment, or rigid, connection. The design intent of a rigid connection is to assure that the connection will develop the moment and shear to transfer both gravity forces and lateral loads from the beam into the column. Connections that are free to rotate under gravity loading are considered simple shear connections. Simple shear connections are designed to transmit only shear forces; therefore, a supplemental system is required to resist the lateral loading induced on the structure. A partially restrained connection is intermediate in degree between the full rigidity of a moment connection and the flexibility of the simple shear connection [1].

The focus of this research is limited to simple shear connections. The model is based on the transfer of shear load only, and moment forces are neglected.

3.1 Connection Layout

Once the connection type has been established, a connection model is developed. Within the Steel Construction Manual, various Specifications exist to assist in the design of

structural steel systems where the steel elements are defined by AISC. In particular, the Specification for Structural Joints Using ASTM A325 or A490 Bolts [20] by the Research Council on Structural Connections (RCSC) contains guidelines specifically for the design of bolted joints. Chapter J in the Specification for Structural Steel Buildings [19] provides detailed criteria regarding fastener size, size and use of holes, center to center spacing of fasteners, and edge distance for connection design. The size and thickness of the connecting element must also be considered. The combination of these factors affects the limit states for design of the connection. In order to investigate the design strength of the connection, the number of fasteners and thickness of the connecting element are varied to explore sensitivity.

3.1.1 Fastener and Joint Type

According to the RCSC, there are two types of high strength bolts, Type 1 (ASTM A325) and Type 3 (ASTM A490), which are supplied in diameters from ½ inch to 1½ inch inclusive. The type of high strength bolt is dependant on the chemical composition of the steel and is the same for ASTM A325 and ASTM A490 bolts. A classification of Type 1 includes medium carbon, carbon boron, or medium carbon alloy steel. A Type 3 designation consists of weathering steel to resist the effect of corrosion [20].

For fasteners loaded in shear or combined shear and tension, the joint type must be specified as snug-tightened, pretensioned or slip-critical. Snug tight is defined as the tightness that exists when all plies of a joint are in firm contact. A snug tight joint is utilized when bolts are not subject to direct tension, slip resistance of the connection is not required and for static load applications. A pretensioned joint transmits shear and

tensile loads through bolts that have been pretensioned prior to installation. Applications include joints subject to significant load reversal, fatigue load with no reversal and tensile fatigue. When slip resistance is required, a slip critical, or friction type connection is used. Slip critical connections rely on the faying surfaces to provide a calculable resistance against slip. Design scenarios where slip is not desired include joints that utilize slotted holes and joints subject to fatigue with reversal of the loading direction [20].

The model developed for this research is based on ASTM A325, Type 1 bolts having a diameter of ¾ inches. Slip critical joints are also specified for the design of the connections.

3.1.2 Bolt Holes

For each high strength bolt, a standard, oversized, short-slotted and long-slotted hole is specified in the Specification for Structural Joints Using ASTM A325 or A490 Bolts. As determined in the first publication of these Specifications, the standard bolt hole is $^{1}/_{16}$ inches larger than the nominal diameter of the bolt. Oversized, short-slotted and long-slotted holes are typically used at the discretion of the Engineer since slip resistance and net area of the connected part are generally reduced. A nominal bolt hole of $^{13}/_{16}$ inches is used for the standard ¾ inch diameter bolt.

3.1.3 Spacing and Edge Distance

Chapter J, Section J3 in the Specification for Structural Steel Buildings provides criteria regarding spacing and edge distance for bolted connections. A center to center spacing of

not less than three times the nominal diameter of the fastener is permitted. This translates to a minimum center to center spacing of 2-¼ inches for the ¾ inch diameter bolt used in this research. The minimum distance from the center of a standard hole to the edge of a connected part is summarized in Tables J3.4 and J3.4M in the Specifications. The distances indicated in these tables are based on standard fabrication practices and tolerances which vary depending on the edge condition. A maximum distance of 12 times the thickness of the connected member under consideration, or 6 inches maximum, is allotted from the center of a bolt to the nearest edge [19].

3.1.4 Connection Geometry

Using the criteria described for minimum edge distances, center-to-center spacing and bolt hole sizes, the following connections are constructed. Figures 3.1.4-1 and 3.1.4-2 indicate the single bolt and double bolt shear plate connections, respectively.

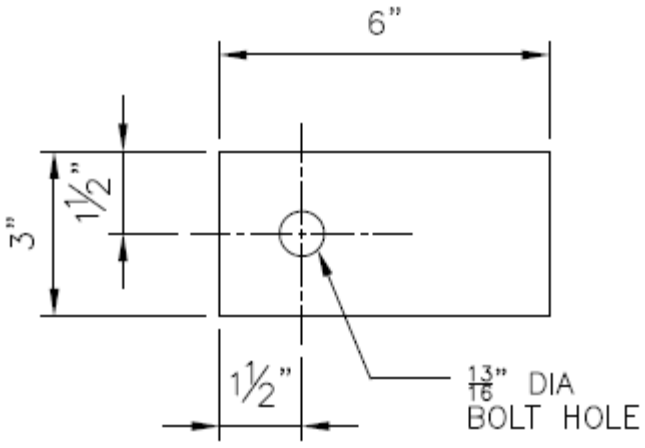

Figure 3.1.4-1: Single Bolt Shear Plate Connection

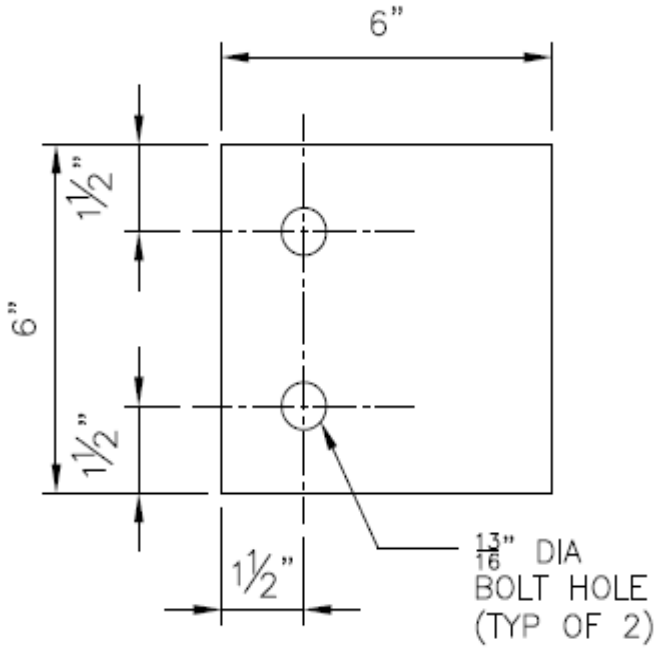

Figure 3.1.4-2: Double Bolt Shear Plate Connection

3.2 Material Properties of Steel at Normal Temperature

Once the connection type is established, the type of steel and the associated material properties of the connecting element must be chosen. Steels for structural use are commonly classified as carbon steel, high-strength low alloy steel and alloy steel. The distinguishing property between these types of steels is the minimum yield stress in tension of the material. The yield stress is defined as the point on the stress-strain curve where perfect elasticity is exceeded. The yield stress and other key values are further described in Section 3.2.2. Carbon and high-strength low alloy steels are characterized as having definitive yield points. The American Society for Testing and Materials (ASTM) [17] has developed, the properties of steels, including the minimum yield stress, as a result of variations in composition, heat treatment, and mechanical working.

3.2.1 ASTM Steel Grades

Carbon steels vary based on the percentage of carbon ranging from less than 0.15% to 1.70% and have a definitive yield point. Structural carbon steels are in the mild carbon range (0.15%-0.29%) and are used for general structural purposes in building construction. ASTM A36 carbon steel having a minimum yield stress of 36 kips per inch used to be the preferred material for rolled shapes until recently. Higher strength, low alloy steels such as ASTM A572 and A992 are more available and have replaced ASTM A36 steel in many applications.

High-strength low alloy steels have a definitive yield point similar to that of carbon steel, however, yielding occurs at a higher stress. The American Society of Testing and Materials has designations for high-strength low alloy steel including steels with yield stresses from 40 to 70 kips per square inch. For structural steel shapes, plates, sheet piling, and bars, ASTM A572 is commonly used. There are five grades of A572 high-strength low alloy steels ranging from Grade 42 to Grade 65. The higher grades of steel are intended for riveted and bolted construction of bridges where a higher yield point is required. The ASTM A572 steel is used for the connecting element in this thesis.

3.2.2 Stress-Strain Diagram for Ductile Steel

Stress-strain diagrams are created using a procedure called tension testing described in ASTM A370, Standard Test Methods and Definitions for Mechanical Testing of Steel Products. To perform a tension test, a round material specimen is used having a cross-sectional area, A_o, and gage marks at a distance L_o apart. The magnitude of the load, P, and the changes in elongation, ΔL, of the member are recorded using dial gages as a force

is applied to the specimen. To plot stress, σ, on the diagram, the load, P, is normalized by the initial cross-sectional area, A_o, of the specimen. Strain, ε, is computed by dividing each increment ΔL of the distance between the gage marks by the initial length L_o. Figure 3.2.2-1 is used to describe the typical stress-strain diagram for ductile steel [21].

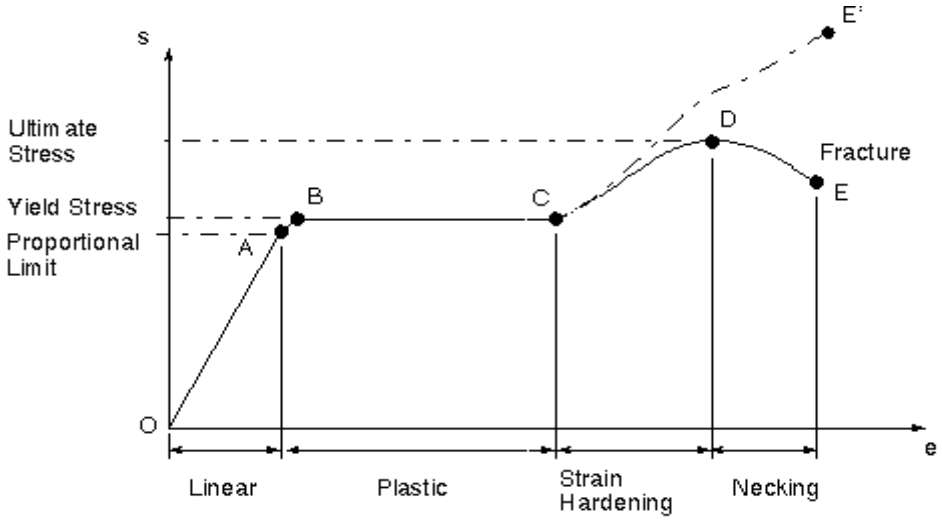

Figure 3.2.2-1: Stress-Strain Diagram for Ductile Steel

As the specimen is subjected to an increasing load, a change in length increases linearly with the load until an elastic limit is reached. The initial portion of the stress-strain diagram is a straight line with a steep slope since the deformations are small hence the material exhibits linear-elastic behavior. This area, identified as the elastic region, represents the region where permanent strains are not an effect upon the complete release of the stress. The relationship of stress directly proportional to strain within the elastic region is known as Hooke's Law [21]:

$$\sigma = E\varepsilon \qquad \text{[Eq. 3.2.2-1]}$$

The coefficient, *E*, defined as the modulus of elasticity (or Young's modulus) measures the elastic stiffness of the material. For carbon steels, the value used for the modulus of elasticity is 29,000 kips per square inch. The proportional limit, Point A in Figure 3.2.2-1, is the maximum stress that can be used in Hooke's Law. Beyond the proportional limit, the response becomes non-linear, (i.e. the load and displacement are no longer proportional) and the deformations become permanent (plastic) beyond the elastic limit.

Past the elastic limit, the yield stress, Point B, is quickly obtained as shown in Figure 3.2.2-1. The yield stress is important for design purposes, since it provides a limit to the amount of stress a material can sustain without becoming permanently stretched. The yield stress is considered the point where plastic elongation of the material begins, and large deformations occur with small increases in load. The stress remains constant for a large range of values after the onset of yield, and the material is said to have perfectly plastic behavior.

As the capacity for perfectly plastic deformation is used up, strain hardening begins indicated at Point C on the figure. The deformations are still plastic, but increasing stresses are required. As the strain hardening capacity is exhausted, the curve flattens. The maximum load normalized by the original area is called the ultimate stress indicated at Point D. Past the peak load, the steel appears to soften and necking begins where the cross sectional area of the specimen is reduced due to local instability. In reality, as necking occurs, the steel is no longer in a simple uniaxial state of stress, and the load is carried across a greatly reduced area. Since a lower load is sufficient to keep the

specimen elongating, the specimens actually breaks at Point E, the fracture stress, which is somewhat lower than the ultimate strength [21].

The ASTM A572, Grade 50 steel used for this research has a yield stress of 50 kips per square inch and an ultimate stress of 65 kips per square inch at normal temperatures [17].

3.3 Material Properties of Steel at Elevated Temperatures

When steel is subjected to high temperatures, the material properties change based on increases in temperature. In particular, the yield stress and the modulus of elasticity decrease and the thermal expansion of the material increases when high temperatures are obtained. The SFPE Handbook of Fire Protection Engineering provides equations to calculate these changing properties. Physical testing known as the stress rupture test is the means of deriving these equations.

3.3.1 Physical Testing of Steel at Elevated Temperatures

The stress rupture test replaces the tensile test as the method to determine the behavior of steel at elevated temperatures. The recorded strain value for a given stress can change if time is permitted to vary, however this effect is very small at room temperature. Therefore, at lower temperatures and at stresses below the yield strength there is essentially no change in the stress-strain curve with time. At high temperatures, the mechanical properties as well as the nature of deformation and fracture demonstrate significant changes depending on the time to complete the test [10].

The stress rupture test is similar to the creep test by the nature of the test, the measurements and the results, however, temperature, load and strain are thoroughly monitored. The common method of performing stress rupture testing is to apply a load on a test bar at a given temperature and measure the elongation as a function of time until fracture occurs. The test specimen is typically a standard ½-inch diameter by 2-inch gage length bar, however a gage length of up to 10 inches may be used. Necking is not common as in low temperature tensile testing and deformation occurs over the entire gage length. The load may be applied directly to the test bar or through use of a beam system. Temperature is controlled to within 0.5% of the test temperature since steel has recrystallization characteristics, where new grains of the metal are formed due to heating and cooling of the material, above room temperature. Strain is measured using a dial gage, a mechanical extensometer attached to the specimen or using optical methods. The elongation is measured as a function of time for a particular load which is converted to stress based on the original cross-section. Stress rupture testing usually takes from approximately 10 to 2000 hours until failure occurs [10].

It is common practice to repeat the testing at various temperatures to provide numerous data points. Once the stress rupture testing is complete, data plots are created and evaluated to determine the effect of time or strain rate on the behavior of the steel under stress at elevated temperature. From a series of data curves it is possible to determine all of the conditions of stress, strain, and temperature for the steel alloy tested [10].

3.3.2 Mechanical Steel Properties at Elevated Temperatures

Using the results of tensile testing and stress rupture testing, mathematical relationships are developed to describe the mechanical properties of steel including the yield strength, σ_y, and modulus of elasticity, E, based on temperature changes. An expression for the coefficient of thermal expansion, α, also varies with temperature and ultimately affects the thermal strain of the member. The SFPE Handbook of Fire Protection Engineering [9] outlines the mathematical equations to compute the mechanical properties based on temperature changes. The material properties for ASTM A572, Grade 50 steel are computed for varying temperatures using the following equations from the Handbook and the results are tabulated in Table 3.3.2-1.

$$\sigma_y = \sigma_{yo}(1 - 0.78\theta - 1.89\theta^4) \qquad \text{for } \theta < 0.63 \qquad \text{[Eq. 3.3.2-1]}$$

$$E = E_o(1 - 2.04\theta^2) \qquad \text{for } \theta < 0.63 \qquad \text{[Eq. 3.3.2-2]}$$

$$\alpha = (6.1 + 0.0019T) \times 10^{-6} \qquad \text{for } \theta < 0.68 \qquad \text{[Eq. 3.3.2-3]}$$

where

σ_y = yield strength at elevated temperature (psi)

σ_{yo} = yield strength at 68 °F (20 °C) (psi)

E = modulus of elasticity at elevated temperature (psi)

E_o = modulus of elasticity at 68 °F (20 °C) (psi)

α = coefficient of thermal expansion at temperature, T (in./in.°F)

T = temperature difference [steel temperature – (100 °F)]

$$\theta = \frac{T' - 68}{1800} \qquad T' \text{ in °F}$$

T' = steel temperature

$$\theta = \frac{T' - 20}{1000} \qquad T' \text{ in } °C$$

Table 3.3.2-1: Temperature Effects on Mechanical Properties of ASTM A572, Grade 50 Steel

Steel Temperature			**Steel Properties**		
°C	**°F**	**θ value**	**σ_y (psi)**	**E (psi)**	**α (in/in°F)**
0	32	-0.02	50,780	28,976,336	5.9708E-06
20	68	0	50,000	29,000,000	6.0392E-06
30	86	0.01	49,610	28,994,084	6.0734E-06
40	104	0.02	49,220	28,976,336	6.1076E-06
50	122	0.03	48,830	28,946,756	6.1418E-06
100	212	0.08	46,876	28,621,376	6.3128E-06
150	302	0.13	44,903	28,000,196	6.4838E-06
200	392	0.18	42,881	27,083,216	6.6548E-06
250	482	0.23	40,766	25,870,436	6.8258E-06
300	572	0.28	38,499	24,361,856	6.9968E-06
350	662	0.33	36,009	22,557,476	7.1678E-06
400	752	0.38	33,210	20,457,296	7.3388E-06
450	842	0.43	29,999	18,061,316	7.5098E-06
500	932	0.48	26,264	15,369,536	7.6808E-06
538	1000	0.52	22,994	13,125,952	7.8108E-06
550	1022	0.53	21,873	12,381,956	7.8518E-06
600	1112	0.58	16,686	9,098,576	8.0228E-06
650	1202	0.63	10,543	5,519,396	8.1938E-06
700	1292	0.68	3,275	1,644,416	8.3648E-06

The values obtained using the mathematical expressions indicate that the elastic and ductile properties of steels are greatly reduced with increases in temperatures. When temperatures rise above 200 °F, the stress-strain curve exhibits nonlinear properties, gradually eliminating the well-defined yield point. The range from 800 °F to 1000 °F is where the rate of decrease of strength is at a maximum.

Figure 3.3.2-1, indicates the temperature effects on the yield strength of ASTM A572, Grade 50 steel. The yield strength, σ_y, at 1000 °F (538 °C) is approximately 60 percent

of the yield strength at ambient temperature, 68 °F. Due to this decrease in strength, the American Institute of Steel Construction limits the permissible design stress to approximately 60 percent of the yield strength [19].

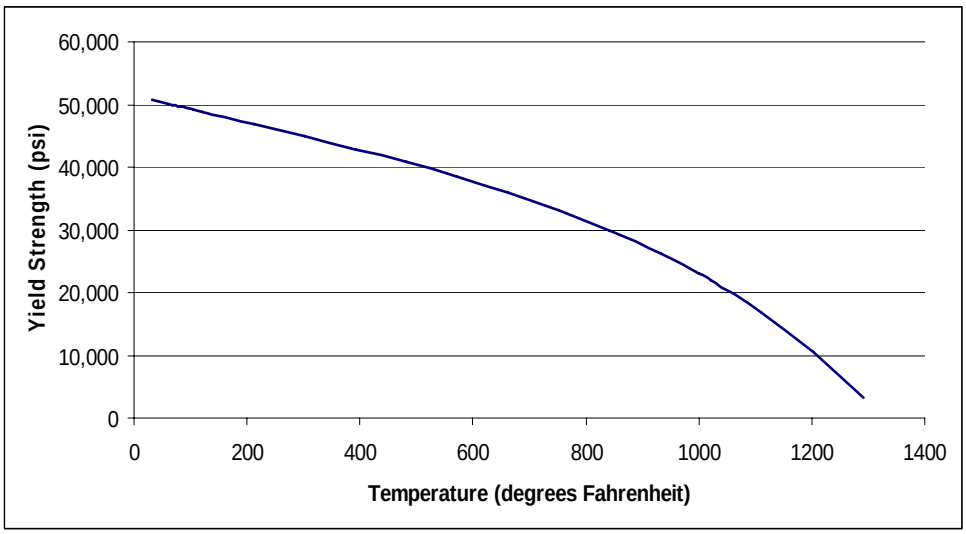

Figure 3.3.2-1: Temperature Effects on Yield Strength of ASTM A572, Grade 50 Steel

In addition to the yield strength, significant changes occur in the modulus of elasticity with increasing temperatures. As shown in Figure 3.3.2-2, when the temperature of a steel member increases, the modulus of elasticity decreases from 29,000 kips per square inch at 68 °F (20 °C) to approximately 13,000 kips per square inch at 1000 °F (538 °C). Beyond 1000 °F, the modulus of elasticity decreases at a faster rate, thus impacting the load carrying capacity, deflection, and buckling capability of a member.

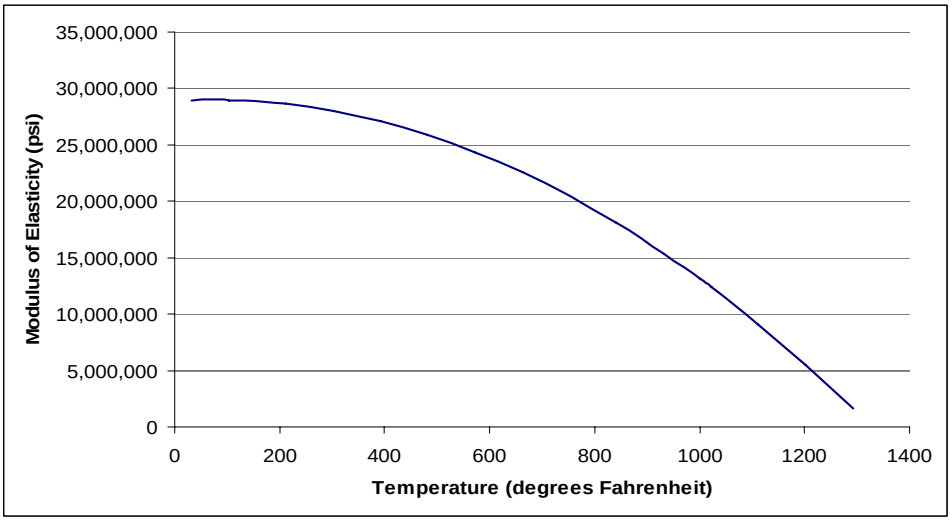

Figure 3.3.2-2: Temperature Effects on Modulus of Elasticity of ASTM A572, Grade 50 Steel

With the onset of increasing temperatures, the coefficient of thermal expansion becomes a characteristic of the material. The coefficient of thermal expansion relates the temperature change in a member to deflection and strain values. At 68 °F, room temperature, the coefficient of thermal expansion for structural steel is approximately 6.0 x 10^{-6} inches/inch °F. This value increases as temperature rises in a steel member as shown in Figure 3.3.2-3.

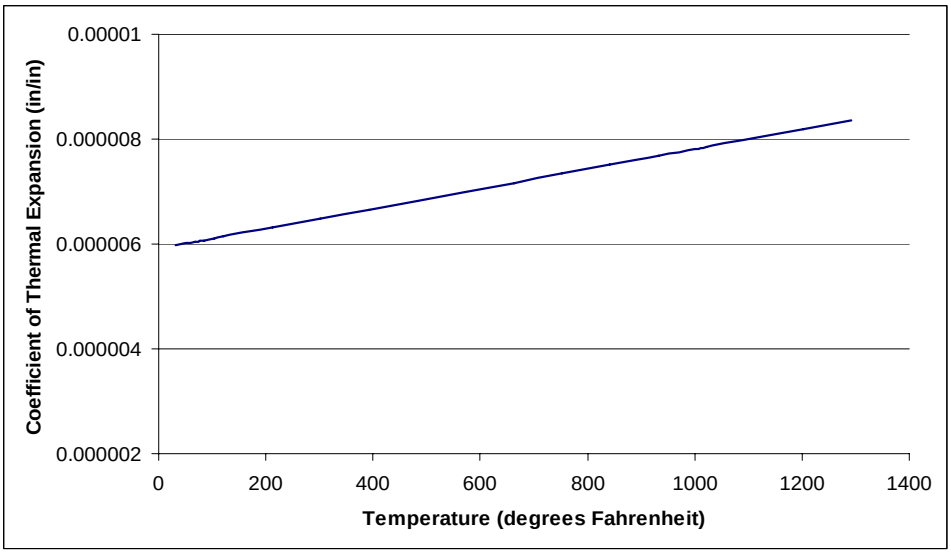

Figure 3.3.2-3: Increasing Coefficient of Thermal Expansion of ASTM A572, Grade 50 Steel

In addition to the changing mechanical properties of the steel at elevated temperatures, changes occur in the specific heat and thermal conductivity of the steel. These thermal properties are typically used in heat transfer analysis calculations and ultimately affect the load carrying capacity of the steel member. Table 3.3.2-2 provides values for the thermal conductivity and specific heat at elevated temperatures. Note that the density of the steel remains unchanged even at increased temperatures.

Table 3.3.2-2: Thermal Conductivity and Specific Heat Values for ASTM A572, Grade 50 Steel

Thermal Conductivity (Btu/ft hr°F)	Specific Heat (Btu/lb °F)	Density (lb/ft^3)
30.0 @ 0 °F	0.107 @ 0 °F	480.0
24.7 @ 600 °F	0.144 @ 750 °F	480.0
20.1 @ 1100 °F	0.172 @ 1100 °F	480.0
15.0 @ 2000 °F	0.172 @ 2000 °F	480.0

3.4 Mathematical Analysis

The American Institute of Steel Construction permits two types of design procedures; allowable stress design (ASD) and load and resistance factor design (LRFD). ASD is characterized by the use of unfactored service loads in conjunction with a single factor of safety applied to the resistance. The designer ensures that the stresses developed do not exceed the allowable elastic limit usually, which is equal to some percentage of the yield stress. LRFD, as its name implies, is based on a limit state philosophy which uses separate factors for each load and the resistance. The two categories of limit states are strength and serviceability. Strength limit states are based on the load-carrying capacity of the structure while serviceability refers to the performance of the structure under loads [1].

ASD and LRFD, as presented in the Steel Construction Manual, are equally valid for the design of steel members and connections and there is no preference stated or implied. Design according to the current edition of the Manual, whether ASD or LRFD, is based on limit state design principles described above. Both approaches are used for the design of the connections in this thesis to highlight how similar ASD and LRFD are in their formulation.

Chapter J in the Specification for Structural Steel Buildings [19], provides equations for the design of bolted connections and connecting elements such as plates, gussets, angles and brackets. The design tensile strength, ϕR_n, and the allowable tensile strength, R_n/Ω, of a connected element loaded in tension is determined when the limit states of excessive

deformation or fracture are reached. Excessive deformation may occur due to the yielding of the gross section along the cross-section of the member. Fracture of the net section occurs when the stress at the net section reaches the ultimate stress, F_u, of the metal. In addition to the tensile strength, the available bearing strength at the bolt hole must be determined to satisfy the limit state of bearing which may also determine the capacity of the connecting element.

The limit states of yielding in the gross section, fracture of the net section and bearing strength are determined for each connecting element and their varying properties. Using Mathcad [22], a technical calculation software package, computations are created for the ASD and LRFD equations of each limit state. The design equations and results of the computations are presented in the following sections and the Mathcad worksheets are provided in Appendix A.

3.4.1 Yielding in the Gross Section

For the limit state of yielding in the gross section, intended to prevent excessive elongation of the member, the nominal yield strength, R_n, equals the following:

$$R_n = F_y A_g \qquad \text{[Eq. 3.4.1-1 / AISC Equation J4-1]}$$

As indicated previously in Section 3.2.2, F_y, the specified minimum yield stress, equals 50 kips per square inch for ASTM A572 Grade 50 steel. The gross area of the member, A_g, is the cross-sectional width of the plate multiplied by the thickness of the plate. To

obtain the design strength (LRFD), the nominal yield strength is multiplied by a factor, ϕ, equal to 0.90. The nominal yield strength is divided by a Ω factor of 1.67 to determine the allowable strength (ASD).

For purposes of comparison, the thickness of the plate is varied as well as the cross-sectional width of the plate. For a single bolt connection, a cross-section of three inches is used while six inches accommodates a double bolt connection. Varying plate thicknesses of ⅜", ¼" and ⅛, are used to compare the performance of the connecting elements under fire conditions.

Table 3.4.1-1 provides the results from the mathematical analysis for the limit state of yielding in the gross section. From these results, it is apparent that the cross-sectional increase from three inches to six inches doubles the capacity of the plate. A comparison of the plate thicknesses indicates that the yield strength varies by a factor of two from the ⅛ inch to the ¼ inch thickness, and a factor of one and a half from the ¼ inch to the ⅜ inch thickness. The ASD and the LRFD results are also compared and it is apparent that there is a higher yield point for the LRFD procedure due to the different safety factors used in each procedure. The LRFD results are approximately one-third higher than the ASD results. This is acceptable, however, since the load combinations used in LRFD are multiplied by load factors. The load combinations used in the ASD approach are not multiplied by load factors except for a few cases where minimal reductions are allowed for multiple time-varying loads.

Table 3.4.1-1: LRFD and ASD Yielding in the Gross Section Results

Connection Element	LRFD Design Yield Strength, ϕR_n (kips)	ASD Allowable Yield Strength, R_n/Ω (kips)
⅜" Plate, Single Bolt Connection	50.6	33.7
¼" Plate, Single Bolt Connection	33.8	22.5
⅛" Plate, Single Bolt Connection	16.9	11.2
⅜" Plate, Double Bolt Connection	101.3	67.4
¼" Plate, Double Bolt Connection	67.5	44.9
⅛" Plate, Double Bolt Connection	33.8	22.5

3.4.2 Fracture in the Net Section

The limit state of fracture in the net section is yielding which results in a fracture through the effective net area at the bolt holes. Section J4 of the Specification for Structural Steel Buildings expresses the nominal fracture strength, R_n as:

$$R_n = F_u A_e \qquad \text{[Eq. 3.4.2-1 / AISC Equation J4-2]}$$

The specified minimum tensile strength, F_u, equals 65 kips per square inch as indicated in Section 3.2.2 for ASTM A572 Grade 50 steel. The effective net area, A_e, that can be assumed to resist tension at the section through the bolt holes is determined by multiplying the net area, A_n, by a shear lag factor, U [19].

Shear lag is the non-uniform stress reduction which occurs in a member adjacent to a connection in which all elements of the cross section are not directly connected. This effect reduces the strength of the connection since the entire cross section is not fully effective at the critical section location. According to Section D3.3 in the Specification for Structural Steel Buildings, the equation to compute the shear lag factor, U, for all

tension members where the tension load is transmitted to some but not all of the cross-sectional elements is:

$$U = 1 - \frac{\bar{x}}{L} \leq 0.9 \qquad \text{[Eq. 3.4.2-1 / AISC Table D3.1]}$$

The length L is the distance, parallel to the line of force, between the first and last row of fasteners in a line. For any given profile of connected elements, $\bar{x}$ is the perpendicular distance from the connecting plane to the centroid of the member resisting the connection force. For short connecting elements, where the connecting elements of the cross-section lie in essentially a common plane, U can conservatively be taken as 1.0. The net area, A_n, is the gross cross-sectional area, A_g, minus the removal of any bolt holes through the section. In computing the net area, the total width of a standard bolt hole to be deducted shall be taken as the nominal hole diameter normal to the direction of the applied load plus 1/16 inches. To obtain the design fracture strength (LRFD), the nominal strength is multiplied by a factor ϕ equal to 0.75. The nominal strength is divided by a factor Ω of 2.0 to determine the allowable fracture strength (ASD) [19].

The computations for the fracture in the net section of each connection are included in Appendix A and a summary of the results is shown in Table 3.4.2-1.

Table 3.4.2-1: LRFD and ASD Fracture in the Net Section Results

Connection Element	LRFD Design Fracture Strength, ϕR_n (kips)	ASD Allowable Fracture Strength, R_n/Ω (kips)
⅜" Plate, Single Bolt Connection	40.0	26.7
¼" Plate, Single Bolt Connection	26.7	17.8
⅛" Plate, Single Bolt Connection	13.3	8.9
⅜" Plate, Double Bolt Connection	80.0	53.3
¼" Plate, Double Bolt Connection	53.3	35.5
⅛" Plate, Double Bolt Connection	26.7	17.8

These results indicate that the double bolt connection for each plate thickness has a fracture strength two times greater than the single bolt connection. The net area is calculated based on the cross-sectional width of the connection which varies from three inches to six inches; a factor of two. A comparison of the plate thicknesses indicates that the fracture strength varies by a factor of two from the ⅛-inch to the ¼-inch plate and a factor of one and a half from the ¼-inch to the ⅜-inch plate. The bolt hole reduction in the net area calculation is also doubled when designing a two bolted connection. Similar conclusions to the yield strength computations are made between the LRFD and the ASD approaches. The ASD computations provide a fracture strength roughly one-third lower than the LRFD method.

Comparing the two failure modes, the fracture strength is approximately 25 percent lower than the yield strength. Therefore, the capacity of the connection is determined by the fracture strength thus far.

3.4.3 Bearing Strength at Bolt Holes

According to Section J3 of the Specification for Structural Steel Buildings, the bearing strength of a bolted connection results from the strength of the parts being connected and the arrangement of the bolts. Factors including the spacing of the bolts, edge distances, tensile strength and thicknesses of the connected parts may impact the bearing strength. The bearing strength for bolted connections using standard sized holes when deformation at service load is a design consideration is determined by the equation:

$$R_n = 1.2L_ctF_u \leq 2.4dtF_u \qquad \text{[Eq. 3.4.3-1 / AISC Equation J3-6a]}$$

This equation is used when the deformations are limited to be less than or equal to a ¼ inch. When deformations are not a design consideration, in other words the acceptable deformation can be greater than a ¼ inch, the limiting nominal strength is $3.0dtF_u$ [19].

The variable L_c represents the clear distance from the edge of the bolt hole to the edge of the connected material. The thickness t of the connected material and the nominal diameter d of the bolt are also expressed in the above equation. The nominal bearing strength is multiplied by the number of bolts perpendicular to the direction of the applied load. A resistance factor ϕ equal to 0.75 is multiplied by the nominal bearing strength to obtain the design bearing strength, ϕR_n, for LRFD. The ASD allowable bearing strength, R_n/Ω, is established when the nominal bearing strength is divided by a safety factor Ω equal to 2.0 [19].

The design bearing strength and the allowable bearing strength results are tabulated in Table 3.4.3-1 and the calculations are presented in Appendix A. Similar to the other

failure modes, the allowable bearing strength (ASD) is approximately one-third less than the design bearing strength (LRFD) and the double bolt connection provides a strength two times greater than the single bolt connection based on the amount of bolts. The plate thicknesses also vary by the same factors as indicated in the yielding in the gross and the net fracture computations. A comparison of the three modes indicates that the capacity of the connection is determined by the bearing strength at the bolt holes.

Table 3.4.3-1: LRFD and ASD Bearing Strength at Bolt Holes Results

Connection Type	LRFD Design Bearing Strength, ϕR_n (kips)	ASD Allowable Bearing Strength, R_n/Ω (kips)
⅜" Plate, Single Bolt Connection	24.7	16.5
¼" Plate, Single Bolt Connection	16.5	11.0
⅛" Plate, Single Bolt Connection	8.2	5.5
⅜" Plate, Double Bolt Connection	49.4	32.9
¼" Plate, Double Bolt Connection	32.9	21.9
⅛" Plate, Double Bolt Connection	16.5	11.0

This chapter focused on the development of the material properties of steel at ambient and elevated temperature based on guidelines provided by AISC, ASTM and the NFPA. The capacities determined in Section 3.4 from the mathematical analysis will provide a baseline for comparison against the computer analysis for each failure mode.

4.0 FINITE ELEMENT MODEL DEVELOPMENT

The finite element method (FEM) is a numerical technique used to obtain approximate solutions to complex engineering, mathematical and physics problems. When problems involve complicated geometries, loadings, or material properties, it is generally not possible to determine closed-form mathematical solutions, therefore, the finite element method is used to achieve acceptable solutions. In finite element modeling, a large region is divided, or meshed, into small sub-regions called finite elements and an approximate solution of the governing equations of mechanics is obtained. These equations are formulated for each element and combined to obtain the solution for the entire model. The solution for most structural problems involves the determination of displacements at each node and the stresses within the elements creating the structure that is subjected to applied loads [11].

4.1 History of Finite Element Analysis

The term "finite element method" was coined by Professor Ray Clough in a 1960 paper entitled, "The Finite Element Method in Plane Stress Analysis" [Clough 1960], however, the ideas of finite element analysis date back much further. In 1943, a mathematician, R. Courant [24], proposed dividing up a continuum into triangular regions and replacing the fields with piecewise approximations within the triangles. The flexibility or force method was developed by Levy [25] in 1947, and in 1953 his work suggested that the stiffness or displacement method could be useful in analyzing aircraft structures [26]. Argyris and Kelsey [27] developed the matrix structural analysis methods using energy principles in 1954. For aircraft structural analysis, the team of Turner, Clough, Martin and Topp [28] applied the displacement method to solve plane stress problems by

subdividing the structure into triangular or rectangular elements in 1956. During the decade of 1960-1970, the finite element method was used to solve three-dimensional problems using a tetrahedral stiffness matrix, large deflection, thermal, fluid and material nonlinearity problems. The finite element method has become a practical solution to solve numerous engineering problems over the past 40 years especially with advancements in computer technology [11].

4.2 Finite Element Analysis Process

To solve any finite element problem, a step-by-step process is followed to develop the model and obtain the results. The six major steps of the finite element method are [29]:

1. Establish the Governing Equations and Boundary Conditions
2. Divide Solution Domain into Elements
3. Determine Element Equations
4. Assemble Global Equations
5. Solve the System of Equations
6. Verify the Results

Steps 1 and 2 are considered to be the preprocessing phase where the mesh is developed and the material properties and boundary conditions are applied. In the solution phase, steps 3 through 5, the program develops and solves the governing matrix equations based on $[K]\{r\}=\{d\}$, where $[K]$ is the system stiffness matrix, $\{r\}$ is the displacement vector including all nodes, and $\{d\}$ is the applied nodal load vector. The postprocessing phase, step 6, allows the analyst to check the validity of the solution. This can be done by

verifying that the applied forces balance the reaction forces in magnitude and direction, checking that the model deforms as intended based on the boundary conditions, and through verification against hand derived computations [29].

There are several commercial software packages, such as ABAQUS [14], ALGOR [13], ANSYS [15] and Nastran [16], that can be used for finite element analysis. Using these programs, much of the work for the engineer is in the model development and interpreting the results. The formulation of the element behavior and the formation of the element and global stiffness matrices are performed automatically by the finite element software. For the work of this thesis, the software program, ALGOR, is used.

4.3 Constructing the Finite Element Model

The ALGOR software package consists of four main interfaces: Superdraw III, CAD Interface, FEA Editor, and Superview. These functions assist in creating a model and viewing the results. Superdraw III contains CAD tools used to create the geometry of a model within the ALGOR program. Models developed using Superview III can be meshed automatically or "by hand" through this function. The geometry of a model constructed by a CAD solid model package compatible with ALGOR can be imported through use of the CAD Interface. The CAD Interface feature allows the user to apply a surface mesh to the imported model. Whether Superdraw III or the CAD Interface is used to create the model, the FEA Editor is used to input the material properties, boundary constraints and loading. The compiled model and the results can be viewed graphically through the Superview function.

4.3.1 Establishing the Type of Analysis

Prior to constructing a structural finite element model the analysis type, either linear or nonlinear, must be determined. A linear analysis is only accurate for a model in which the relationship between the forces and stresses/deflections is a linear function. There are various types of linear analysis applications, however, the stress-strain curve results remain in the elastic range for all cases. Deflections are typically small and the magnitude of the load does not change over time.

A nonlinear analysis approach is used when forces do not display a linear relationship with the resulting displacements and stresses. Nonlinearity is established through the material, geometry or the elements in the model. Materials that do not have a linear stress-strain curve, such as carbon steel, are nonlinear. Up to the yield point, steel is elastic in nature and has a linear stress-strain curve as shown in Figure 3.2.2-1. Beyond the point of yield, the steel enters the plastic range and becomes nonlinear. When loading steel materials into the plastic range, a nonlinear computer analysis is required. Geometric nonlinearity occurs in models that are subjected to large deformations or strains, therefore, impacting the geometric characteristics of the model. Once the geometry of the model is compromised, the model behaves differently under load. The final type of nonlinearity occurs within the elements in the model. Element nonlinearity is exemplified through use of contact elements where the stiffness matrix of elements changes as a function of some specified variable. The study of stresses in the vicinity of the bolt holes requires that a nonlinear stress analysis be performed due to the steel

properties beyond yielding and the large deflections anticipated from a ramp loading which will later be defined.

In addition to linear and nonlinear analyses, heat transfer, electrostatic and fluid flow analyses can be performed with the ALGOR software package. The second part of this research combines the use of a nonlinear mechanical analysis with a heat transfer analysis. A nonlinear thermal stress analysis calculates the stress in a nonlinear model or mechanical event simulation (MES) due to temperature loads from a thermal model. The MES/nonlinear software reads the nodal temperatures obtained from a transient heat transfer analysis and calculates the stress at each step provided that the thermal model and stress model are identical. Each node must be at the same position for the integrated thermal stress analysis to work as intended. Minimal changes to the stress model such as the addition of stress boundary conditions or the addition of forces, moments and pressures, can be done, and the models will remain identical for a direct approach. If the nodes in the heat transfer model are not in the same position as the stress model, the direct transfer will not work and an indirect analysis to transfer the information is required.

4.3.2 Generate Model Geometry in Superdraw III

The preprocessing phase begins with the development of the model in Superdraw III, ALGOR's finite element model-building tool. Once in the Superdraw III interface, the program functions are accessed through pull-down menus and toolbars. Superdraw III allows the user to specify a global coordinate system and define the overall dimensions of the model as well as the individual elements that comprise the model.

First, the “Tools: Model Data Control” pull-down menu is used to establish a file name, a unit system, and the analysis type (MES with Nonlinear Material Models). Next, a global coordinate system is created using the “View: Pre-Defined Views” menu. A two dimensional model is sufficient for the analysis, therefore, the model must be constructed in the YZ plane, ALGOR’s default. Following this setup, the rectangular outline of the connection and the bolt holes begin to take shape using the “Add”, “Construct” and “Modify” commands.

Once the outline of the connection model is complete, a mesh is applied to divide the model into quadrilateral or triangular elements. Mesh density is a term used to describe the amount of elements in the mesh in proportion to the size of the model. By increasing the mesh density, the triangular and quadrilateral elements increase in number but decrease in size. The density of the mesh affects the accuracy of the model especially at curved edges. However, the increase in accuracy may not be worth the increase in processing time required. It is best to determine the areas of importance in the model and increase the mesh in these areas.

Models can be automatically meshed by Superdraw III or the mesh can be created “by hand”. The pull-down menu, “FEA Mesh” indicates the “Automatic Mesh” and “Two-Dimensional Mesh Generation” options. There are five different automatic mesh generation techniques that can be performed using objects, points, or a combination of the two. There are two auxiliary commands that allow the user to control the density of

the mesh and limit the points or objects that are being meshed between. It is important to note that complex models sometimes require lines to be added connecting different points to create mesh regions. The two-dimensional mesh generation option provides a simple method for refining the mesh of a model by adding more elements at critical points. The quadrilateral, triangular or mixed elements can be specified using a mesh density or mesh size. Also, if various groups are specified in the model, different meshes can be applied for each group.

Creating a mesh for a model is a trial and error process. The connection models are meshed several times using the two-dimensional mesh generator to find an efficient yet accurate model. The finely meshed models result in very long computer processing and errors. The final mesh, indicated in Figure 4.3.2-1, provides a denser mesh in the vicinity of the bolt for more accurate results. This model contains 516 quadrilateral elements and 546 nodes.

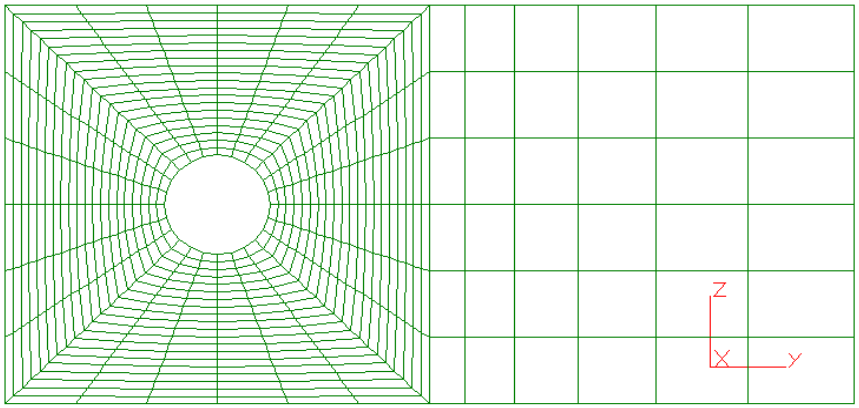

Figure 4.3.2-1: Meshed Connection Model

Each entity in the model has a surface, layer and a group property associated with it. Surfaces are used to assign surface loads such as applied pressures to specific elements. Layers are used to group sections of a model together and are generally used in complex models where graphical filtering is required to view portions of the model while it is constructed. Linear beams are the only elements that have properties associated with the layer property. Group properties separate different materials, multiple elements or element properties in the same model. Each group defined in the model must consist of complete elements. Therefore, one of each group number is required at the interface between groups. To view these different properties, use the "Tools" pull-down menu and access the "Surface Control", "Layer Control" and "Model Data Control" options. Due to the simplicity of the connections, the models are created on one layer and as a single group.

4.3.3 Element and Material Specification

Elements define how the degrees of freedom of one node relate to the next. There are several types of elements depending on the type of object being modeled and the type of phenomena and analysis being investigated. Element types include lines (beams), areas (2-D or 3-D plates) and solids (bricks). Typically for a stress analysis, either plane stress or plane strain, 2-D plate elements are specified. In a plane strain analysis, the model exhibits no deflection normal to the Y-Z plane. Therefore, a thickness of 1 unit is assumed. Plane stress analysis, on the other hand, models elements of a specified thickness exhibiting no stress normal to the Y-Z plane. For this research, the 2-D plate elements are used in the model [12].

The material type of the elements must be defined to complete the model description. In Superview III, under the "Tools: Model Data Control" menu, a comprehensive material library is accessed. A material from the library can be selected or a "Customer Defined" material can be input. Values for the mass density, modulus of elasticity, poisson's ratio, yield stress, and strain hardening modulus must be supplied to create a new material. The following table indicates the "Customer Defined" material created for the ASTM A572, Grade 50 steel used to model the connections.

Table 4.3.3-1: "Customer Defined" Material Properties for ASTM A572, Grade 50 Steel

Material Property	**Value**
Mass Density	7.35×10^{-4} lbf-s^2/in/in^3
Modulus of Elasticity	29×10^6 lbf/in^2
Poisson's Ratio	0.29
Yield Stress	50,000 lbf/in^2
Strain Hardening Modulus	1×10^6 lbf/in^2

4.3.4 Yield Criterion

The yield surface of a material is expressed in terms of the three dimensional principle stresses. The state of stress inside the yield surface is elastic. Once the state of stress is on the surface, the material is considered to have reached its yield point and is in a plastic state. There are two criterions, von Mises and Tresca, typically used to define the yield surface of a material [12].

The von Mises criterion states that a material will yield when the distortion energy, or energy associated with the change in shape of the material, reaches a critical value known as the yield strength. In other words, a material will stay elastic as long as the distortion

energy remains smaller than the distortion energy that causes yield in a tensile test specified for the same material. The von Mises criterion [30] written in terms of the two-dimensional principle stresses, σ_1 and σ_2, and the yield stress, σ_y, is:

$$\sigma_1^2 - (\sigma_1 \sigma_2) + \sigma_2^2 \leq \sigma_y^2 \qquad \text{[Eq. 4.3.4-1]}$$

The Tresca criterion [30], often called the maximum shear stress criterion, similarly relates the shear stress to the principle stresses. This criterion requires the principle stress difference along with the principle stresses themselves to be less than the yield shear stress. Mathematically,

$$|\sigma_1| \leq \sigma_y, \ |\sigma_2| \leq \sigma_y, \ and \ |\sigma_2 - \sigma_1| \leq \sigma_y \qquad \text{[Eq. 4.3.4-2]}$$

Figure 4.3.4-1 provides a projection of the von Mises and the Tresca criterions into the σ_1 and σ_2 plane. The von Mises envelope is shown as an ellipse and the Tresca envelope is the prism based on the equations above. Since the Tresca envelope appears inside the ellipse of the von Mises envelope, the Tresca criterion is more conservative and the yielding using this theory is predicted at a lower stress [30].

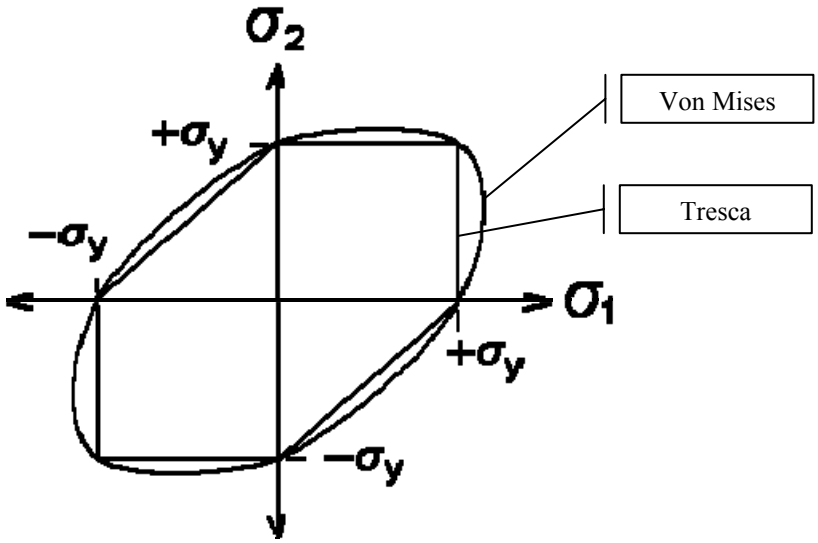

Figure 4.3.4-1: Von Mises and Tresca Yield Envelopes

When compared to actual experiments, the yield stress is closer to the von Mises condition. For hand calculations, the Tresca is easy to implement, however, the von Mises criterion is convenient for computer analysis since the entire envelope can be represented with a single equation. Since the von Mises criterion is often used to estimate the yield of ductile materials such as steel, this criterion is used for this computer analysis [30].

4.3.5 Strain Hardening

Experiments show that when a material is plastically deformed, then unloaded and further loaded to go into a plastic region, its resistance to plastic flow will increase. This increased resistance to plastic flow is known as strain hardening. Isotropic hardening and kinematic hardening are two methods to model strain hardening by relating the size and shape of the yield surface to plastic strain.

Isotropic hardening models the yield surface as increasing in size but remaining the same shape as a result of plastic straining. After a few iterations, however, the solid hardens until it acts elastically. Isotropic hardening is not effective in situations where solids are subjected to cyclic loading because at any state of loading, the center of the yield surface remains at the origin.

The hardening is said to be kinematic in the sense that at any state of loading, the size of the yield surface cannot change and its center can move with respect to the origin. As the material in tension is deformed, the yield surface is pulled in the direction of increasing stress allowing cyclic, plastic deformation to occur.

The stress-strain curves for kinematic and isotropic strain hardening are compared in Figure 4.3.5-1. The stress-strain diagram using the kinematic strain hardening rule, shows the translation that occurs when the material is loaded, unloaded and reloaded. Isotropic strain hardening produces a stress-strain diagram that unloads and reloads along the same path. A kinematic strain hardening law is applied to the connection models to most accurately observe the nonlinear stresses.

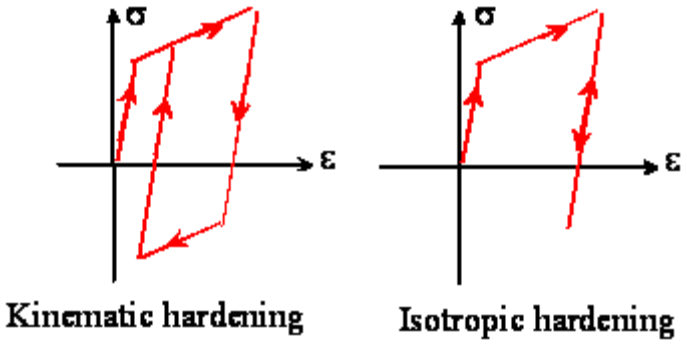

Figure 4.3.5-1: Stress-Strain Diagrams for Kinematic and Isotropic Strain Hardening

4.3.6 Symmetry Axis

When creating a model, it is important for the analyst to be cognizant of situations of symmetry that allow reduction in the size of the model to be analyzed. Reflective symmetry is defined as the "correspondence in size, shape, and position of loads; material properties; and boundary conditions that are on opposite sides of a dividing line or plane." [11] A series of rollers is used along the Y axis of the plate at the centerline to model a double bolt connection as shown in Figure 4.3.6-1. The use of symmetry allows a problem to be modeled using a reduced stiffness matrix, therefore, decreasing the computing time.

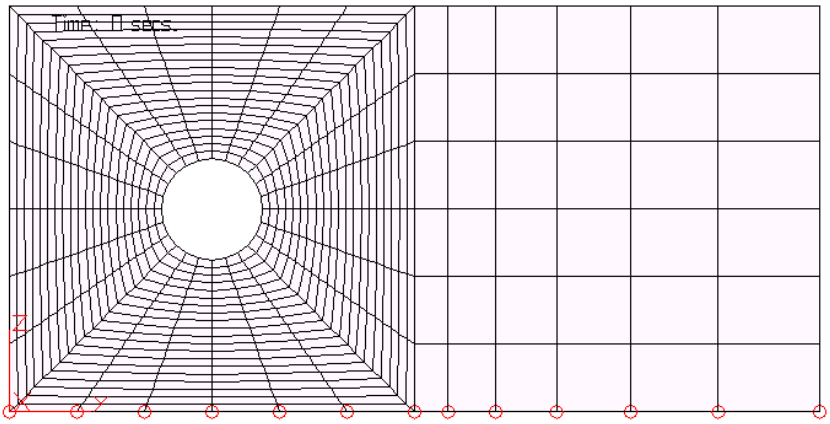

Figure 4.3.6-1: Reflective Symmetry

Now that the analysis type, geometry and element/material properties have been defined, the model is transferred to the FEA Object Editor in the ALGOR interface where external loads and boundary conditions are applied.

4.4 Boundary Conditions

During analysis, an equation is generated for each degree of freedom at every node. However, when a boundary condition is applied at a node, no equation is generated since it is prevented from translating or rotating in a specified direction. There are four predefined boundary conditions in ALGOR: fixed, free, pinned and no rotation [12]. A fixed condition restrains all degrees of freedom at a node while a free condition allows translation and rotation in any direction. A pinned condition constrains all translational degrees of freedom. No rotation indicates that all rotational degrees of freedom are constrained. If a predefined boundary condition is not used, the analyst can choose to restrict translation or rotation in any direction at any node. Boundary conditions are added through use of pull-down menus once the model is transferred back into the ALGOR FEA Object Editor.

In order to accurately simulate the restraint at the bolt, nodes must be fixed around the edges of the bolt hole to constrain translation and rotation in all directions. A trial-and-error approach is used to monitor the restraint at the bolt holes through observation of the deformations at specific nodes. Three bolt hole restraint conditions are studied to make a comparison. The varying amounts of restrained nodes are located in a 60 degree, 90 degree and 180 degree circumference around the bolt hole as shown in Figure 4.4-1.

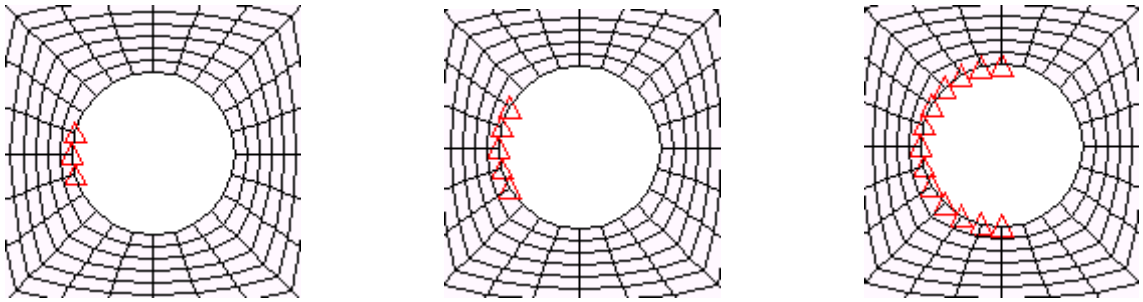

a) 60 degree restraint b) 90 degree restraint c) 180 degree restraint

Figure 4.4-1: Varying Degrees of Restraint at Bolt Hole

A nonlinear analysis is performed for each bolt condition using a 100-pound ramp load applied at the edge of the ⅜" connection plate. Once each connection has been analyzed, the displacement results are compared. Five nodes located around the bolt, indicated in Figure 4.4-2, are identified to compare the displacement of the bolt.

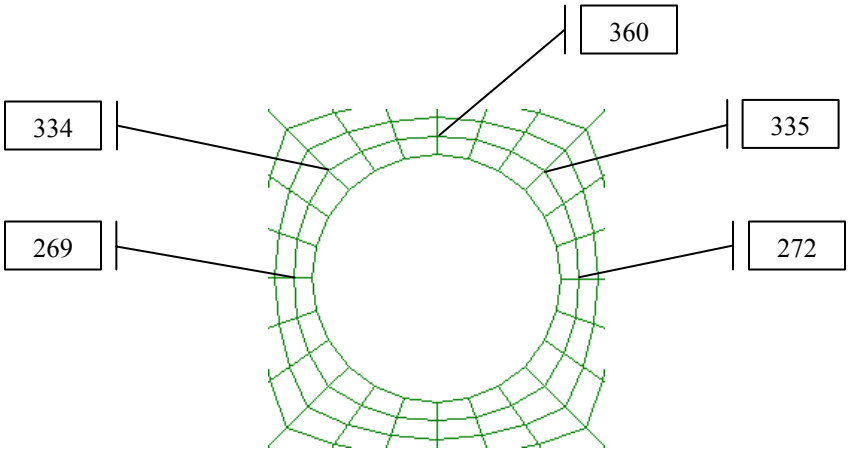

Figure 4.4-2: Nodes Used for Comparing Restraint at Bolt Hole

From the ALGOR output files, the graphs shown in Figures 4.4-3, 4.4-4 and 4.4-5 are created to compare the deformations at the five nodes for the three restraint conditions. In the 60 degree and 90 degree cases, node 269 shows minimal movement due to its direct location behind the fixed node. Nodes 334, 360, 335 and 272 exhibit a rapid increase in deflection at 0.007 seconds and 0.011 seconds for the 60 degree and 90 degree cases, respectively. The 180 degree case in Figure 4.4-5, however, depicts a gradual increase in deflection at all nodes with no excessive deformation.

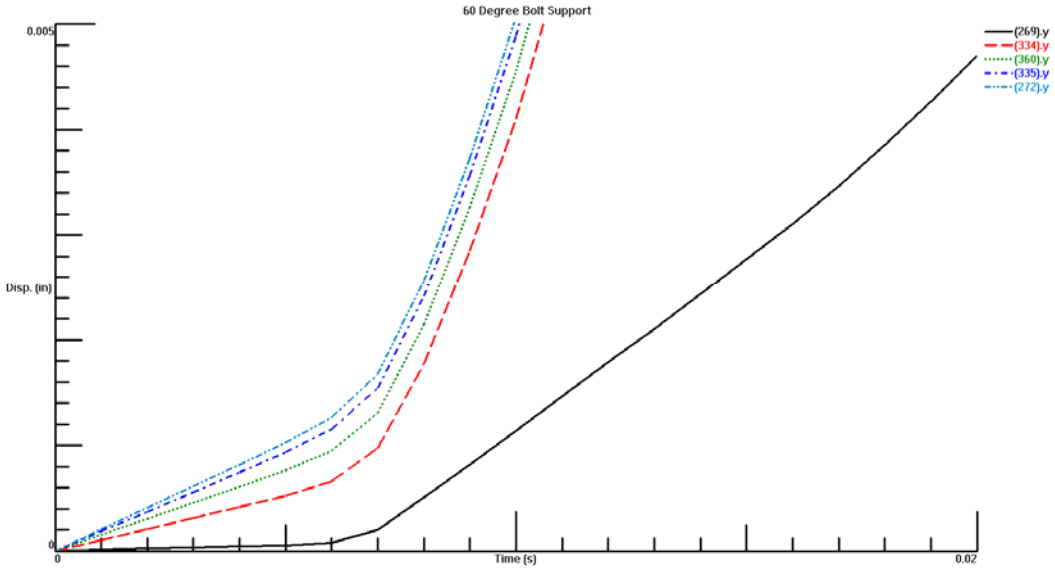

Figure 4.4-3: 60 Degree Bolt Restraint – Time vs. Displacement

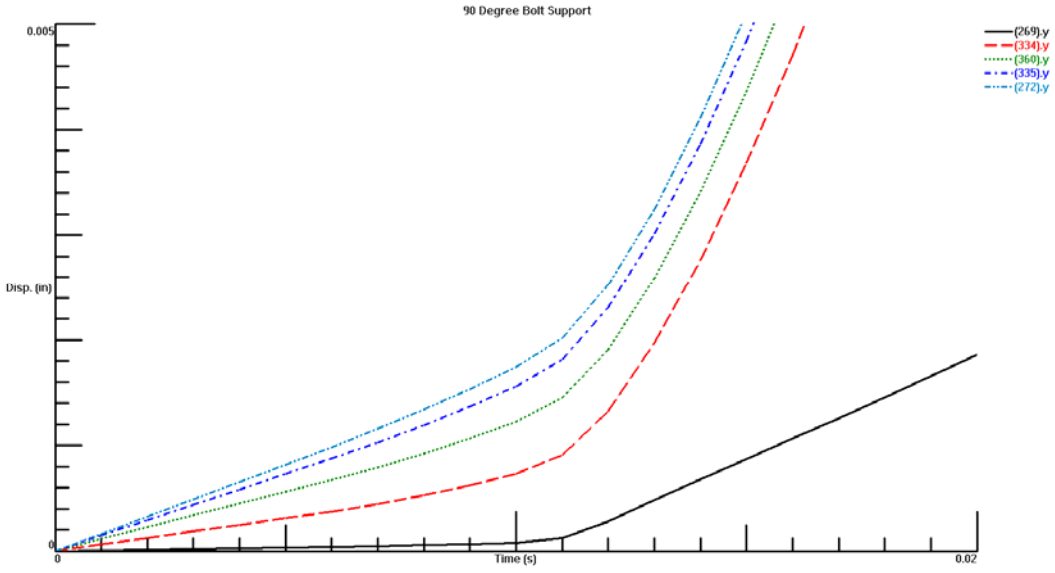

Figure 4.4-4: 90 Degree Bolt Restraint – Time vs. Displacement

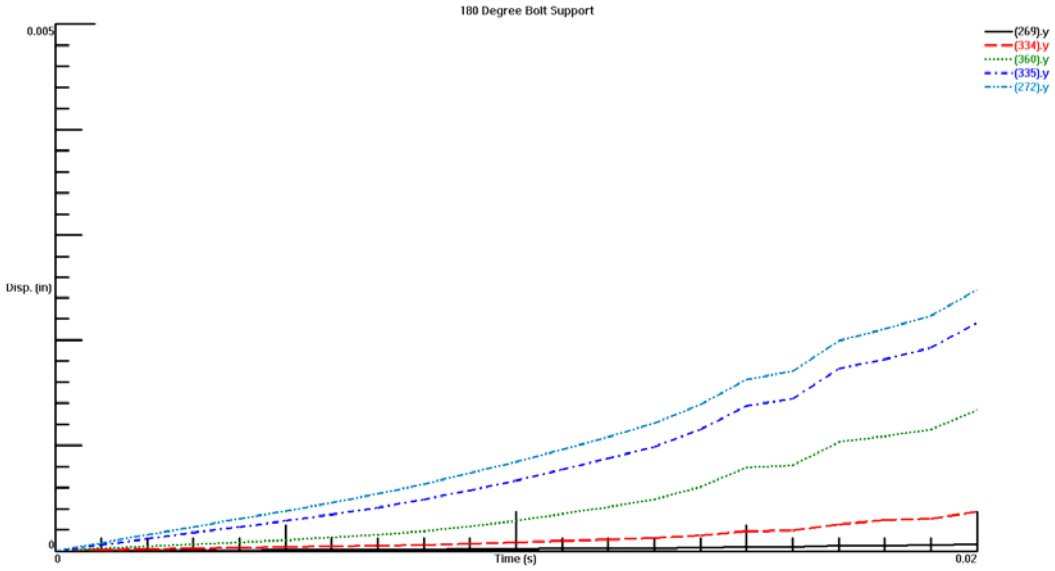

Figure 4.4-5: 180 Degree Bolt Restraint – Time vs. Displacement

From this comparison, it is determined that the most accurate approximation of the bolt is the 180 degree model. This model provides sufficient restraint to depict a bolted connection, however, minimal movement around the bolt is also seen as the yield load approaches. As a result, each connection is modeled using a similar 180 degree bolted restraint.

4.5 Applied Forces

In order to observe the behavior of the connections, external forces are applied at nodes in the model. Displacement at the nodes occurs as a result of the applied force. The amount of displacement is dependent on the geometry and material properties of the model. Other nodes adjacent to the applied force displace since the nodes are connected by the element mesh. Through this interaction, the external force affects the entire model.

Forces are applied to the model as load curves in the Global Analysis Screen in ALGOR's FEA Object Editor. The event duration and capture rate, the amount of times the results will be output, are required to develop a load curve. Ideally, the capture rate should be large enough and the time step small enough so the processor can converge on a solution. Through trial-and-error, a duration time of 0.5 seconds and a capture rate of 1000 seconds^{-1} is chosen. Loads can be applied as forces or moments at nodes in the model. To define a load curve, a load multiplier is input at a start and an end time. The multiplier corresponds to the load input as a nodal force. Numerous load curves can be applied to any model.

Typically there are two types of loads: point loads and distributed loads. Point loads are applied at individual nodes, while distributed loading is applied along a surface. Since the ALGOR program only allows nodal forces and moments, a distributed load case must be applied as fractions of the total load along the surface. A comparison is performed to determine the effect of point loads and distributed loads on the single bolt, ¼" connection model. Connection "A" is modeled using a single ramp load up to 500,000 pounds at node 297 as shown in Figure 4.5-1. Figure 4.5-2 indicates Connection "B" modeled having the 500,000 pound distributed among seven nodes. This is represented as individual ramp loads up to 71,428.5 pounds at nodes 13, 77, 170, 297, 384, 477, and 546.

Also indicated in Figures 4.5-1 and 4.5-2 are the additional nodes used for comparing the displacement due to the distributed and point loading in each case. It is important to

compare the results across the free field of the connection as well as along the face where the loads are applied. Therefore, nodes 274 and 294 are used within the free field and nodes 297, 477 and 77 are chosen along the face of the connection where the loads are applied.

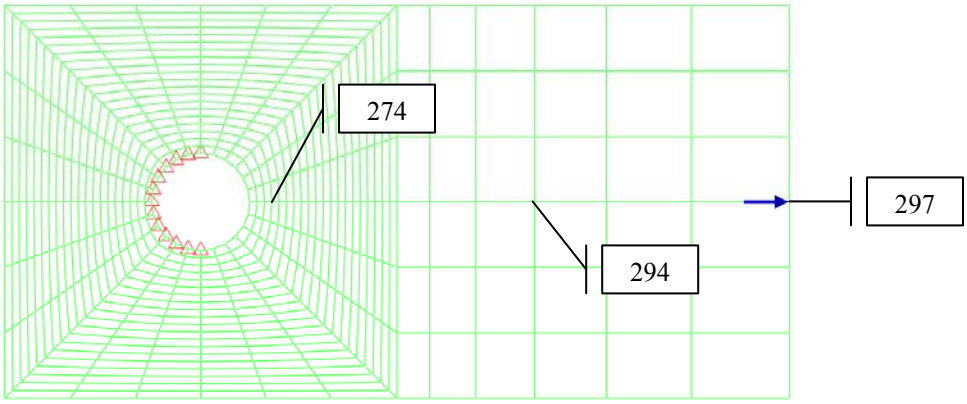

Figure 4.5-1: Connection"A" – Point Load

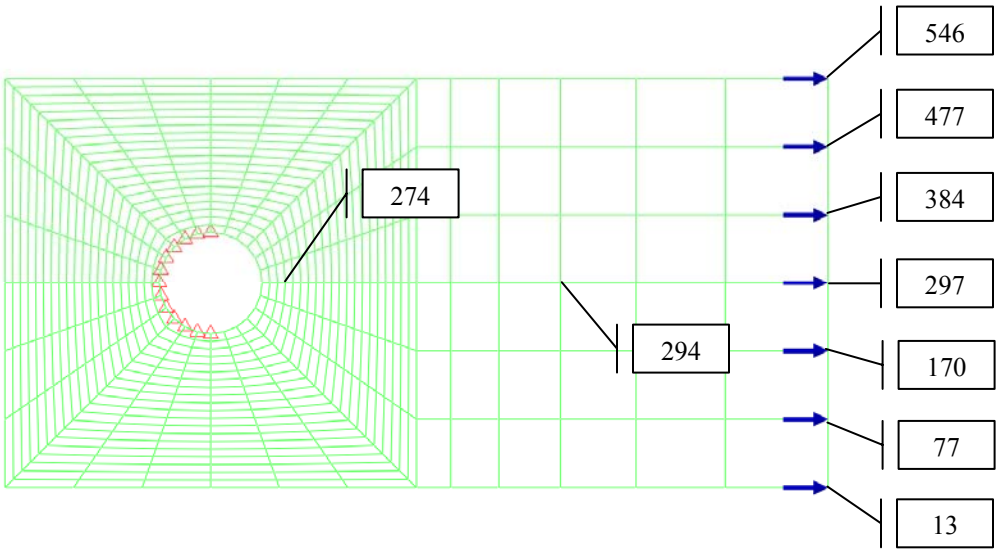

Figure 4.5-2: Connection "B" – Distributed Load

The point load and the distributed load cases are analyzed in ALGOR and the results are viewed as graphs plotting displacement against time as shown in Figures 4.5-3 and 4.5-4.

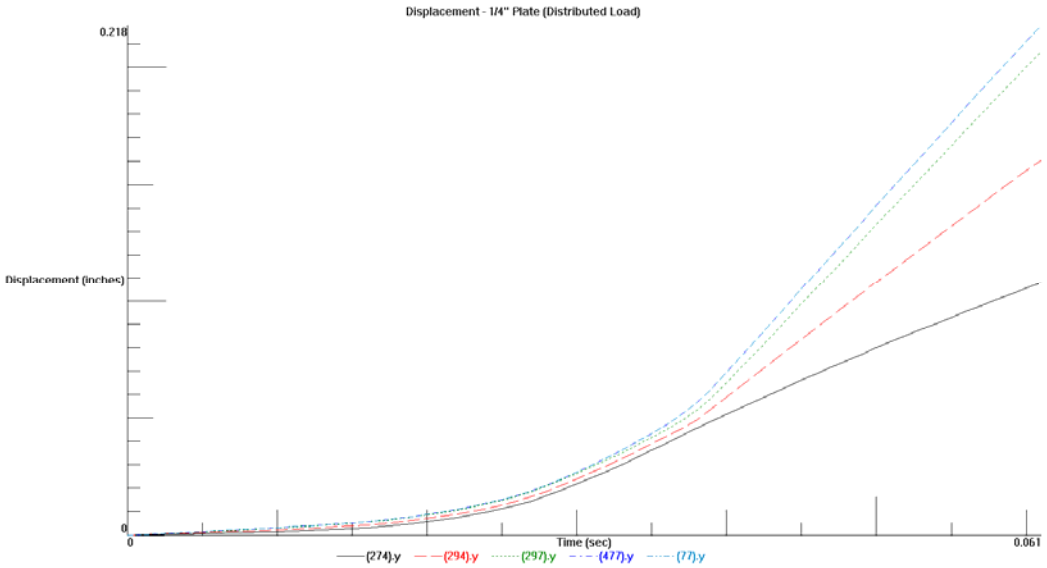

Figure 4.5-3: Displacement Results of Distributed Load

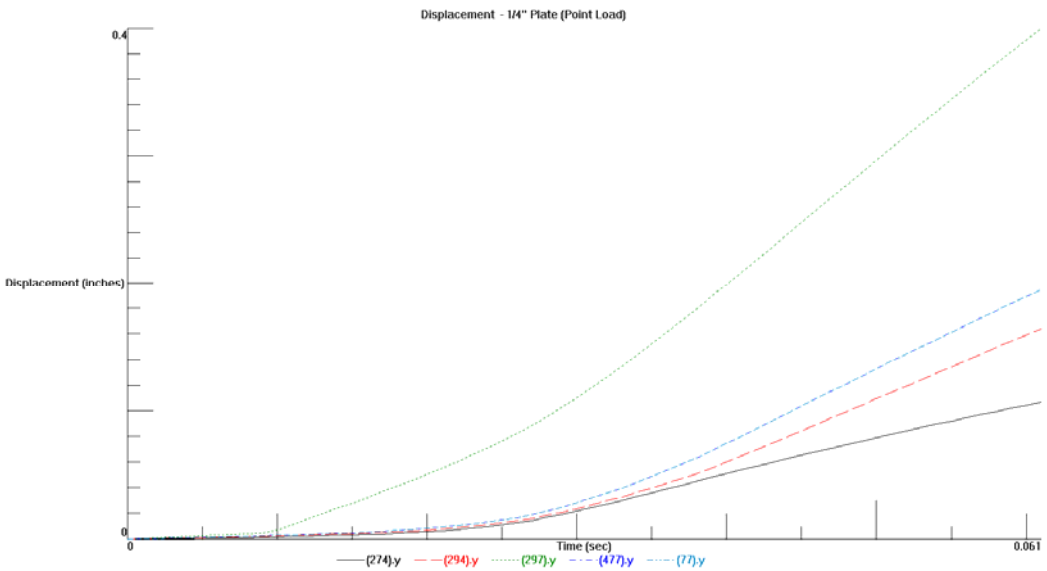

Figure 4.5-4: Displacement Results of Point Load

Using these graphs, the displacement at nodes 274, 294, 297, 477 and 77 are monitored at time step 30 and time step 60 and the results are tabulated in Tables 4.5-1 and 4.5-2 for each case. In the point load comparison, the largest displacements of 0.15 inches at time step 30 and 0.387 inches at time step 60 occur at node 297, the location of the applied external load. At time step 30, the remaining nodes have displacements within a range of 0.020 inches to 0.024 inches, a value seven times smaller than the displacement at node 297. At time step 60, the remaining nodes displace from 0.10 inches to 0.185 inches, approximately four times smaller than at node 297.

The distributed load, on the other hand, produces a relatively uniform displacement for each node at time step 30 and time step 60. The displacements of the nodes at time step 30 ranges from 0.020 inches to 0.026 inches, having a maximum deviation of 0.006 inches. The displacements of the nodes at time step 60 ranges from 0.14 inches to 0.21 inches.

Table 4.5-1: Displacement Results at Time Step 30

Node #	Point Load Displacement at Time Step 30 (inches)	Distributed Load Displacement at Time Step 30 (inches)
274	0.020	0.020
294	0.022	0.022
297	0.150	0.024
477	0.024	0.026
77	0.024	0.026

Table 4.5-2: Displacement Results at Time Step 60

Node #	Point Load Displacement at Time Step 60 (inches)	Distributed Load Displacement at Time Step 60 (inches)
274	0.100	0.140
294	0.160	0.157
297	0.387	0.200
477	0.185	0.210
77	0.185	0.210

The results tabulated show the uniformity in displacements when the loading is applied in a distributed manor rather than as a single point. The point load produces a significantly higher displacement thus skewing the displacement data adjacent to the applied load. With exception to the displacement of node 297 in the point load case, the displacement results are very similar among the two loading cases. It is apparent that reducing the load value and spreading the load out among various nodes results in more accurate deflections. For this reasoning, the external loading is applied as a distributed load for this thesis.

4.6 Applied Thermal Loading

In order to include thermal effects in the connection design, a nonlinear thermal stress analysis must be performed. This type of analysis calculates stresses in the nonlinear model due to nodal temperatures obtained from a thermal model. The thermal analysis may be performed as a steady-state heat transfer or as a transient heat transfer. A steady-state heat transfer analysis is used to determine the steady-state temperature distribution and heat flow when the temperature is independent of time. A transient heat transfer analysis determines the temperature distribution and heat flow within an object having time dependent temperature conditions.

For the computer-based simulation, the ASTM E-119 standard time-temperature curve is applied to the nonlinear model and a transient heat transfer analysis is used. In any type of heat transfer analysis, the stress model and the thermal model must be identical so the program can interpolate exactly from one model to the other. This implies that the type of elements and the number of nodes in each model remain the same, however, applied loading and stress boundary conditions may change if necessary. A transient heat transfer analysis requires that the material properties, temperature boundary conditions, initial temperatures and time-dependent heat flow characteristics be specified.

Once the thermal analysis is performed, the thermal model is converted to a nonlinear stress model using ALGOR's Mechanical Event Simulation processor. Boundary conditions, service loading and the temperature distribution output, as well as element and material information are added for the stress analysis. The final analysis provides stresses and displacements at various times and locations as a result of the combination of thermal effects and external loads induced on the connections.

4.6.1 Thermal Material Properties

Material properties for the transient heat transfer analysis are defined for each connection model. For the transient heat transfer portion of analysis, two-dimensional isotropic elements in which the thermal conductivity is constant in all directions are used. Furthermore, material properties such as thermal conductivity and specific heat are independent of temperature. A thermal conductivity value of 5.84 in·lbf/(s·in·°F) and a

specific heat of 0.172 $in^2/(s^2 \cdot °F)$ are used. Since the geometry of the element is planar, the thickness is input as ⅜, ¼, or ⅛ inch for each connection.

Under thermal conditions, the material properties for the nonlinear stress analysis are also affected. Nonlinear, two-dimensional thermoplastic elements are used where the modulus of elasticity, the thermal coefficient of expansion, and the yield stress vary with temperature. The values determined from the equations in Section 3.3 are input into ALGOR's customer-defined element material specification table. Poisson's ratio, determined by dividing the negative lateral strain by the axial strain for an axially loaded member, is input as 0.29 at each temperature. The slope of the stress versus strain curve after the point of yield, or strain hardening modulus, is entered as 1,000,000 in the table. As previously determined in Section 3.3.2, the steel properties are calculated to a temperature of 1202 °F (650 °C).

4.6.2 Thermal Boundary Conditions

Thermal boundary elements are input to the transient heat transfer model as applied temperatures. An applied temperature is used to fix a node to a specific temperature throughout the analysis. An additional node, which is held at a specified temperature, is added to the model. The heat is transferred from the new node to the node on the model through an element having a thermal stiffness. The temperature of the node on the model depends on the stiffness value. A high stiffness value will cause the temperature of the node on the model to be very close to that of the new node. For a low stiffness, the boundary element absorbs some of the heat, and the temperature of the node on the model will be significantly lower than the new node.

For an applied temperature to be used correctly, a Boundary Multiplier must be input. The product of the Multiplier and the Magnitude is the temperature value applied to the new node. Through a trial-and-error process, a temperature of 68 °F is applied to nodes 1, 70, 163, 250, 377, 470, and 534 on the connection model as shown in Figure 4.6.2-1. A stiffness value of 1000 inch-pounds per °F is used which retains the temperature at approximately 68 °F. By applying this temperature limitation to the connection, an insulated boundary condition is represented.

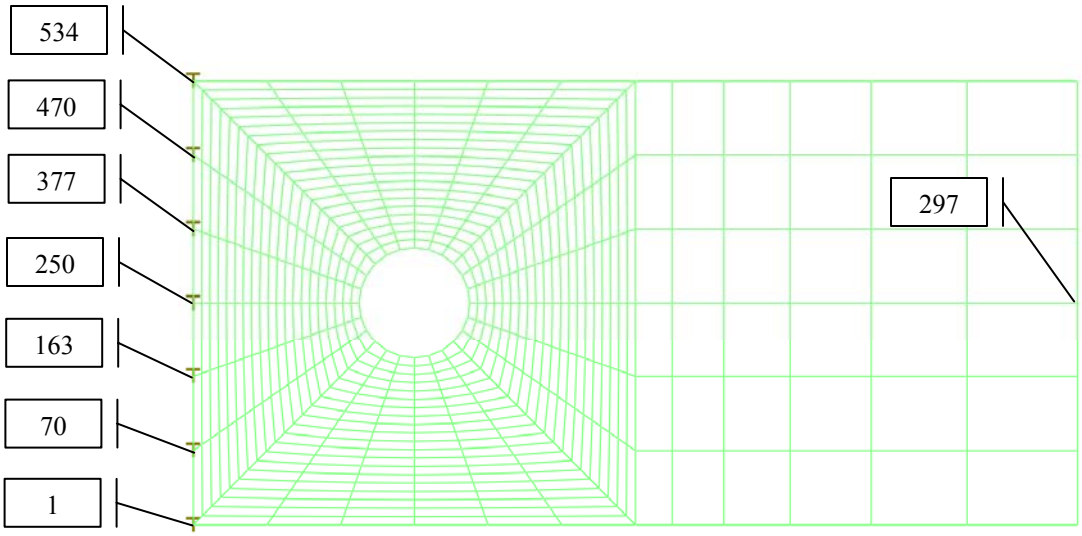

Figure 4.6.2-1: Thermal Boundary Conditions

4.6.3 Time-Temperature Curve Data

In a transient heat transfer analysis, a time-dependant temperature curve is required to apply a thermal condition to the model. The ASTM E-119 [17] time-temperature curve, as previously shown in Figure 2.1-1, is applied at node 297 to simulate conditions in a fully developed room fire. Node 297 is located at the centerline on the side of the

connection opposite the boundary condition as depicted in Figure 4.6.2-1. Upon heating the connection at this location, one assumes that the thermal activity is initiated in the span of the connecting steel member.

As the ASTM E-119 curve is applied, the steel gains internal heat causing a rise in temperature at a rapid rate. Therefore, the time it takes for the connection to reach a temperature of 1202 °F is less than the time on the actual ASTM E-119 curve due to the lack of heat escaping the system. The material thickness is also a factor in the rate of the thermal process in the connection. The ⅜ inch plate attains the temperature of 1202 °F in 276 time steps, while the ¼ inch plate and the ⅛ inch plate reach 1202 °F in 184 time steps and 92 time steps, respectively.

4.6.4 External Load Curve Data

In addition to the ASTM E-119 time-temperature curve, an external load is applied to the connection model so the temperature effects may be observed. Once the heat transfer analysis is complete, the model is converted to an MES/nonlinear stress model where the external loads are applied. For the first trial, a total distributed ramp loading of 500,000 pounds is applied similar to the normal temperature analysis. This loading, applied to nodes 13, 77, 170, 297, 384, 477 and 546, produces an error and aborts the program due to the high stresses and displacements in the model. This result indicates that the maximum ramp load must be reduced.

The second trial uses a reduced ramp load which is determined by doubling the maximum yield load obtained in the normal temperature analysis for each plate. The maximum

yield loads found for normal conditions are summarized in Table 5.3-2. The loads in this Table are doubled to achieve a failure condition for the elevated temperature analysis without overstressing the model. The ramp load for each plate begins with no load at time equals zero and ends at the maximum loads indicated in Table 4.6.4-1 for each plate thickness and configuration.

Table 4.6.4-1: Applied Ramp Loadings for Elevated Temperature Models

Connection	Max Load Used in Thermal Analysis (Pounds)
⅜" plate, single bolt	122,600
¼" plate, single bolt	81,600
⅛" plate, single bolt	40,800
⅜" plate, double bolt	229,680
¼" plate, double bolt	153,120
⅛" plate, double bolt	76,560

5.0 RESULTS

Once the connection models are created and analyzed using the ALGOR analysis processor, the analysis results can be viewed. ALGOR's Superview program serves as a comprehensive postprocessing tool to graphically examine the displacements and stresses obtained from the analysis processor. The outputs of displacements and stresses can also be viewed as data coordinates and converted into Excel worksheets. These methods, combined, facilitate presentation, review and interpretation of the results.

5.1 Definition of Offset Method

The offset method is an accepted method to define the yield strength of a ductile material where the stress on the stress-strain curve continues to increase and a definitive yield point is not reached. Due to the nonlinearity of the material and the high displacements, the offset method is used to define the yield point in this analysis since a definitive yield point cannot be obtained.

A convention has been established where a straight line is constructed parallel to the elastic portion of the stress-strain curve at some specified strain offset, usually 0.002 (or 0.2 %). The stress corresponding to the intersection of this line and the stress-strain curve as it bends over in the plastic region is defined as the yield strength.

5.2 Establishing Nodes for Comparison

Due to the extensive range of output information from ALGOR, specific nodes must be identified for comparison purposes in each connection model. In Section 3.4, three modes of failure are established based on the AISC criteria for connection design. With

these modes in mind, it is important to observe the displacements and stresses near the bolt hole and in the free field of the plate. These locations refer to the limit states of the bolt bearing capacity and yielding in the gross section. The four nodes used for comparing the results are located around the bolt hole at nodes 270 and 272 and in the free field at nodes 294 and 295 as shown in Figure 5.2-1.

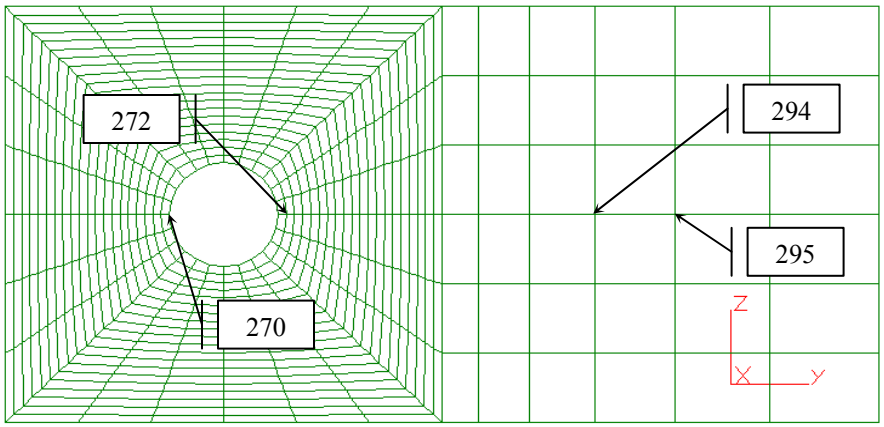

Figure 5.2-1: Node Locations Used for Evaluation

Node 270 and node 272 measure 0.80625 inches apart at the initial time step of zero seconds and are used to observe the behavior around the bolt hole. Nodes 294 and 295 are located 0.55 inches apart at time step zero and are used to observe the yielding in the gross area of the connection. As the load is applied and increased throughout the duration of the analysis, the displacements of these nodes also increased. The relative displacements between each pair of nodes are used to determine the average strains at each location throughout the analysis. The stresses at each of these nodes are also recorded and observed at each time step to create the stress strain diagrams.

5.3 Connection Results at Normal Temperatures

The results of each connection for normal temperatures are presented herein through use of the Excel program. The stresses and displacement are imported from ALGOR into an Excel spreadsheet to easily view the results. The average strain values at each step of the analysis are computed by dividing the change in distance between a pair of nodes, ΔL, by the initial length, L_o, at time zero. The initial length, L_o, is 0.80625 inches for nodes 270 and 272 and 0.55 inches for nodes 294 and 295 as discussed in Section 5.2. The Excel spreadsheet showing the computed average strain and the nodal stresses from the finite element analysis at each time step are provided for the ⅜ inch, ¼ inch and ⅛ inch single and double bolt shear connections in Appendix B.

Graphs of the calculated average strain versus the computed nodal stress from the finite element analysis are then created for each connection. Figure 5.3-1 and Figure 5.3-2 indicate the stress-strain diagrams for the ⅜ inch, ¼ inch and ⅛ inch single bolt connections at nodes 270-272 and 294-295, respectively. Using the offset method established in Section 5.1 a 0.2% offset strain, indicated as a parallel line to the initial curve on the stress-strain diagram, is also indicated on the stress-strain diagrams. A similar graphical presentation is provided for the double bolt connection, and the results are shown in Figures 5.3-3 and 5.3-4.

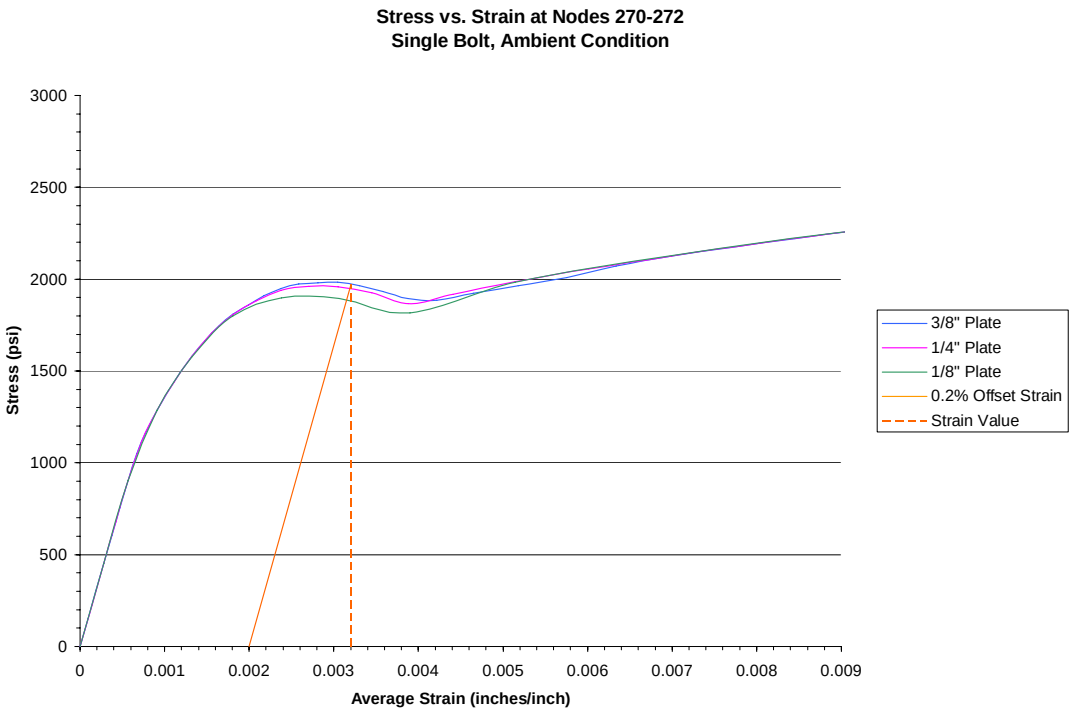

Figure 5.3-1: Stress vs. Strain Diagram Nodes 270 and 272, Single Bolt Connection

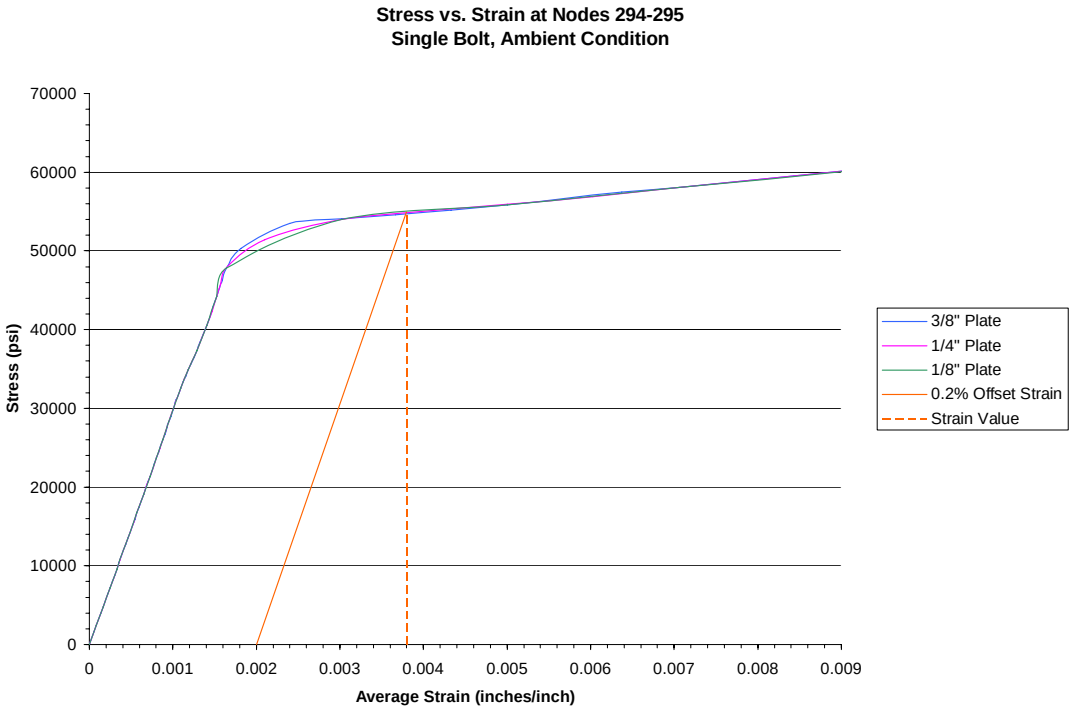

Figure 5.3-2: Stress vs. Strain Diagram Nodes 294 and 295, Single Bolt Connection

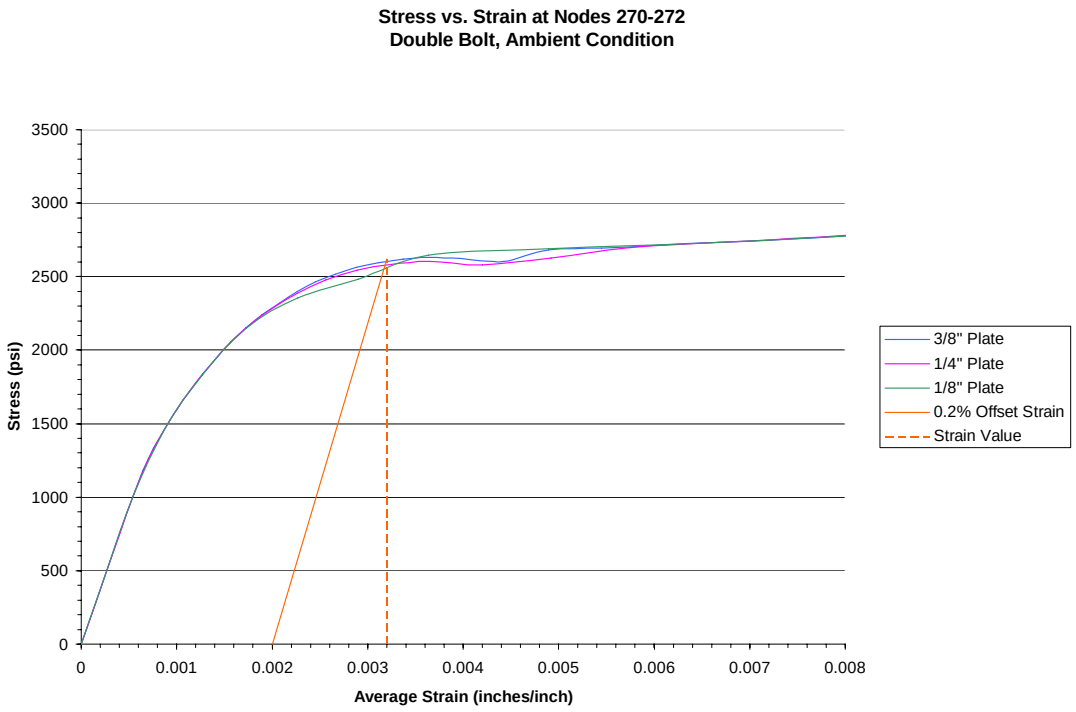

Figure 5.3-3: Stress vs. Strain Diagram Nodes 270 and 272, Double Bolt Connection

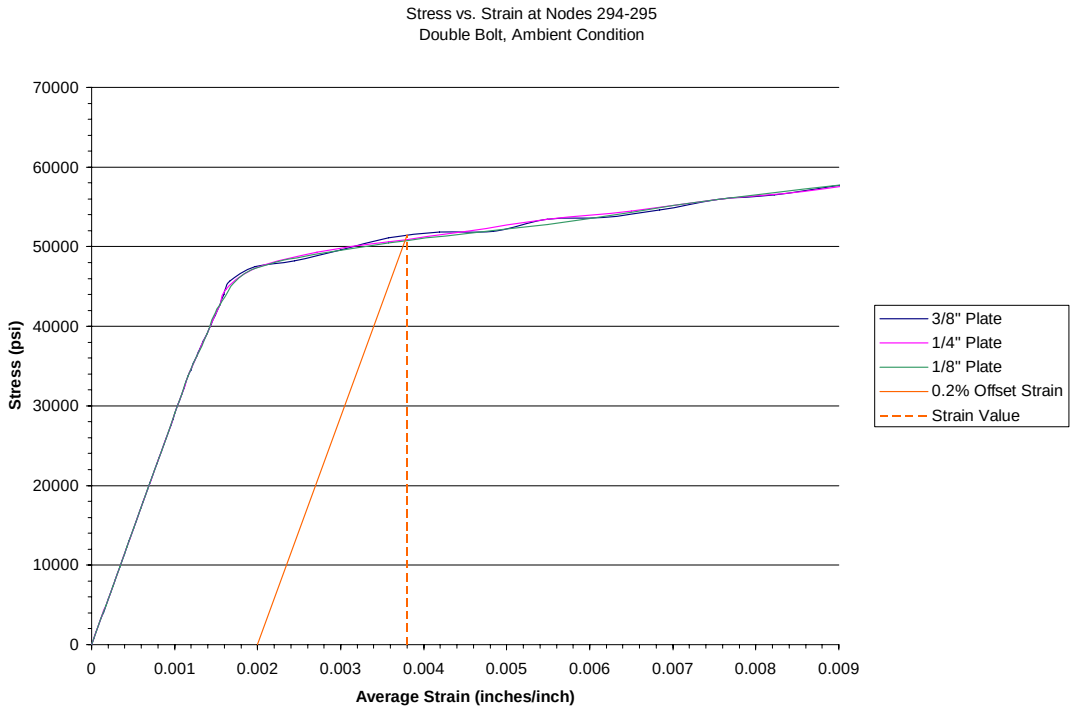

Figure 5.3-4: Stress vs. Strain Diagram Nodes 294 and 295, Double Bolt Connection

An offset strain value of 0.0032 inches/inch is observed from Figures 5.3-1 (single bolt condition) and 5.3-3 (double bolt condition) at nodes 270 and 272. The stress-strain diagram for nodes 294 and 295 produces an offset strain value of 0.0037 inches per inch for the ⅜ inch, ¼ inch and ⅛ inch single and double bolt connections. In both cases, it is important to note that the initial curve for each connection thickness is similar, therefore resulting in the same offset strain value.

Once the offset strain values are established from the stress-strain diagrams, graphs are created to determine the load at which yielding occurs. Figures 5.3-5 and 5.3-6 represent graphs of the load versus average strain at nodes 270 and 272 for the single and double bolt connections, respectively. The offset strain value, indicated as a horizontal line, is plotted on the graph. This line is then used to determine the load at which yielding occurs for each connection. Similar graphical analyses are shown in Figures 5.3-7 and 5.3-8 for nodes 295 and 294.

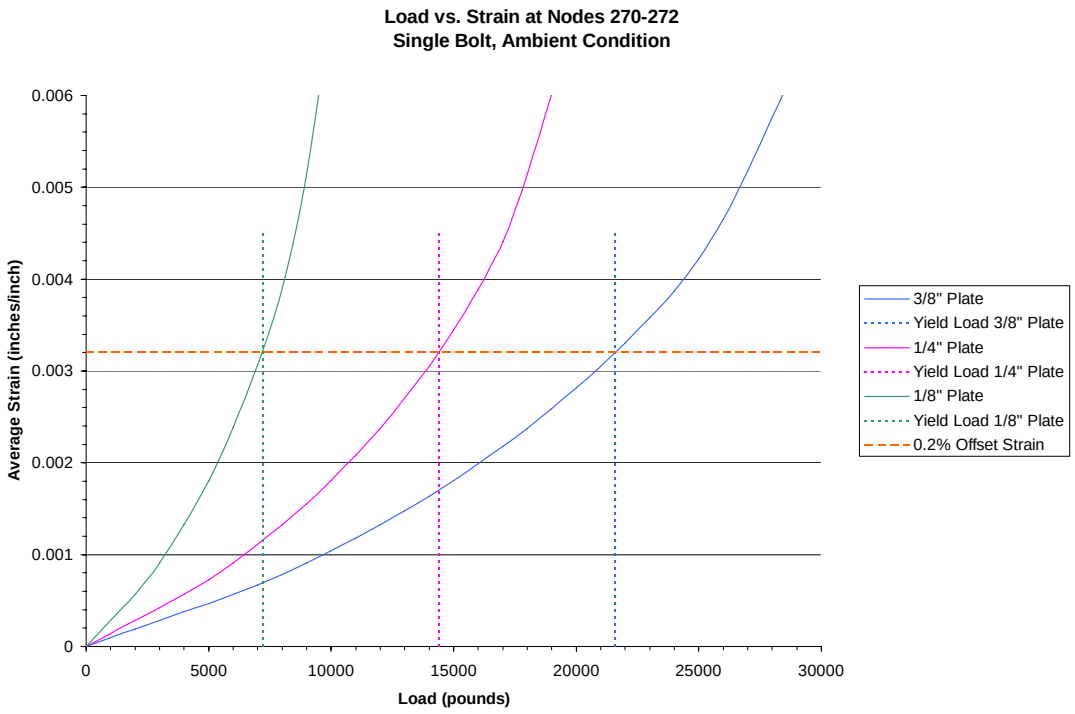

Figure 5.3-5: Load vs. Average Strain Diagram at Nodes 270 and 272, Single Bolt Connection

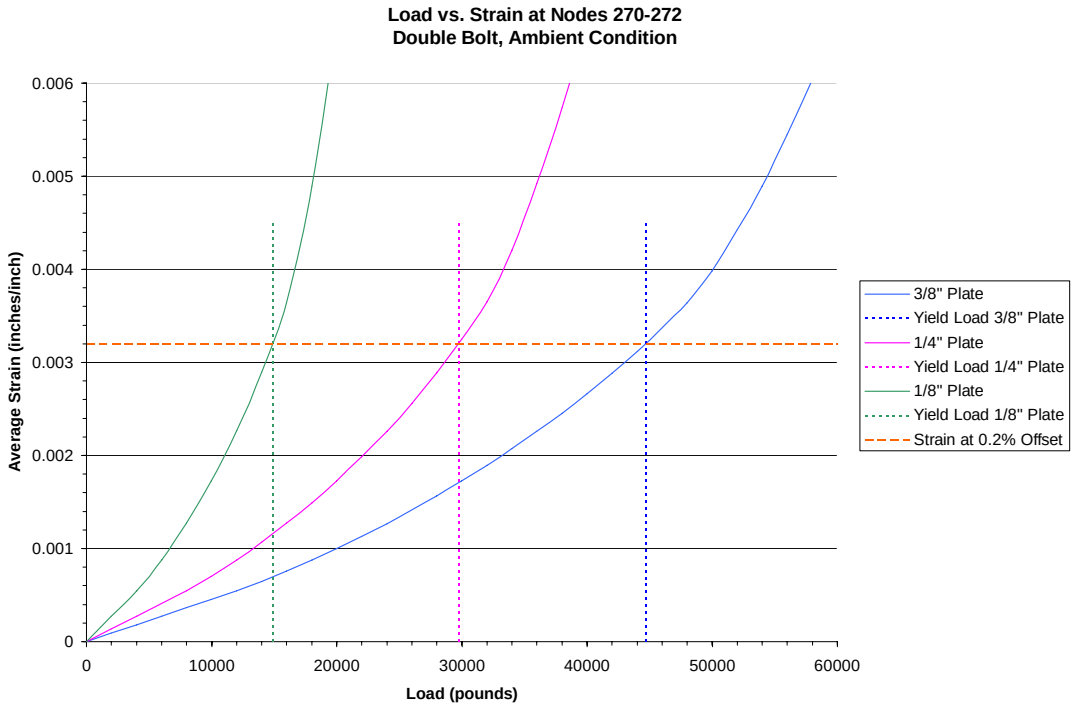

Figure 5.3-6: Load vs. Average Strain Diagram at Nodes 270 and 272, Double Bolt Connection

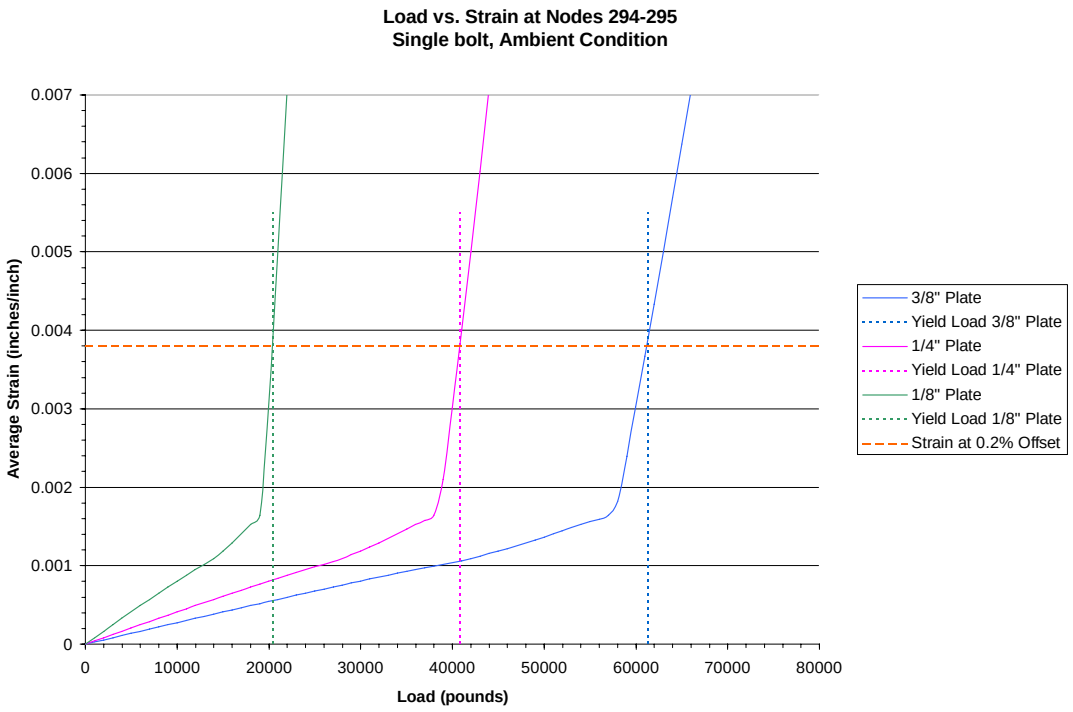

Figure 5.3-7: Load vs. Average Strain Diagram at Nodes 294 and 295, Single Bolt Connection

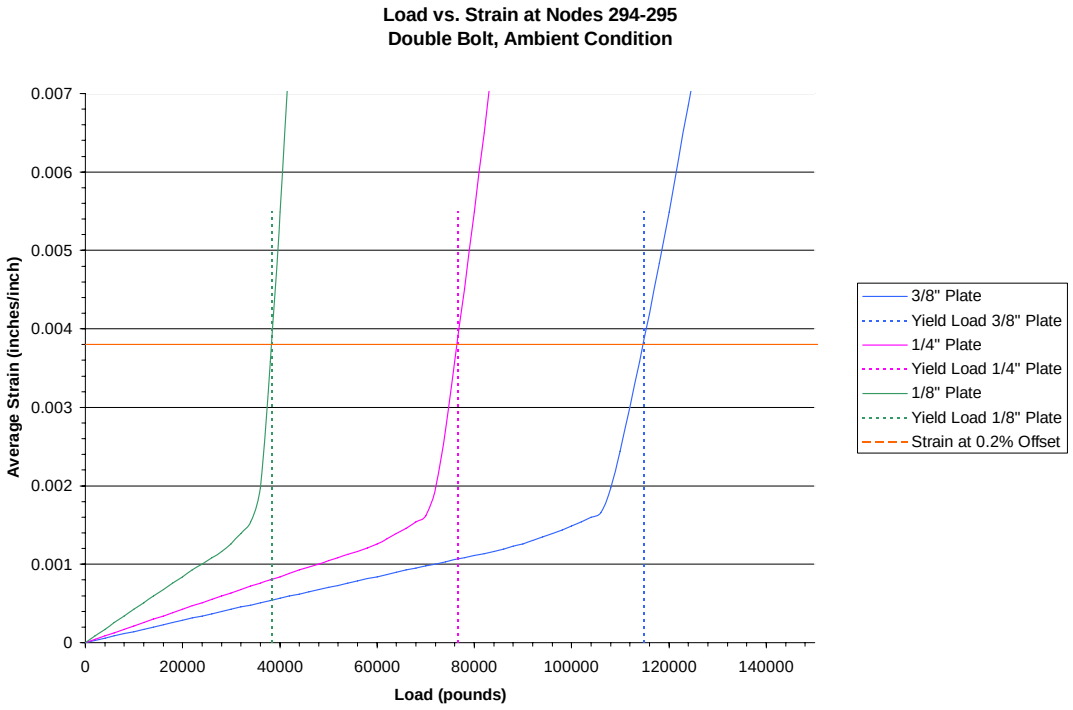

Figure 5.3-8: Load vs. Average Strain Diagram Nodes at 294 and 295, Double Bolt Connection

A summary of the yield loads derived from the finite element analysis for each connection thickness and bolting condition is provided in Tables 5.3-1 and 5.3-2 in the vicinity of the bolt hole and in the free field of the plate.

Table 5.3-1: Summary of Yield Loads at Bolt Hole at Normal Temperatures

Connection	Yield Load (Pounds)
⅜" plate, single bolt	21,600
¼" plate, single bolt	14,400
⅛" plate, single bolt	7,200
⅜" plate, double bolt	44,700
¼" plate, double bolt	29,800
⅛" plate, double bolt	14,900

Table 5.3-2: Summary of Yield Loads in Free Field at Normal Temperatures

Connection	Yield Load (Pounds)
⅜" plate, single bolt	61,300
¼" plate, single bolt	40,800
⅛" plate, single bolt	20,400
⅜" plate, double bolt	114,840
¼" plate, double bolt	76,560
⅛" plate, double bolt	38,280

5.4 Connection Results at Elevated Temperatures

Similar to the results at normal temperatures, the stresses and displacements for the thermal connections are imported from ALGOR and presented through use of the Excel program. Again, nodes 270 and 272 are used for investigation in the vicinity of the bolt hole and nodes 294 and 295 are used to study response in the gross cross-sectional area of the plate.

As in the normal temperature analysis, the average strain values at each step of the analysis are computed by dividing the change in distance of the nodes, ΔL, by the initial length, L_o, at time zero. The initial length, L_o, is 0.80625 inches for nodes 270 and 272 and 0.55 inches for nodes 294 and 295. The Excel spreadsheets indicating the computed average strains and the nodal stresses from the finite element analysis at each time step are provided for the ⅜ inch, ¼ inch and ⅛ inch single and double bolt connections in Appendix C.

Graphs of the calculated average strain versus the nodal stress computed from the finite element analysis are then created for each connection. Figure 5.4-1 and Figure 5.4-2 indicate the stress-strain diagrams for the ⅜ inch, ¼ inch and ⅛ inch single bolt connections at nodes 270 and 272 and nodes 294 and 295, respectively. Similarly, Figures 5.4-3 and 5.4-4 show the stress-strain diagrams for the double bolt connections. Due to the temperature increase in the connection models, the initial data points are not uniform as observed under normal conditions. Therefore, a curve is superimposed to normalize the data for the stress-strain curve as shown in the figures. The 0.2% offset line is shown parallel to the normalized curve to determine the yield strain as well.

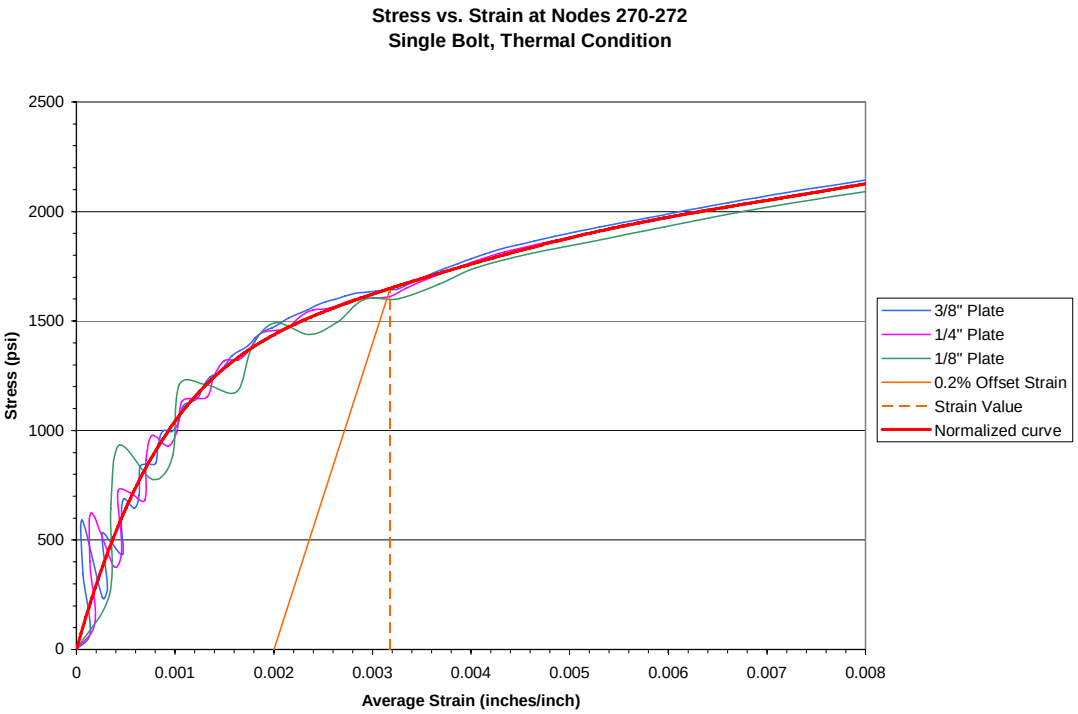

Figure 5.4-1: Stress vs. Strain Diagram at Nodes 270 and 272, Single Bolt Connection

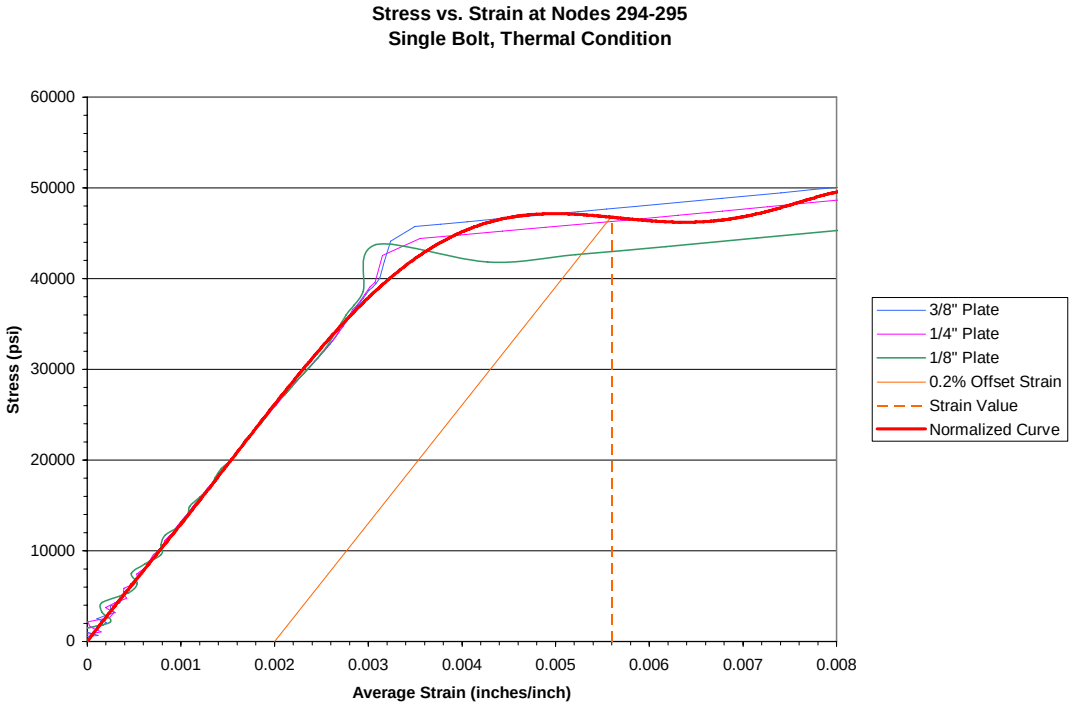

Figure 5.4-2: Stress vs. Strain Diagram at Nodes 294 and 295, Single Bolt Connection

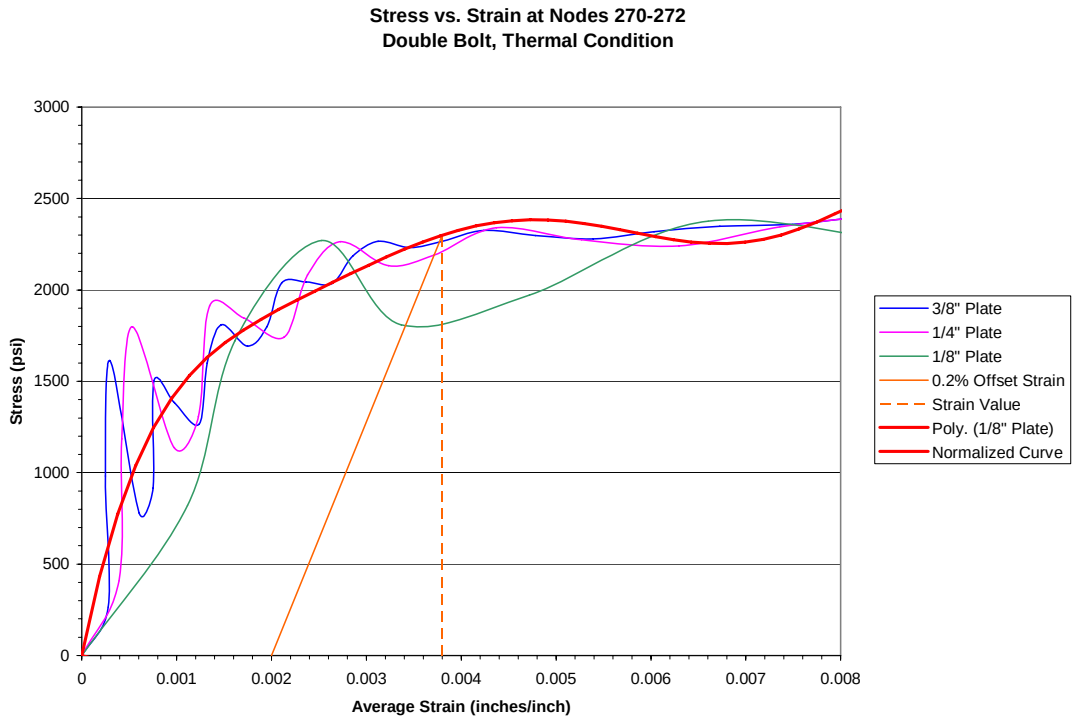

Figure 5.4-3: Stress vs. Strain Diagram at Nodes 270 and 272, Double Bolt Connection

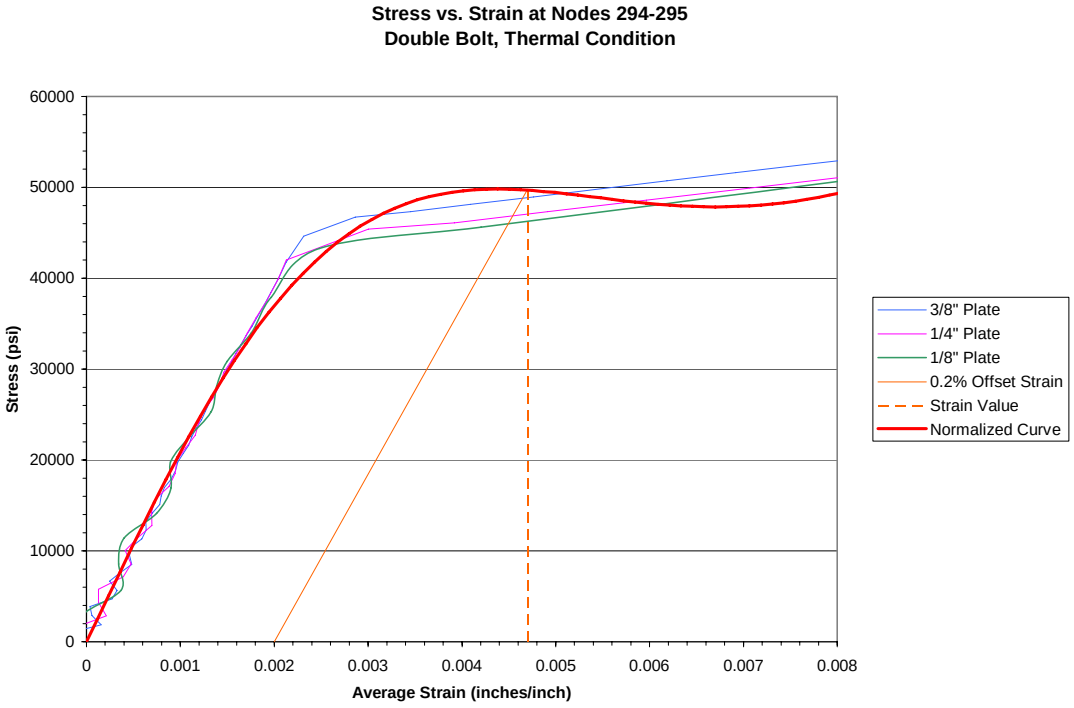

Figure 5.4-4: Stress vs. Strain Diagram at Nodes 294 and 295, Double Bolt Connection

An offset strain value of 0.00318 inches per inch is observed from Figure 5.4-1 for the elevated temperature, single bolt connection at nodes 270 and 272. The stress-strain diagram for the double bolt connection at the same location produces an offset strain of 0.0038 inches per inch. The elevated temperature stress-strain diagrams for nodes 294 and 295 produce an offset strain value of 0.0056 inches per inch for the single bolt connection and a strain value of 0.0047 inches per inch for the double bolt connection. Unlike the normal temperature models, the offset strain values vary between the single and double bolt connections at elevated temperatures.

Once the offset strain values are established from the stress-strain diagrams, graphs are created to determine the load at which yielding occurs. Figures 5.4-3 and 5.4-4 represent graphs of the load versus average strain at nodes 270 and 272 and at nodes 294 and 295, respectively for the single bolt connection. The load capacities for the double bolt connections are shown in Figures 5.4-5 and 5.4-6. The offset strain value, indicated as a horizontal line, is plotted on the graph. This line is then used to determine the load at which yielding occurs for each connection.

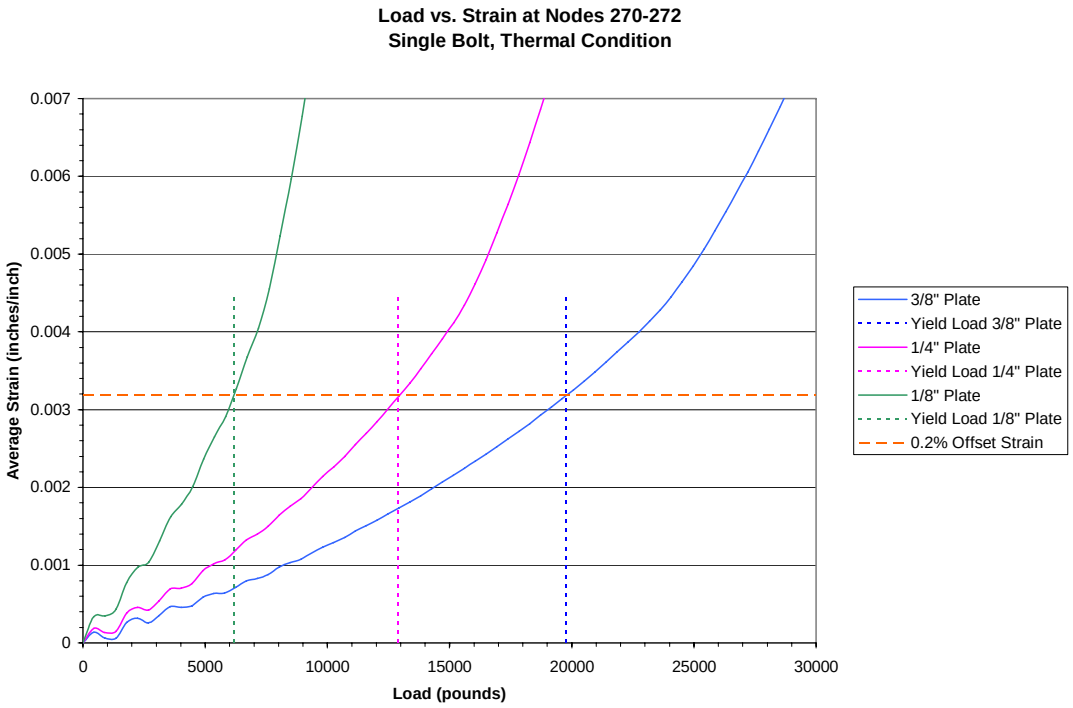

Figure 5.4-5: Load vs. Average Strain Diagram at Nodes 270 and 272, Single Bolt Connection

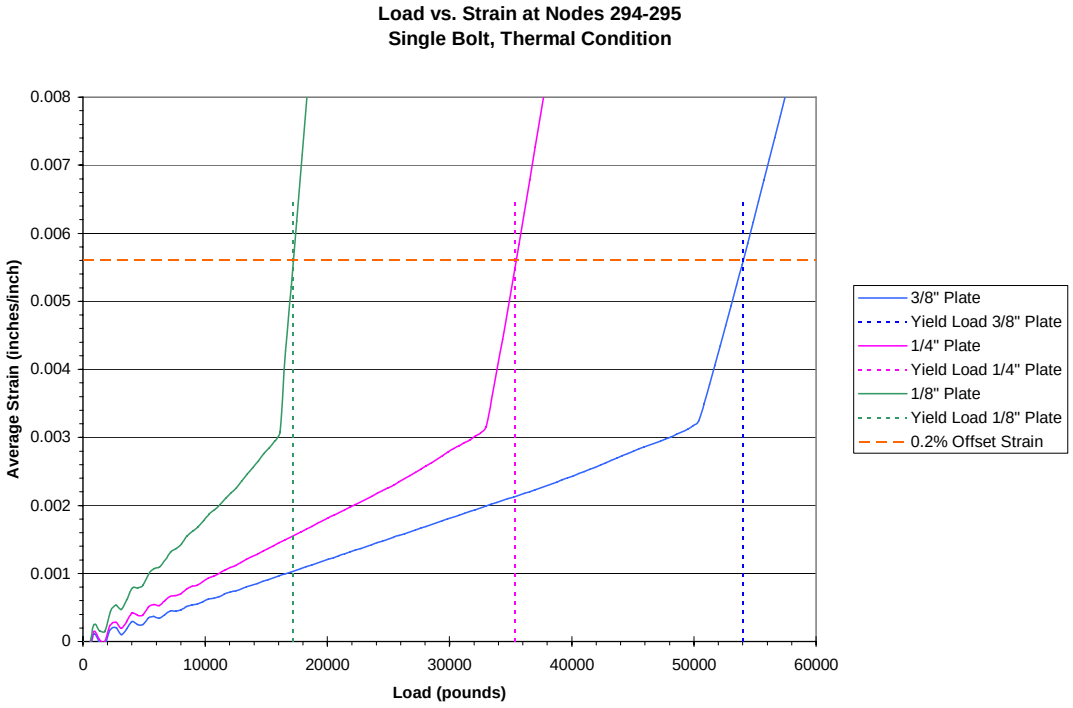

Figure 5.4-6: Load vs. Average Strain Diagram at Nodes 294 and 295, Single Bolt Connection

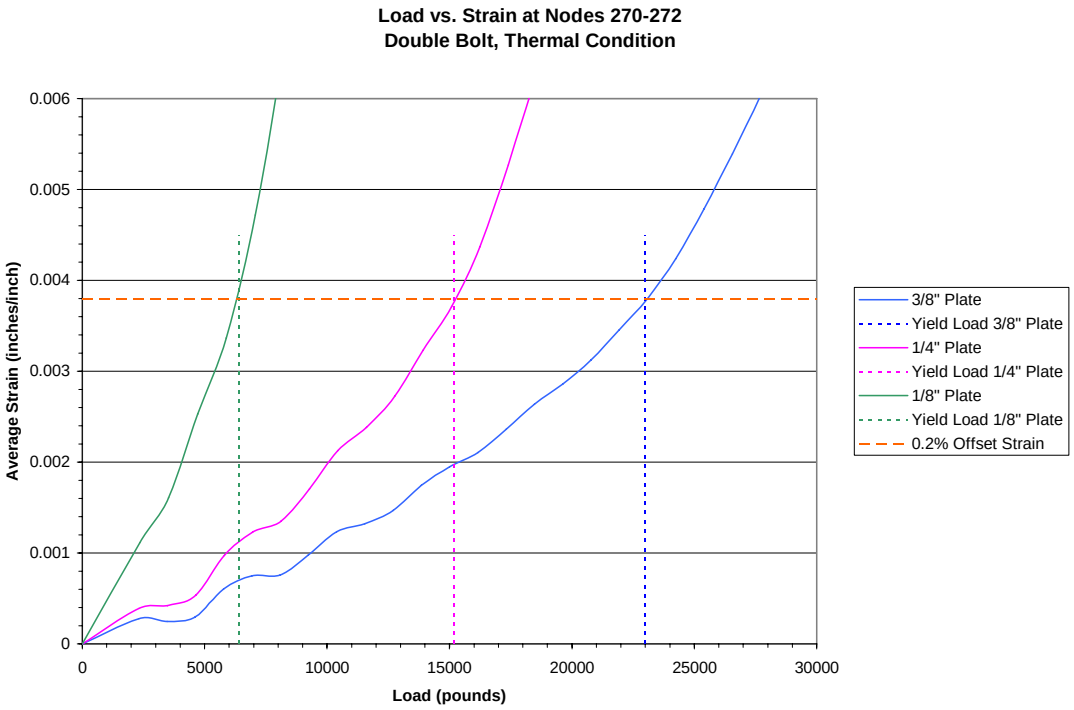

Figure 5.4-7: Load vs. Average Strain Diagram at Nodes 270 and 272, Double Bolt Connection

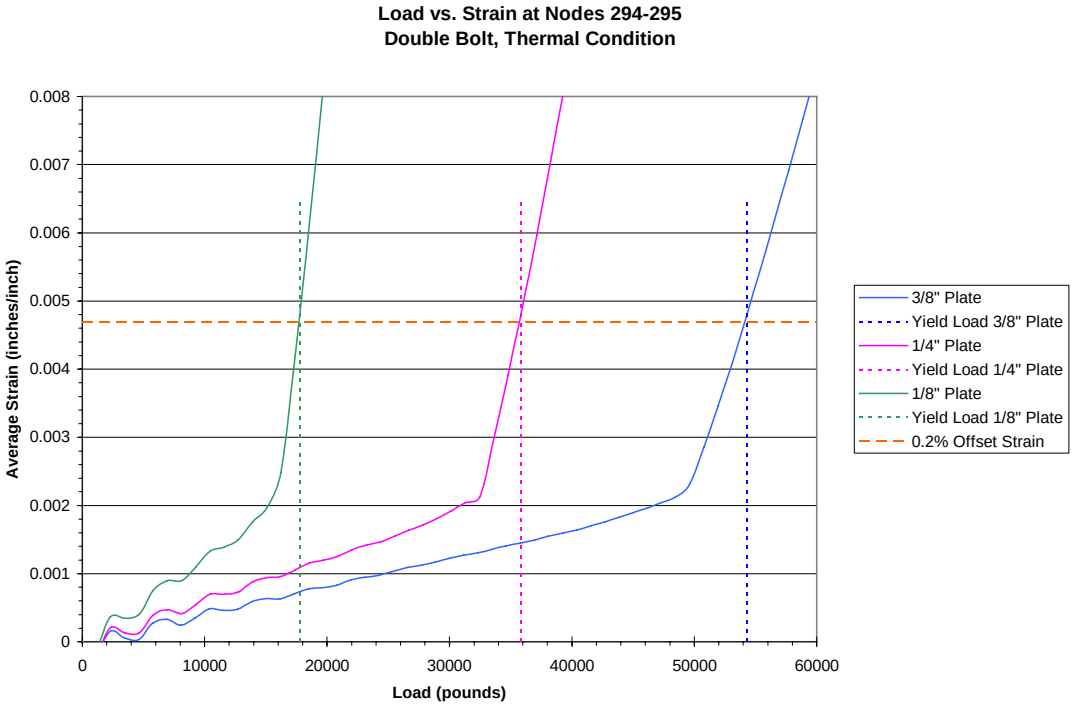

Figure 5.4-8: Load vs. Average Strain Diagram at Nodes 294 and 295, Double Bolt Connection

A summary of the yield loads derived from the elevated temperature finite element analysis for each connection thickness is provided in Tables 5.4-1 and 5.4-2 at each node location under observation.

Table 5.4-1: Summary of Yield Loads at Bolt Hole at Elevated Temperatures

Connection	Yield Load (Pounds)
⅜" plate, single bolt	19,750
¼" plate, single bolt	12,900
⅛" plate, single bolt	6,200
⅜" plate, double bolt	23,000
¼" plate, double bolt	15,200
⅛" plate, double bolt	6,400

Table 5.4-2: Summary of Yield Loads in Free Field at Elevated Temperatures

Connection	Yield Load (Pounds)
⅜" plate, single bolt	54,000
¼" plate, single bolt	35,400
⅛" plate, single bolt	17,200
⅜" plate, double bolt	54,300
¼" plate, double bolt	35,800
⅛" plate, double bolt	17,800

6.0 EVALUATION OF RESULTS

Now that the results have been presented, several comparisons can be performed to determine the behavior of the connections at elevated temperatures. First, the ALGOR results at normal temperatures are compared to the design values determined using the AISC Specifications. The specific point of interest is the accuracy of the results from the finite element computer analysis versus the values determined using the Chapter J equations in the Specification for Structural Steel Buildings. The second part of the evaluation compares the elevated temperature results against the same design values from the Specifications. Comparisons of the varying plate thicknesses and the bolting conditions provide further insight into the behavior of steel connections.

6.1 ALGOR Results at Normal Temperatures versus AISC Design Values

The ALGOR model compared against the AISC design values at normal temperatures is important to determine the accuracy of the computer modeling software. It validates the results for the second part of the analysis which is performed at elevated temperatures. It was determined in Section 3.4 that the ASD design equations produced capacities that were approximately 33 percent lower than the LRFD design equations. The ASD approach is known to be more conservative due to the higher safety factors and this is demonstrated in the results. The following tables provide a side by side comparison of the yield load values obtained for the bearing at the bolt and the yielding in the gross section at normal temperatures.

Table 6.1-1 presents the load capacities obtained using the LRFD and ASD design equations for the bearing at the bolt hole as well as the capacities determined from the

ALGOR model at nodes 270 and 272. These tabulated results indicate that the finite element model produces a bolt bearing capacity approximately 14 percent lower than the LRFD design approach. The ALGOR model results in capacities 30 percent higher than the ASD design equations.

Table 6.1-1: Comparison of Bolt Bearing Capacities at Normal Temperatures

Connection	LRFD Load (Pounds)	ASD Load (Pounds)	ALGOR Load (Pounds)
⅜" plate, single bolt	24,700	16,500	21,600
¼" plate, single bolt	16,500	11,000	14,400
⅛" plate, single bolt	8,200	5,500	7,200
⅜" plate, double bolt	49,400	32,900	44,700
¼" plate, double bolt	32,900	21,900	29,800
⅛" plate, double bolt	16,500	11,000	14,900

Table 6.1-2 provides the capacity values for yielding in the gross section. Results are provided for the two AISC design approaches and the computer model at nodes 294 and 295. The ALGOR model produces capacities approximately 20 percent higher than the LRFD approach and 45 percent higher than the ASD design equations.

Table 6.1-2: Comparison of Yielding In the Gross Section Capacities at Normal Temperatures

Connection	LRFD Load (Pounds)	ASD Load (Pounds)	ALGOR Load (Pounds)
⅜" plate, single bolt	50,600	33,700	61,300
¼" plate, single bolt	33,800	22,500	40,800
⅛" plate, single bolt	16,900	11,200	20,400
⅜" plate, double bolt	101,300	67,400	114,840
¼" plate, double bolt	67,500	44,900	76,560
⅛" plate, double bolt	33,800	22,500	38,280

Overall, the computer results are within 20 percent of the LRFD design equations and within 45 percent of the ASD equations. Since safety factors are not applied to the computer model, the capacities in general, are higher than both design approaches. The

safety factors indicate a conservatism that is typical in design. The ALGOR model proves to be relatively accurate and representative of the connections, therefore, it can be used as a basis to evaluate the behavior at elevated temperatures.

6.2 ALGOR Results at Elevated Temperatures versus AISC Design Values

Similar to the normal temperature results, the elevated temperature results are compared to the LRFD and ASD design values derived from application of the Specification for Structural Steel Buildings. Nodes 270 and 272 are used as comparison against the bolt bearing capacity, and nodes 294 and 295 are compared against the capacity for yielding in the gross section.

Table 6.2-1 summarizes the finite element model results at elevated temperatures versus the LRFD and ASD equation results for the bolt bearing capacity as determined in Section 3.4. In this comparison, the LRFD equations produce a capacity 30 percent higher than the computer model, however, the ASD equations remain lower by approximately 20 percent. It is apparent from the finite element modeling that there is a reduction in capacity when temperatures of the steel are elevated.

Table 6.2-1: Comparison of Bolt Bearing Capacities at Elevated Temperatures

Connection	LRFD Load (Pounds)	ASD Load (Pounds)	ALGOR Load (Pounds)
⅜" plate, single bolt	24,700	16,500	19,750
¼" plate, single bolt	16,500	11,000	12,900
⅛" plate, single bolt	8,200	5,500	6,200
⅜" plate, double bolt	49,400	32,900	23,000
¼" plate, double bolt	32,900	21,900	15,200
⅛" plate, double bolt	16,500	11,000	6,400

Table 6.2-2 provides a similar summary of the results for the yielding in the gross capacities. The computer model produces yielding within 6 percent of the LRFD equation and within 35 percent of the ASD equation.

Table 6.2-2: Comparison of Yielding In the Gross Section Capacities at Elevated Temperatures

Connection	LRFD Load (Pounds)	ASD Load (Pounds)	ALGOR Load (Pounds)
⅜" plate, single bolt	50,600	33,700	54,000
¼" plate, single bolt	33,800	22,500	35,400
⅛" plate, single bolt	16,900	11,200	17,200
⅜" plate, double bolt	101,300	67,400	54,300
¼" plate, double bolt	67,500	44,900	35,800
⅛" plate, double bolt	33,800	22,500	17,800

It is observed that the elevated temperature computer model produces lower capacities than the normal temperature condition, and these capacities are closer to the design values in the Steel Construction Manual where safety factors have been applied to the results. The following Section will further investigate the normal temperature model and the high temperature model.

6.3 Normal Temperature Model versus Elevated Temperature Model

Now that the computer model has proven to be reasonably accurate against the AISC design equations, the ALGOR models can be examined to determine the reduction in strength due to increases in temperature. Table 6.3-1 provides the capacities, as determined from the stress-strain curves of the finite element models in Chapter 5, of the bearing at the bolt hole at normal temperatures and at elevated temperatures.

Table 6.3-1: Bearing at Bolt Hole Capacities at Normal and Elevated Temperatures, Based on ALGOR Model

Connection	Capacity at Normal Temp. (Pounds)	Capacity at Elevated Temp. (Pounds)	Reduction in Capacity (%)
⅜" plate, single bolt	21,600	19,750	9%
¼" plate, single bolt	14,400	12,900	10%
⅛" plate, single bolt	7,200	6,200	14%
⅜" plate, double bolt	44,700	23,000	48%
¼" plate, double bolt	29,800	15,200	49%
⅛" plate, double bolt	14,900	6,400	57%

The single bolt connection indicates a strength reduction of 9 percent to 14 percent for the three connection thicknesses due to the bolt bearing capacity at elevated temperatures. The elevated temperature model for the double bolt connection produced a bolt bearing capacity 48 percent to 57 percent less than the normal temperature model. A reduction in the capacity is expected at high temperatures; however, these results indicate that the double bolt model loses half of its capacity when elevated to high temperatures.

Similar observations are made in the free field of the connection model. Table 6.3-2 summarizes the capacities found using the ALGOR models at normal and at elevated temperatures for the yielding in the gross cross-sectional area.

Table 6.3-2: Yielding in the Gross Section Capacities at Normal and Elevated Temperatures, Based on ALGOR Model

Connection	Capacity at Normal Temp. (Pounds)	Capacity at Elevated Temp. (Pounds)	Reduction in Capacity (%)
⅜" plate, single bolt	61,300	54,000	12%
¼" plate, single bolt	40,800	35,400	13%
⅛" plate, single bolt	20,400	17,200	15%
⅜" plate, double bolt	114,840	54,300	53%
¼" plate, double bolt	76,560	35,800	53%
⅛" plate, double bolt	38,280	17,800	53%

From these results, the elevated temperature model of the single bolt connection produces an anticipated yield load 12 percent to 15 percent lower than the single bolt connection at normal temperatures. Similar to the study at the bolt hole, the double bolt connection loses 53 percent of the capacity when subjected to high temperatures.

The results of the double bolt connection under elevated temperatures are surprising. Since the double bolt connection models produced approximately twice the capacity at normal temperatures, this result was expected for the high temperature model as well. The loss of half of the capacity is significant and may have resulted due to high stresses According to these results, the single and double bolt connections have essentially the same capacities at elevated temperatures.

Through correlation of the offset strain values, the temperatures at which the strength reduction begins to occur can also be determined. Recall that the single bolt connection produces an offset strain of 0.00318 inches per inch for the bearing at the bolt and 0.0056 inches per inch for the yielding in the gross section. For each plate thickness, the offset strain of 0.00318 inches per inch corresponds to a temperature at the bolt hole of 125 degrees Fahrenheit. In the free field of the plate, the offset strain is associated with a temperature of 365 degrees Fahrenheit for all three plates. Offset strains of 0.0038 inches per inch and 0.0047 inches per inch are found for the bearing at the bolt and yielding in the gross section, respectively. These strains correspond to yield temperatures for the three plate thicknesses of 98 degrees Fahrenheit in the vicinity of the bolt and 183 degrees Fahrenheit in the free field of the plate.

These temperatures, especially in the vicinity of the bolt hole, are not extreme temperature conditions. The premature yielding at the bolt may be due to the loss of material and heat at the bolt hole. A more accurate model of the bolted assembly as a unit may produce higher temperatures around the bolt hole. It is also important to note that the temperature capacity is governed by the limit state of bearing at the bolt similar to the yield load capacity.

6.4 Plate Thickness Comparison

The effect of the plate thickness on the capacity of the connections has been compared several times throughout this research. The mathematical computations performed in Section 3.4 using the AISC Manual of Steel Construction are the first indication of the behavior of the connections based upon plate thickness. Geometrically, the ⅜-inch plate is one and a half times thicker than the ¼-inch plate and three times thicker than the ⅛-inch plate.

The capacities derived from the ASD and LRFD mathematical computations of the yielding in the gross section, the bearing capacity and the fracture in the net section correlate in a similar manner. Table 6.4-1 summarizes the load values obtained for these failure modes using the LRFD design equations. It is observed that a ⅜-inch plate yields a bolt bearing capacity of 24,700 pounds which is three times higher than the ⅛-inch plate (8,200 pounds) and one and a half times higher than the ¼-inch plate (16,500 pounds). The other limit states prove to compare similarly as shown.

Table 6.4-1: Comparison of Plate Thicknesses using LRFD Computation Results

Connection	LRFD Bolt Bearing Capacity (pounds)	LRFD Yielding In the Gross Section (pounds)	LRFD Fracture In the Net Section (pounds)
⅜" plate, single bolt	24,700	50,600	40,000
¼" plate, single bolt	16,500	33,800	26,700
⅛" plate, single bolt	8,200	16,900	13,300
⅜" plate, double bolt	49,400	101,300	80,000
¼" plate, double bolt	32,900	67,500	53,300
⅛" plate, double bolt	16,500	33,800	26,700

Following the mathematical computations, the finite element model was constructed based on the three varying plate thicknesses. The connections were subject to the same loadings so the results due to different plate thicknesses could be observed. The ALGOR results presented in Table 6.4-2 and Table 6.4-3 for the normal and elevated temperature conditions show a similar comparison to the mathematical computations. At the bolt hole and in the free field, the ⅜ inch plate produces results three times the ⅛ inch plate and one and a half times the ¼ inch plate at normal temperatures.

Table 6.4-2: Plate Thicknesses Comparison of ALGOR Model at Normal Temperatures

Connection	ALGOR Bolt Bearing Capacity (pounds)	ALGOR Yielding In the Gross Section (pounds)
⅜" plate, single bolt	21,600	61,300
¼" plate, single bolt	14,400	40,800
⅛" plate, single bolt	7,200	20,400
⅜" plate, double bolt	44,700	114,840
¼" plate, double bolt	29,800	76,560
⅛" plate, double bolt	14,900	38,280

Table 6.4-3: Plate Thicknesses Comparison of ALGOR Model at Elevated Temperatures

Connection	ALGOR Bolt Bearing Capacity (pounds)	ALGOR Yielding In the Gross Section (pounds)
⅜" plate, single bolt	19,750	54,000
¼" plate, single bolt	12,900	35,400
⅛" plate, single bolt	6,200	17,200
⅜" plate, double bolt	23,000	54,300
¼" plate, double bolt	15,200	35,800
⅛" plate, double bolt	6,400	17,800

Overall, it can be concluded that the load capacity varies based on the thickness of the connecting plate as one would expect. The ⅜ inch plate produces a capacity three times greater than the ⅛ inch plate and one and a half times greater than the ¼ inch plate.

6.5 Single Bolt versus Double Bolt Comparison

The number of bolts used in the connection models provides another comparison to determine the behavior of connections. By adding another bolt to the model, an increase to the connection plate size also occurs. Similar to the plate thickness comparison, the results of the mathematical analysis are tabulated in Table 6.5-1, this time for the single and double bolt conditions. It is simple to observe that the increase from one bolt to two bolts, doubles the capacity of the connection. This increase in capacity by a factor of two occurs for the varying plate thicknesses as well.

Table 6.5-1: Comparison of Bolt Conditions using LRFD Computation Results

Connection	LRFD Bolt Bearing Capacity (pounds)	LRFD Yielding In the Gross Section (kips)	LRFD Fracture In the Net (kips)
⅜" plate, single bolt	24,700	50,600	40,000
¼" plate, single bolt	16,500	33,800	26,700
⅛" plate, single bolt	8,200	16,900	13,300
⅜" plate, double bolt	49,400	101,300	80,000
¼" plate, double bolt	32,900	67,500	53,300
⅛" plate, double bolt	16,500	33,800	26,700

At normal temperatures, the ALGOR model was constructed for a single bolt condition and a double bolt condition. The results from these analyses are shown in Table 6.5-2 for the bolt bearing capacity and the yielding in the gross section. The ALGOR finite element model produced bolt bearing capacity results for the double bolt connection that are twice those for the single bolt. However, the gross section result capacities varied by a factor of 1.87, which is slightly less than two.

Table 6.5-2: Bolt Condition Comparison of ALGOR Models at Normal Temperatures

Connection	ALGOR Bolt Bearing Capacity (pounds)	ALGOR Yielding In the Gross Section (pounds)
⅜" plate, single bolt	21,600	61,300
¼" plate, single bolt	14,400	40,800
⅛" plate, single bolt	7,200	20,400
⅜" plate, double bolt	44,700	114,840
¼" plate, double bolt	29,800	76,560
⅛" plate, double bolt	14,900	38,280

7.0 CONCLUSIONS

The scope of work for this thesis included the development of comprehensive finite element models to observe the behavior of connections, in particular their strength capacities under elevated fire conditions. The modeling proved to be complex when the heat transfer analysis was combined with the mechanical simulation analysis. The following are observations regarding the analysis of the results as well as discoveries on the modeling procedures using the finite element software.

Finite Element Models Compared Against AISC Design Equations

The LRFD and the ASD design equations found in Chapter J of the AISC Specifications are the baseline for evaluation of the finite element models. The LRFD equations are known to have lower, less conservative factors of safety which produce capacities approximately 20 to 30 percent higher than the ASD approach. The capacities predicted through use of the finite element models at normal temperatures are found to be 20 percent higher than those obtained from the LRFD equations and 45 percent higher than the ASD equations. It is expected that the computer model produces higher capacities since a factor of safety is not applied to the results. Therefore, it is reasonable to assume that the finite element modeling of the connection at normal temperatures is accurate when compared to the AISC design equations. The finite element modeling and the AISC design equations are both governed by the limit state of bearing at the bolt.

Plate Thickness and Bolt Conditions

At normal temperatures, the varying thicknesses of the connection plates and the addition of a bolt to the connection produces results as one would expect. The ⅜ inch plate thickness results in capacities three times greater than the ⅛ inch plate, and one and a half times greater than the ¼ inch plate. The increase from one bolt to two bolts, produces bolt bearing capacity results for the double bolt connection that are twice the single bolt connection. However, the yielding in the gross section capacities increased by a factor of 1.87 with the addition of a second bolt. This may be due to the location of the observation nodes in the free field which are near the applied external loading. The stresses may have increased at a faster rate at this location, resulting in slightly lower capacities.

The elevated temperature single bolt connection model produces capacities varying with the plate thickness similar to the normal temperature condition. For the double bolt condition at elevated temperatures, the ⅜ inch plate has a capacity three and a half times greater than the ⅛ inch plate. On the other hand, the capacities resulting from the number of bolts are not as straightforward. At elevated temperatures, the double bolt connection indicates an increase in capacity of only about 12 percent compared to the single bolt connection capacity. This result is not consistent with the results from the normal temperature connections described above. From these comparisons it is apparent that at elevated temperatures, high stresses are produced in the models at a faster rate which results in lower capacities of the connections.

Elevated Temperature Model Results

The elevated temperature finite element models are created using temperature-dependent values for the yield stress and modulus of elasticity which are shown to decrease with increases in temperatures. Therefore, the introduction of high temperatures results in a decrease in strength of the connection. The elevated temperature models produce yield capacities 15 percent and 50 percent lower than the normal temperature models for the single bolt and double bolt connections, respectively.

The temperature results indicate that the critical temperature is dependent on the limit state. For the single bolt condition, the yield temperature which occurs due to bolt bearing is 125 degrees Fahrenheit. A higher temperature of 365 degrees Fahrenheit occurs in the gross section of the plate for the same single bolt models. The double bolt connection produces critical temperatures of 98 and 183 degrees Fahrenheit for the yielding at the bolt bearing and the yielding in the gross section, respectively. It is important to note that the critical temperatures did not vary with the plate thicknesses.

The critical temperatures in the vicinity of the bolt hole are not extreme temperature conditions. This premature yielding at the bolt hole may be due to the loss of material when the bolt hole is modeled. A more accurate model of the bolted connection as a unit may indicate a transfer of heat through the actual bolt.

Observations on Modeling Procedures

There are several challenges to overcome when constructing a computerized finite element model. The following are some of the items which deemed problematic during the modeling procedure.

- The mesh development for the model was done using a trial-and-error procedure. When the mesh was too fine, there were a large number of elements and nodes resulting in long processing for the computer analysis. A few various mesh patterns were tried until a mesh was found which produced accurate results in a reasonable amount of time.

- The modeling of the bolt and the temperature boundary conditions were also determined through trial-and-error. Experimenting with various fixed nodes produced a range of displacements. When too many nodes were fixed, the bolt became extremely fixed and very small displacements occurred at the bolt. The opposite occurred when there were minimal fixed nodes at the bolt. The fixed nodes arranged in a 180 degree circumference around the bolt hole seemed to produce fairly accurate displacements and stresses at the bolt.

  Several trials of the temperature boundary conditions were also performed to produce accurate temperatures in the model. Without any temperature boundaries, the time-temperature curve continually increased to temperatures well beyond the capacity of the material. However, when too many nodes were chosen

as boundaries, the temperature change in the model remained minimal. The temperatures boundary conditions ultimately chosen produced maximum temperatures of 1200 degrees Fahrenheit within the connection.

- The external ramp loading applied to the model was changed several times before a final load was chosen. When the ramp load increased to a load well beyond the plate capacity, the program would abort and fail because the stresses became too large. A small ramp load would not induce the failure characteristics that were trying to be achieved through the model. The results of the mathematical analysis were a good starting point to gage a ramp loading that would produce the desired results.

- The ALGOR finite element program produced temperature, displacement and stress results at all nodes for each time step once the analysis of the model was complete. The displacement and temperature results were tabulated in a separate file which could easily be converted into an Excel worksheet. However, the stress results at each time step did not have a pre-tabulated form to convert into Excel. This required that the stresses at each time step be input manually for each node. This proved to be a very time consuming procedure for obtaining the stress results. The addition of another function to the ALGOR program similar to what is used for the displacements and temperatures could easily remedy the problem.

Possible Future Work of Bolted Shear Connections at Elevated Temperatures

The analysis of the strength of bolted shear connections is a topic that has seldom been studied. The following are recommendations of areas that may be of interest to future researchers on this topic:

- Further study of the connection in the vicinity of the bolt. In particular, it may be advantageous to provide a more accurate representation of the bolt and plate as a unit. This may produce temperature results around the bolt and provide investigation into the tension loss at the bolt hole.

- Produce finite element models which contain staggered bolt connections. This would give more insight into the behavior of multiple bolted connections and the effect of locations of the bolt holes in the plates.

- Using the finite element models, determine the actual length of time it takes to obtain the critical temperature and the capacity of the connection.

REFERENCES

1. Steel Construction Manual, Thirteenth Edition. Chicago: American Institute of Steel Construction, 2005.

2. Iding, R. H. and Bresler, B. "Effect of Restraint Conditions on Fire Endurance of Steel-Framed Construction." Proceedings of the 1990 National Steel Construction Conference, AISC Chicago, Mar. 1990.

3. Iding, R. H., Nizamuddin, Z. and Bresler, B. "A Computer Program for the FIre REsponse of Structures – Thermal Three-Dimensional Version." Report No. UCB FRG 77-15, Fire Research Group, Structural Engineering and Structural Mechanics, Department of Civil Engineering, University of California, Berkeley, Oct. 1977.

4. Franssen, J-M. "SAFIR: A Thermal/Structural Program Modeling Structures Under Fire." Proceedings of the 2003 National Steel Construction Conference, AISC, Baltimore, MD, Apr. 2003.

5. Bletzacker, R. W. "Effect of Structural Restraint on the Fire Resistance of Steel Beam Floor and Roof Assemblies." Report No. EES 246/266, AISI, Ohio State University, Columbus, OH, Sept. 1966.

6. Iding, R. H. and Bresler, B. "Prediction of Fire Response of Buildings Using Finite Element Methods."

7. Iding, R. H. and Bresler, B. "Effect of Fire Exposure on Steel Frame Buildings." Final Report, Vols. 1 and 2, AISI, Wiss, Janney, Elstner Associates, Inc., Mar. 1982.

8. Khan, F.R. and Nassetta, A.F. "Temperature Effects on Tall Steel Framed Buildings." AISC Engineering Journal. Oct. 1970.

9. The SFPE Handbook of Fire Protection Engineering, Second Edition. Quincy, MA: Society of Fire Protection Engineers and National Fire Protection Association, 1995.

10. Grant, Nicholas J. and Mullendore, Arthur W. "Deformation and Fracture at Elevated Temperatures." Cambridge, MA: MIT, 1965. 3-33

11. Logan, Daryl L. A First Course in the Finite Element Method Using Algor. 2nd edition. Pacific Grove: Brooks-Wadsworth, 2001.

12. DocuTech-Software Documentation Information Resource, Revision 1.00. Algor, Inc., 1999.

13. ALGOR. Algor Inc. <http://www.algor.com>.

14. Abaqus. 2004. Dassault Systemes SIMULIA. <http://www.simulia.com>.

15. ANSYS. 1970. ANSYS, Inc. <http://www.ansys.com>.

16. Nei Nastran. Nei Software, Inc. <http://www.nenastran.com>.

17. American Society of Testing and Materials. ASTM International. <http://www.astm.org>.

18. AISC. American Institute of Steel Construction. <http://www.aisc.org>.

19. Specification for Structural Steel Buildings. Chicago: American Institute of Steel Construction, 2005.

20. Specification for Structural Joints Using ASTM A325 or A490 Bolts. Chicago: Research Council on Structural Connections, 2004.

21. Beer, F. P. and Johnston, E. R., Mechanics of Materials, Second Edition. New York: McGraw-Hill. Inc., 1992.

22. Mathcad. Mathsoft. <http://www.mathsoft.com>.

23. Clough, R. W., "The Finite Element Method in Plane Stress Analysis." Proceedings of Second ASCE Conference on Electronic Computation, Pittsburg, PA, Sept. 1960.

24. Courant, R., "Variational Methods for Solution of Equilibrium and Vibration." Bulletin American Math Society, Volume 49, 1943.

25. Levy, S., "Computation of Influence Coefficients for Aircraft Structures with Discontinuities and Sweepback." Journal of Aeronautical Science, Volume 14, 1947.

26. Levy, S., "Structural Analysis and Influence Coefficients for Delta Wings." Journal of Aeronautical Science, Volume 20, 1953.

27. Argyris, J. and Kelsey, S., "Energy Theorems and Structural Analysis." Butterworth, London, 1960.

28. Turner, M., Clough, R. W., Martin, H. C., and Topp, L. J., "Stiffness and Deflection Analysis of Complex Structures." Journal of Aeronautical Science, Volume 23, Sept. 1956.

29. Pepper, D. W. and Heinrich, J. C., The Finite Element Method: Basic Concepts and Applications, Second Edition. Taylor and Francis Publishing Co., 2005.

30. Young, W. C. and Budynas, R. G., Roark's Formula for Stress and Strain, Seventh Edition. McGraw Hill, 2002.

APPENDIX A. MATHEMATICAL ANALYSIS COMPUTATIONS

DESIGN CRITERIA

UNIT CONVERSIONS:

$k := 1000 \cdot lb \quad klf := \frac{k}{ft} \quad ksf := \frac{k}{ft^2} \quad kcf := \frac{k}{ft^3} \quad ksi := \frac{k}{in^2} \quad plf := \frac{lb}{ft} \quad psf := \frac{lb}{ft^2} \quad pcf := \frac{lb}{ft^3} \quad psi := \frac{lb}{in^2}$

REFERENCE: AISC Manual of Steel Construction, Thirteenth Edition

MATERIAL PROPERTIES:	Yield Stress:	$F_y := 50ksi$
	Ultimate Stress:	$F_u := 65ksi$
	Modulus of Elasticity:	$E_s := 29000ksi$
RESISTANCE FACTORS: (LRFD)	Resistance factor for tensile yielding:	$\phi_{t1} := 0.90$
	Resistance factor for tensile rupture:	$\phi_{t2} := 0.75$
	Resistance factor for bearing strength:	$\phi_{t3} := 0.75$
SAFETY FACTORS: (ASD)	Safety factor for tensile yielding:	$\Omega_{t1} := 1.67$
	Safety factor for tensile rupture:	$\Omega_{t2} := 2.0$
	Safety factor for bearing strength:	$\Omega_{t3} := 2.0$

STRENGTH OF 3/8" PLATE, SINGLE BOLT CONNECTION

YIELDING IN THE GROSS SECTION

Plate Dimensions: $t_{p1} := 0.375in$ $w_{p1} := 3in$

Gross Area, A_g: $A_{g1} := t_{p1} \cdot w_{p1}$ $A_{g1} = 1.125\,in^2$

Nominal Strength, R_n: $R_{n1} := A_{g1} \cdot F_y$ $R_{n1} = 56.25\,k$

Design Tensile Strength, $\phi_t R_n$: $\phi_{t1} \cdot R_{n1} = 50.6\,k$ (LRFD)

Allowable Tensile Strength, R_n/Ω: $\frac{R_{n1}}{\Omega_{t1}} = 33.7\,k$ (ASD)

FRACTURE IN THE NET SECTION

Bolt Diameter, d_b: $d_b := 0.75in$

Shear Lag Factor, U: $U := 1.0$

Net Area, A_n: $A_{n1} := A_{g1} - \left[\left(d_b + .0625in\right) \cdot t_{p1}\right]$ $A_{n1} = 0.82\,in^2$

Effective Net Area, A_e: $A_{e1} := U \cdot A_{n1}$ $A_{e1} = 0.82\,in^2$

Nominal Strength, R_n: $R_{nf1} := A_{e1} \cdot F_u$ $R_{nf1} = 53.32\,k$

$\phi_{t2} \cdot R_{nf1} = 40\,k$ (LRFD)

$\frac{R_{nf1}}{\Omega_{t2}} = 26.7\,k$ (ASD)

BEARING STRENGTH AT BOLT HOLES

Clear Distance, L_c: $L_{c1} := 1.125in$

Nominal Strength, R_n: $R_{nb1} := 1.2 \cdot L_{c1} \cdot t_{p1} \cdot F_u$ $R_{nb1} = 32.91\,k$

Maximum Nominal Strength, R_{nmax}: $R_{nbmax1} := 2.4 \cdot d_b \cdot t_{p1} \cdot F_u$ $R_{nbmax1} = 43.87\,k$

$\phi_{t3} \cdot \left(\min\left(R_{nb1}, R_{nbmax1}\right)\right) = 24.7\,k$ (LRFD)

$\frac{\min\left(R_{nb1}, R_{nbmax1}\right)}{\Omega_{t3}} = 16.5\,k$ (ASD)

STRENGTH OF 1/4" PLATE, SINGLE BOLT CONNECTION

YIELDING IN THE GROSS SECTION

Plate Dimensions: $t_{p2} := 0.25in$ $w_{p2} := 3in$

Gross Area, A_g: $A_{g2} := t_{p2} \cdot w_{p2}$ $A_{g2} = 0.75in^2$

Nominal Strength, R_n: $R_{n2} := A_{g2} \cdot F_y$ $R_{n2} = 37.5k$

$\phi_{t1} \cdot R_{n2} = 33.8k$ (LRFD) $\frac{R_{n2}}{\Omega_{t1}} = 22.5k$ (ASD)

FRACTURE IN THE NET SECTION

Plate Dimensions: $t_{p2} = 0.25in$ $w_{p2} = 3in$

Bolt Diameter: $d_b = 0.75in$

Gross Area, A_g: $A_{g2} = 0.75in^2$

Shear Lag Factor, U: $U = 1.0$

Net Area, A_n: $A_{n2} := A_{g2} - \left[\left(d_b + .0625in\right) \cdot t_{p2}\right]$ $A_{n2} = 0.547in^2$

Effective Net Area, A_e: $A_{e2} := U \cdot A_{n2}$ $A_{e2} = 0.547in^2$

Nominal Strength, R_n: $R_{nf2} := A_{e2} \cdot F_u$ $R_{nf2} = 35.547k$

$\phi_{t2} \cdot R_{nf2} = 26.7k$ (LRFD) $\frac{R_{nf2}}{\Omega_{t2}} = 17.8k$ (ASD)

BEARING STRENGTH AT BOLT HOLES

Clear Distance, L_c: $L_{c2} := 1.125in$

Bolt Diameter, d_b: $d_b = 0.75in$

Nominal Strength, R_n: $R_{nb2} := 1.2 \cdot L_{c2} \cdot t_{p2} \cdot F_u$ $R_{nb2} = 21.94k$

Maximum Nominal Strength: $R_{nbmax2} := 2.4 \cdot d_b \cdot t_{p2} \cdot F_u$ $R_{nbmax2} = 29.25k$

$\phi_{t3} \cdot \left(\min\left(R_{nb2}, R_{nbmax2}\right)\right) = 16.5k$ (LRFD) $\frac{\min\left(R_{nb2}, R_{nbmax2}\right)}{\Omega_{t3}} = 11k$ (ASD)

STRENGTH OF 1/8" PLATE, SINGLE BOLT CONNECTION

YIELDING IN THE GROSS SECTION

Plate Dimensions: $t_{p3} := 0.125in$ $w_{p3} := 3in$

Gross Area, A_g: $A_{g3} := t_{p3} \cdot w_{p3}$ $A_{g3} = 0.375\,in^2$

Nominal Strength, R_n: $R_{n3} := A_{g3} \cdot F_y$ $R_{n3} = 18.75\,k$

$\phi_{t1} \cdot R_{n3} = 16.9\,k$ (LRFD) $\frac{R_{n3}}{\Omega_{t1}} = 11.2\,k$ (ASD)

FRACTURE IN THE NET SECTION

Plate Dimensions: $t_{p3} = 0.125\,in$ $w_{p3} = 3\,in$

Bolt Diameter: $d_b = 0.75\,in$

Gross Area, A_g: $A_{g3} = 0.375\,in^2$

Shear Lag Factor, U: $U = 1.0$

Net Area, A_n: $A_{n3} := A_{g3} - \left[\left(d_b + .0625in\right) \cdot t_{p3}\right]$ $A_{n3} = 0.273\,in^2$

Effective Net Area, A_e: $A_{e3} := U \cdot A_{n3}$ $A_{e3} = 0.273\,in^2$

Nominal Strength, R_n: $R_{nf3} := A_{e3} \cdot F_u$ $R_{nf3} = 17.773\,k$

$\phi_{t2} \cdot R_{nf3} = 13.3\,k$ (LRFD) $\frac{R_{nf3}}{\Omega_{t2}} = 8.9\,k$ (ASD)

BEARING STRENGTH AT BOLT HOLES

Clear Distance, L_c: $L_{c3} := 1.125in$

Bolt Diameter, d_b: $d_b = 0.75\,in$

Nominal Strength, R_n: $R_{nb3} := 1.2 \cdot L_{c3} \cdot t_{p3} \cdot F_u$ $R_{nb3} = 10.97\,k$

Maximum Nominal Strength: $R_{nbmax3} := 2.4 \cdot d_b \cdot t_{p3} \cdot F_u$ $R_{nbmax3} = 14.62\,k$

$\phi_{t3} \cdot \left(\min\left(R_{nb3}, R_{nbmax3}\right)\right) = 8.2\,k$ (LRFD) $\frac{\min\left(R_{nb3}, R_{nbmax3}\right)}{\Omega_{t3}} = 5.5\,k$ (ASD)

STRENGTH OF 3/8" PLATE, DOUBLE BOLT CONNECTION

YIELDING IN THE GROSS SECTION

Plate Dimensions: $t_{p4} := 0.375in$ $w_{p4} := 6in$

Gross Area, A_g: $A_{g4} := t_{p4} \cdot w_{p4}$ $A_{g4} = 2.25 in^2$

Nominal Strength, R_n: $R_{n4} := A_{g4} \cdot F_y$ $R_{n4} = 112.5 k$

$\phi_{t1} \cdot R_{n4} = 101.3 k$ (LRFD) $\frac{R_{n4}}{\Omega_{t1}} = 67.4 k$ (ASD)

FRACTURE IN THE NET SECTION

Plate Dimensions: $t_{p4} = 0.375 in$ $w_{p4} = 6 in$

Bolt Diameter: $d_b = 0.75 in$

Gross Area, A_g: $A_{g4} = 2.25 in^2$

Shear Lag Factor, U: $U = 1.0$

Net Area, A_n: $A_{n4} := A_{g4} - \left[2\left(d_b + .0625in\right) \cdot t_{p4}\right]$ $A_{n4} = 1.641 in^2$

Effective Net Area, A_e: $A_{e4} := U \cdot A_{n4}$ $A_{e4} = 1.641 in^2$

Nominal Strength, R_n: $R_{nf4} := A_{e4} \cdot F_u$ $R_{nf4} = 106.6 k$

$\phi_{t2} \cdot R_{nf4} = 80 k$ (LRFD) $\frac{R_{nf4}}{\Omega_{t2}} = 53.3 k$ (ASD)

BEARING STRENGTH AT BOLT HOLES

Clear Distance, L_c: $L_{c4} := 1.125in$

Bolt Diameter, d_b: $d_b = 0.75 in$

Nominal Strength, R_n: $R_{nb4} := 1.2 \cdot L_{c4} \cdot t_{p4} \cdot F_u \cdot 2$ $R_{nb4} = 65.81 k$

Maximum Nominal Strength: $R_{nbmax4} := 2.4 \cdot d_b \cdot t_{p4} \cdot F_u \cdot 2$ $R_{nbmax4} = 87.75 k$

$\phi_{t3} \cdot \left(\min\left(R_{nb4}, R_{nbmax4}\right)\right) = 49.4 k$ (LRFD) $\frac{\min\left(R_{nb4}, R_{nbmax4}\right)}{\Omega_{t3}} = 32.9 k$ (ASD)

STRENGTH OF 1/4" PLATE, DOUBLE BOLT CONNECTION

YIELDING IN THE GROSS SECTION

Plate Dimensions: $t_{p5} := 0.25in$ $w_{p5} := 6in$

Gross Area, A_g: $A_{g5} := t_{p5} \cdot w_{p5}$ $A_{g5} = 1.5\,in^2$

Nominal Strength, R_n: $R_{n5} := A_{g5} \cdot F_y$ $R_{n5} = 75\,k$

$\phi_{t1} \cdot R_{n5} = 67.5\,k$ (LRFD) $\frac{R_{n5}}{\Omega_{t1}} = 44.9\,k$ (ASD)

FRACTURE IN THE NET SECTION

Plate Dimensions: $t_{p5} = 0.25\,in$ $w_{p5} = 6\,in$

Bolt Diameter: $d_b = 0.75\,in$

Gross Area, A_g: $A_{g5} = 1.5\,in^2$

Shear Lag Factor, U: $U = 1.0$

Net Area, A_n: $A_{n5} := A_{g5} - \left[2\left(d_b + .0625in\right) \cdot t_{p5}\right]$ $A_{n5} = 1.094\,in^2$

Effective Net Area, A_e: $A_{e5} := U \cdot A_{n5}$ $A_{e5} = 1.094\,in^2$

Nominal Strength, R_n: $R_{nf5} := A_{e5} \cdot F_u$ $R_{nf5} = 71.1\,k$

$\phi_{t2} \cdot R_{nf5} = 53.3\,k$ (LRFD) $\frac{R_{nf5}}{\Omega_{t2}} = 35.5\,k$ (ASD)

BEARING STRENGTH AT BOLT HOLES

Clear Distance, L_c: $L_{c5} := 1.125in$

Bolt Diameter, d_b: $d_b = 0.75\,in$

Nominal Strength, R_n: $R_{nb5} := 1.2 \cdot L_{c2} \cdot t_{p5} \cdot F_u \cdot 2$ $R_{nb5} = 43.88\,k$

Maximum Nominal Strength: $R_{nbmax5} := 2.4 \cdot d_b \cdot t_{p5} \cdot F_u \cdot 2$ $R_{nbmax2} = 29.25\,k$

$\phi_{t3} \cdot \left(\min\left(R_{nb5}, R_{nbmax5}\right)\right) = 32.9\,k$ (LRFD) $\frac{\min\left(R_{nb5}, R_{nbmax5}\right)}{\Omega_{t3}} = 21.9\,k$ (ASD)

STRENGTH OF 1/8" PLATE, DOUBLE BOLT CONNECTION

YIELDING IN THE GROSS SECTION

Plate Dimensions: $t_{p6} := 0.125in$ $w_{p6} := 6in$

Gross Area, A_g: $A_{g6} := t_{p6} \cdot w_{p6}$ $A_{g6} = 0.75 in^2$

Nominal Strength, R_n: $R_{n6} := A_{g6} \cdot F_y$ $R_{n6} = 37.5 k$

$\phi_{t1} \cdot R_{n6} = 33.8 k$ (LRFD) $\frac{R_{n6}}{\Omega_{t1}} = 22.5 k$ (ASD)

FRACTURE IN THE NET SECTION

Plate Dimensions: $t_{p6} = 0.125 in$ $w_{p6} = 6 in$

Bolt Diameter: $d_b = 0.75 in$

Gross Area, A_g: $A_{g6} = 0.75 in^2$

Shear Lag Factor, U: $U = 1.0$

Net Area, A_n: $A_{n6} := A_{g6} - \left[2\left(d_b + .0625in\right) \cdot t_{p6}\right]$ $A_{n6} = 0.547 in^2$

Effective Net Area, A_e: $A_{e6} := U \cdot A_{n6}$ $A_{e6} = 0.547 in^2$

Nominal Strength, R_n: $R_{nf6} := A_{e6} \cdot F_u$ $R_{nf6} = 35.5 k$

$\phi_{t2} \cdot R_{nf6} = 26.7 k$ (LRFD) $\frac{R_{nf6}}{\Omega_{t2}} = 17.8 k$ (ASD)

BEARING STRENGTH AT BOLT HOLES

Clear Distance, L_c: $L_{c6} := 1.125in$

Bolt Diameter, d_b: $d_b = 0.75 in$

Nominal Strength, R_n: $R_{nb6} := 1.2 \cdot L_{c6} \cdot t_{p6} \cdot F_u \cdot 2$ $R_{nb6} = 21.94 k$

Maximum Nominal Strength: $R_{nbmax6} := 2.4 \cdot d_b \cdot t_{p6} \cdot F_u \cdot 2$ $R_{nbmax6} = 29.25 k$

$\phi_{t3} \cdot \left(\min\left(R_{nb6}, R_{nbmax6}\right)\right) = 16.5 k$ (LRFD) $\frac{\min\left(R_{nb6}, R_{nbmax6}\right)}{\Omega_{t3}} = 11 k$ (ASD)

APPENDIX B. STRESSES AND STRAINS FOR SHEAR CONNECTIONS AT NORMAL TEMPERATURES

Bearing at Bolt - Single Bolt, Normal Temperature Condition

		3/8" Plate			1/4" Plate			1/8" Plate		
Time (sec)	Load (lbs)	Disp. Node 272 (in)	Strain,ε = ΔL/L (in/in)	Stress (psi)	Disp. Node 272 (in)	Strain,ε = ΔL/L (in/in)	Stress (psi)	Disp. Node 272 (in)	Strain,ε = ΔL/L (in/in)	Stress (psi)
0	0.0	0	0	0	0	0	0	0	0	0
0.001	1000.0	7.58E-05	9.4E-05	150.785	0.000114	0.000141	226.186	0.000227	0.000282	452.432
0.002	2000.0	0.000152	0.000188	301.597	0.000227	0.000282	452.432	0.000457	0.000567	903.612
0.003	3000.0	0.000227	0.000282	452.435	0.000341	0.000423	678.736	0.000734	0.000911	1284.92
0.004	4000.0	0.000303	0.000376	603.299	0.000457	0.000567	903.61	0.001068	0.001324	1576.9
0.005	5000.0	0.000379	0.00047	754.174	0.000585	0.000726	1112.92	0.001458	0.001808	1800.85
0.006	6000.0	0.000457	0.000567	903.617	0.000735	0.000911	1284.75	0.001922	0.002384	1899.08
0.007	6999.9	0.00054	0.00067	1047.12	0.000896	0.001111	1438.2	0.002472	0.003066	1895.26
0.008	7999.9	0.000633	0.000785	1173.93	0.001067	0.001324	1578.49	0.003148	0.003904	1814.84
0.009	8999.9	0.000735	0.000911	1284.93	0.001253	0.001555	1703.7	0.004152	0.00515	1983.47
0.01	9999.9	0.00084	0.001042	1389.17	0.001457	0.001807	1805	0.005639	0.006994	2127.56
0.011	10999.9	0.000952	0.00118	1486.56	0.00168	0.002084	1881.52	0.007463	0.009256	2267.92
0.012	11999.9	0.001067	0.001324	1579.31	0.001917	0.002378	1940.35	0.009732	0.012071	2375.89
0.013	12999.9	0.00119	0.001476	1664.95	0.002179	0.002702	1961.3	0.012776	0.015846	2513.58
0.014	13999.9	0.001319	0.001636	1742.02	0.002462	0.003053	1958.75	0.016802	0.02084	2799.41
0.015	14999.9	0.001456	0.001806	1808.1	0.002779	0.003446	1925.3	0.021807	0.027047	3529.55
0.016	15999.9	0.001603	0.001989	1861.53	0.00313	0.003883	1866.93	0.027274	0.033829	4740.94
0.017	16999.9	0.001756	0.002178	1909.66	0.003552	0.004406	1918.31	0.033136	0.041098	9654.24
0.018	17999.9	0.001915	0.002376	1949.86	0.004147	0.005143	1985.73	0.039274	0.048712	13260.6
0.019	18999.8	0.002086	0.002587	1973.97	0.00485	0.006015	2054.93	0.045571	0.056522	15398
0.02	19999.8	0.002269	0.002814	1980.29	0.005636	0.006991	2126.74	0.051664	0.064079	15296.9
0.021	20999.8	0.002458	0.003048	1981.73	0.006504	0.008066	2198.06	0.057571	0.071406	15090.4
0.022	21999.8	0.002664	0.003305	1963.4	0.007461	0.009254	2266.56	0.063335	0.078555	15190.4

0.023	22999.8	0.002887	0.003581	1934.15	0.008525	0.010574	2329.53	0.068969	0.085543	7013.07
0.024	23999.8	0.003124	0.003874	1895.11	0.00973	0.012068	2374.85	0.074485	0.092385	7633.65
0.025	24999.8	0.0034	0.004217	1885.7	0.011141	0.013818	2420.49	0.079886	0.099083	12266.4
0.026	25999.8	0.003753	0.004655	1923.37	0.012776	0.015846	2513.15	0.085175	0.105643	16672.7
0.027	26999.8	0.004177	0.00518	1963.04	0.014603	0.018112	2605.09	0.090359	0.112073	9277.36
0.028	27999.8	0.004642	0.005757	2007.7	0.016802	0.02084	2798.32	0.095445	0.118381	13533.5
0.029	28999.8	0.005109	0.006337	2072.2	0.019241	0.023865	3102.72	0.100437	0.124573	10211.1
0.03	29999.8	0.005639	0.006994	2124.73	0.021805	0.027044	3526.94	0.105338	0.130652	10655.7
0.031	30999.8	0.006209	0.007701	2173.01	0.024483	0.030367	4080.96			
0.032	31999.7	0.006812	0.008449	2220.91	0.027275	0.033829	4749.97			
0.033	32999.7	0.007462	0.009255	2266.19	0.030164	0.037413	6683.41			
0.034	33999.7	0.008158	0.010119	2309.18	0.033136	0.041099	9657.87			
0.035	34999.7	0.008908	0.011049	2348.97	0.036176	0.044869	11255.9			
0.036	35999.7	0.009731	0.01207	2374.67	0.039274	0.048712	13262.9			
0.037	36999.7	0.010644	0.013201	2393.54	0.042423	0.052618	14815.6			
0.038	37999.7	0.011667	0.014471	2453.2	0.045571	0.056522	6614.24			
0.039	38999.7	0.012776	0.015846	2513.05	0.048647	0.060337	15409.5			
0.04	39999.7	0.013968	0.017325	2571.71	0.051663	0.064078	15297.2			
0.041	40999.7	0.015275	0.018945	2647.1	0.054637	0.067767	15174.8			
0.042	41999.7	0.016803	0.02084	2798.09	0.057572	0.071407	15089			
0.043	42999.7	0.018411	0.022836	2992.87	0.06047	0.075001	15103.5			
0.044	43999.6	0.020085	0.024912	3227.42	0.063334	0.078554	15190			
0.045	44999.6	0.021806	0.027046	3528.68	0.066167	0.082068	15348.4			
0.046	45999.6	0.023577	0.029243	3885.77	0.068969	0.085543	15525.6			
0.047	46999.6	0.025401	0.031505	4276.23	0.071741	0.088981	7325.88			
0.048	47999.6	0.027277	0.033832	4755.95	0.074485	0.092385	7635.24			
0.049	48999.6	0.029192	0.036207	5867.12	0.0772	0.095751	12024.9			
0.05	49999.6	0.031144	0.038628	7654.38	0.079885	0.099083	12266.5			
0.051	50999.6	0.033136	0.041099	9648.67	0.082543	0.102379	8501.31			
0.052	51999.6	0.035157	0.043605	10717.6	0.085174	0.105643	8769.87			
0.053	52999.6	0.037203	0.046144	11869.7	0.08778	0.108874	16842.4			
0.054	53999.6	0.039274	0.048712	13262.6	0.090359	0.112074	13141.6			

0.055	54999.6	0.041373	0.051315	14444.4	0.092914	0.115242	17161.3
0.056	55999.6	0.043475	0.053922	15089.1	0.095445	0.118381	17308.9
0.057	56999.5	0.045572	0.056523	11005.5	0.097952	0.121491	13722.4
0.058	57999.5	0.047631	0.059078	15414.2	0.100437	0.124573	13908.4
0.059	58999.5	0.049658	0.061592	15393.9	0.102898	0.127625	10434.3
0.06	59999.5	0.051664	0.06408	15297.1	0.105338	0.130652	10655.5
0.061	60999.5	0.053651	0.066544	15210.6			
0.062	61999.5	0.05562	0.068987	15141			
0.063	62999.5	0.057572	0.071407	15092.4			
0.064	63999.5	0.059509	0.073809	15097.2			
0.065	64999.5	0.061429	0.076191	15110			
0.066	65999.5	0.063336	0.078556	15189.4			
0.067	66999.5	0.065228	0.080903	15292			
0.068	67999.5	0.067106	0.083232	15401.8			
0.069	68999.4	0.068971	0.085545	7016.09			
0.07	69999.4	0.070822	0.087841	15652.6			
0.071	70999.4	0.07266	0.090121	7429.98			
0.072	71999.4	0.074486	0.092386	7633.81			
0.073	72999.4	0.076299	0.094635	7834.94			
0.074	73999.4	0.078099	0.096867	12106.2			
0.075	74999.4	0.079887	0.099084	8223.21			
0.076	75999.4	0.081663	0.101288	12432.6			
0.077	76999.4	0.083424	0.103472	8592.42			
0.078	77999.4	0.085175	0.105644	8770.25			
0.079	78999.4	0.086915	0.107802	16788.2			
0.08	79999.4	0.088643	0.109945	9111.91			
0.081	80999.4	0.09036	0.112075	9279.71			
0.082	81999.3	0.092066	0.114191	9439.89			
0.083	82999.3	0.093762	0.116293	13406.4			
0.084	83999.3	0.095446	0.118383	17308.6			
0.085	84999.3	0.09712	0.120459	13659.3			
0.086	85999.3	0.098784	0.122523	10061.6			

0.087	86999.3	0.100438	0.124574	13908.2		
0.088	87999.3	0.102081	0.126612	10360.4		
0.089	88999.3	0.103715	0.128639	14153.5		
0.09	89999.3	0.105339	0.130653	10655.5		

Bearing at Bolt - Double Bolt, Normal Temperature Condition

		3/8" Plate			1/4" Plate			1/8" Plate		
Time (sec)	Load (lbs)	Disp. Node 272 (in)	Strain,ε = ΔL/L (in/in)	Stress (psi)	Disp. Node 272 (in)	Strain,ε = ΔL/L (in/in)	Stress (psi)	Disp. Node 272 (in)	Strain,ε = ΔL/L (in/in)	Stress (psi)
0	0	0	0	0	0	0	0	0	0	0
0.001	1999.984	7.33E-05	9.1E-05	169.702	0.00011	0.000136	254.562	0.00022	0.000273	509.182
0.002	3999.968	0.000147	0.000182	339.429	0.00022	0.000273	509.182	0.000442	0.000548	1018.2
0.003	5999.952	0.00022	0.000273	509.182	0.00033	0.000409	763.859	0.000706	0.000876	1468.53
0.004	7999.936	0.000293	0.000364	678.96	0.000442	0.000548	1018.2	0.001024	0.00127	1833.75
0.005	9999.92	0.000367	0.000455	848.806	0.000565	0.0007	1260.18	0.001393	0.001727	2145.41
0.006	11999.9	0.000442	0.000548	1018.19	0.000706	0.000876	1468.56	0.001828	0.002268	2356.06
0.007	13999.89	0.000522	0.000648	1182.06	0.00086	0.001067	1657.97	0.002335	0.002896	2482.08
0.008	15999.87	0.00061	0.000757	1333.21	0.001024	0.00127	1835.38	0.002934	0.00364	2646.67
0.009	17999.86	0.000706	0.000876	1468.64	0.001201	0.001489	2001.71	0.003947	0.004896	2691.28
0.01	19999.84	0.000808	0.001002	1596.28	0.001392	0.001727	2149.99	0.005384	0.006678	2733.55
0.011	21999.82	0.000914	0.001133	1718.5	0.001601	0.001985	2277.77	0.007121	0.008832	2807.66
0.012	23999.81	0.001024	0.00127	1836.05	0.001824	0.002262	2388.63	0.009182	0.011388	2917.62
0.013	25999.79	0.00114	0.001414	1948.56	0.002065	0.002561	2478.35	0.01169	0.014499	3097.91
0.014	27999.78	0.001262	0.001565	2054.9	0.002326	0.002886	2543.89	0.014751	0.018295	3410.49
0.015	29999.76	0.001391	0.001726	2152.61	0.002618	0.003247	2583.59	0.018367	0.022781	3991.49
0.016	31999.74	0.001528	0.001895	2241.18	0.002943	0.00365	2602.57	0.022689	0.028142	5363.67
0.017	33999.73	0.001672	0.002074	2321.91	0.003388	0.004202	2579.35	0.027484	0.034089	7041.99
0.018	35999.71	0.001822	0.00226	2397.29	0.003967	0.00492	2628.8	0.032865	0.040763	8792.5
0.019	37999.7	0.00198	0.002456	2464.26	0.004629	0.005741	2699.53	0.038755	0.048068	11245.3
0.02	39999.68	0.002148	0.002664	2517.87	0.005384	0.006678	2733.14	0.044651	0.055382	15350.1
0.021	41999.66	0.002323	0.002882	2563.94	0.006214	0.007707	2769.82	0.050431	0.06255	17820.9
0.022	43999.65	0.002512	0.003116	2596.96	0.007119	0.008829	2810.2	0.056075	0.069551	18082.5
0.023	45999.63	0.002717	0.00337	2618.6	0.008104	0.010052	2858.97	0.061581	0.076379	17493.8
0.024	47999.62	0.002937	0.003642	2632.03	0.00918	0.011386	2918.88	0.066954	0.083044	16927.3
0.025	49999.6	0.003211	0.003982	2622.55	0.010364	0.012854	2996.32	0.072209	0.089562	16662.5
0.026	51999.58	0.003568	0.004426	2602.47	0.011689	0.014498	3099.43	0.077355	0.095945	16852.9

0.027	53999.57	0.003948	0.004896	2680.37	0.013162	0.016325	3232.19	0.0824	0.102202	17557.3
0.028	55999.55	0.004392	0.005448	2695.14	0.01475	0.018294	3410.12	0.087346	0.108336	19053.8
0.029	57999.54	0.004872	0.006042	2711.77	0.01648	0.02044	3650.3	0.092199	0.114355	20718.1
0.03	59999.52	0.005383	0.006677	2731.71	0.018368	0.022781	3992.5			
0.031	61999.5	0.005929	0.007353	2754.34	0.020455	0.02537	4573.33			
0.032	63999.49	0.006508	0.008071	2780.7	0.022689	0.028142	5364.4			
0.033	65999.47	0.007119	0.00883	2808.05	0.025026	0.03104	6222.48			
0.034	67999.46	0.007765	0.009631	2837.73	0.027484	0.034089	7041.99			
0.035	69999.44	0.008451	0.010482	2876.72	0.030065	0.03729	7823.47			
0.036	71999.42	0.00918	0.011386	2917.45	0.032865	0.040763	8792.95			
0.037	73999.41	0.009954	0.012347	2966.19	0.035783	0.044382	9828.15			
0.038	75999.39	0.010786	0.013378	3025.3	0.038755	0.048068	11246			
0.039	77999.38	0.011689	0.014497	3096.52	0.041718	0.051743	13034.2			
0.04	79999.36	0.012657	0.015699	3181.95	0.044651	0.055381	15351.8			
0.041	81999.34	0.01368	0.016968	3284.54	0.047556	0.058984	17248.2			
0.042	83999.33	0.014751	0.018296	3410.24	0.050431	0.06255	17819.9			
0.043	85999.31	0.015877	0.019693	3554.9	0.053271	0.066073	17913.7			
0.044	87999.3	0.017094	0.021202	3752.7	0.056075	0.069551	12903.9			
0.045	89999.28	0.018368	0.022782	3992.32	0.058846	0.072987	17842.7			
0.046	91999.26	0.019735	0.024478	4360.72	0.061581	0.076379	17490.3			
0.047	93999.25	0.021188	0.02628	4816.71	0.064284	0.079732	17190.6			
0.048	95999.23	0.022689	0.028142	5364.3	0.066955	0.083045	16925.2			
0.049	97999.22	0.024234	0.030058	5931.07	0.069595	0.08632	16734.8			
0.05	99999.2	0.025833	0.032041	6505.63	0.072209	0.089561	16662.5			
0.051	101999.2	0.027484	0.034089	7041.57	0.074795	0.092769	16733.9			
0.052	103999.2	0.029184	0.036197	7553.74	0.077355	0.095945	16852.5			
0.053	105999.2	0.030976	0.03842	8115.49	0.079891	0.09909	17160.4			
0.054	107999.1	0.032865	0.040763	8791.55	0.082401	0.102202	17552.5			
0.055	109999.1	0.034798	0.04316	9407.59	0.084886	0.105285	18204.2			
0.056	111999.1	0.036772	0.045609	10286.1	0.087346	0.108336	19052.6			
0.057	113999.1	0.038755	0.048068	11246.1	0.089784	0.11136	19894.7			
0.058	115999.1	0.040733	0.050521	12459.4	0.092199	0.114356	20715.3			

0.059	117999.1	0.042699	0.05296	13735.4	0.094592	0.117323	21502.3	
0.06	119999	0.044651	0.055381	15347.2				
0.061	121999	0.046591	0.057787	16689.9				
0.062	123999	0.048518	0.060178	17712				
0.063	125999	0.05043	0.062549	17820				
0.064	127999	0.052329	0.064904	17765.2				
0.065	129999	0.05421	0.067237	18037.2				
0.066	131998.9	0.056075	0.06955	18080.9				
0.067	133998.9	0.057926	0.071846	17943.7				
0.068	135998.9	0.059761	0.074123	17721				
0.069	137998.9	0.061581	0.07638	17493.6				
0.07	139998.9	0.063387	0.078619	17286.8				
0.071	141998.9	0.065178	0.080841	17095				
0.072	143998.8	0.066955	0.083045	16912.9				
0.073	145998.8	0.068719	0.085232	16780.1				
0.074	147998.8	0.070471	0.087405	16719.3				
0.075	149998.8	0.072215	0.089569	16646.5				
0.076	151998.8	0.073936	0.091704	16872.8				
0.077	153998.8	0.075652	0.093832	16766.3				
0.078	155998.8	0.077356	0.095945	16855.9				
0.079	157998.7	0.079048	0.098044	12876.6				
0.08	159998.7	0.08073	0.10013	17289.1				
0.081	161998.7	0.0824	0.102202	17556.2				
0.082	163998.7	0.08406	0.10426	17917.3				
0.083	165998.7	0.085708	0.106305	18483.2				
0.084	167998.7	0.087346	0.108337	19050.3				
0.085	169998.6	0.088974	0.110356	19615.4				
0.086	171998.6	0.090593	0.112363	20162.1				
0.087	173998.6	0.092199	0.114356	20714.4				
0.088	175998.6	0.093797	0.116337	21246.8				
0.089	177998.6	0.095385	0.118307	21751.7				

Free Field - Single Bolt, Normal Temperature Condition

		3/8" Plate				1/4" Plate				1/8" Plate			
Time (sec)	Load (lbs)	Disp. Node 294 (in)	Disp. Node 295 (in)	Strain,ε = ΔL/L (in/in)	Stress (psi)	Disp. Node 294 (in)	Disp. Node 295 (in)	Strain,ε = ΔL/L (in/in)	Stress (psi)	Disp. Node 294 (in)	Disp. Node 295 (in)	Strain,ε = ΔL/L (in/in)	Stress (psi)
0	0	0	0	0	0	0	0	0	0	0	0	0	0
0.001	999.992	0.000132	0.000147	2.76E-05	801.985	0.000197	0.00022	4.14E-05	1202.98	0.000395	0.00044	8.29E-05	2406.03
0.002	1999.984	0.000263	0.000293	5.52E-05	1604	0.000395	0.00044	8.29E-05	2406.03	0.000791	0.000882	0.000166	4812.06
0.003	2999.976	0.000395	0.00044	8.29E-05	2406.05	0.000592	0.00066	0.000124	3609.14	0.001229	0.001366	0.000248	7210.47
0.004	3999.968	0.000526	0.000587	0.00011	3208.12	0.000791	0.000882	0.000166	4812.06	0.001717	0.001898	0.00033	9599.72
0.005	4999.96	0.000658	0.000734	0.000138	4010.22	0.001001	0.001115	0.000207	6013.14	0.002256	0.002481	0.000411	11981.7
0.006	5999.952	0.000791	0.000882	0.000166	4812.1	0.001229	0.001366	0.000248	7210.45	0.002861	0.003131	0.000491	14351.6
0.007	6999.944	0.000929	0.001035	0.000193	5613.24	0.001468	0.001627	0.000289	8405.84	0.003544	0.003858	0.00057	16709.6
0.008	7999.936	0.001076	0.001197	0.000221	6412.65	0.001716	0.001898	0.00033	9599.86	0.004345	0.004701	0.000649	19051.6
0.009	8999.928	0.001229	0.001366	0.000248	7210.52	0.001978	0.002182	0.00037	10792.2	0.005479	0.005879	0.000727	21398.3
0.01	9999.92	0.001387	0.001538	0.000275	8007.66	0.002256	0.002481	0.000411	11982	0.007087	0.007529	0.000805	23722.9
0.011	10999.91	0.00155	0.001716	0.000302	8804.08	0.002551	0.002799	0.000451	13169	0.009029	0.009513	0.00088	26021.2
0.012	11999.9	0.001716	0.001898	0.00033	9600.01	0.002858	0.003128	0.000491	14354.3	0.011414	0.011937	0.000952	28257.6
0.013	12999.9	0.00189	0.002086	0.000357	10395.2	0.003188	0.00348	0.000531	15535.9	0.01458	0.01514	0.001019	30382.2
0.014	13999.89	0.002068	0.002279	0.000384	11189.4	0.003538	0.003852	0.000571	16714.5	0.018758	0.019359	0.001093	32561.3
0.015	14999.88	0.002255	0.002481	0.000411	11982.4	0.003919	0.004254	0.00061	17889	0.023958	0.02461	0.001187	34905.7
0.016	15999.87	0.00245	0.002691	0.000438	12774	0.004333	0.00469	0.000649	19059.4	0.029639	0.030348	0.001289	37383.9
0.017	16999.86	0.00265	0.002906	0.000464	13565	0.00482	0.005198	0.000689	20233	0.035722	0.036496	0.001406	40551.8
0.018	17999.86	0.002857	0.003127	0.000491	14355.2	0.005474	0.005874	0.000728	21399.3	0.042128	0.042966	0.001523	44202.4
0.019	18999.85	0.003074	0.003358	0.000518	15143.8	0.006237	0.006658	0.000766	22562.8	0.049267	0.05017	0.001642	47854.9
0.02	19999.84	0.003302	0.003601	0.000544	15930.4	0.007084	0.007526	0.000805	23722.6	0.05886	0.060521	0.00302	54004.9
0.021	20999.83	0.003535	0.003849	0.000571	16716.4	0.00801	0.008474	0.000843	24876.6	0.068766	0.071519	0.005005	55846.1
0.022	21999.82	0.003785	0.004113	0.000597	17500	0.009026	0.00951	0.00088	26020.5	0.078683	0.082565	0.007058	58059.5
0.023	22999.82	0.00405	0.004393	0.000623	18282	0.010149	0.010653	0.000917	27149.7	0.088562	0.093579	0.009121	60215.2
0.024	23999.81	0.004328	0.004685	0.000649	19062.4	0.011411	0.011935	0.000952	28257.5	0.098382	0.10453	0.011178	62520.8
0.025	24999.8	0.004644	0.005015	0.000675	19839.9	0.012882	0.013424	0.000986	29333	0.108143	0.115418	0.013227	62824.6
0.026	25999.79	0.005036	0.005421	0.000701	20613.9	0.01458	0.01514	0.001019	30382.2	0.117839	0.126236	0.015267	67160.5

0.027	26999.78	0.005497	0.005897	0.000727	21387.4	0.016473	0.017052	0.001051	31412.4	0.127467	0.136982	0.0173	69526.2
0.028	27999.78	0.006002	0.006415	0.000752	22160.9	0.018758	0.019359	0.001093	32561.3	0.137022	0.147654	0.019331	72921.1
0.029	28999.77	0.006515	0.006943	0.000779	22946.1	0.021292	0.021918	0.001139	33736.9	0.1465	0.158247	0.021358	74345.1
0.03	29999.76	0.007085	0.007528	0.000805	23721.4	0.023956	0.024608	0.001187	34905.6	0.155899	0.168761	0.023385	76915.7
0.031	30999.75	0.007695	0.008152	0.00083	24491.7	0.026739	0.027419	0.001235	36090.2				
0.032	31999.74	0.008338	0.008809	0.000855	25259.2	0.02964	0.030349	0.001289	37384.7				
0.033	32999.74	0.009027	0.009511	0.00088	26020.4	0.032636	0.033376	0.001346	38873.5				
0.034	33999.73	0.009762	0.01026	0.000905	26775.6	0.035722	0.036496	0.001406	40548.1				
0.035	34999.72	0.010551	0.011062	0.000929	27522.6	0.038888	0.039695	0.001466	42311.6				
0.036	35999.71	0.011413	0.011936	0.000952	28257.6	0.042128	0.042966	0.001523	44203.3				
0.037	36999.7	0.012364	0.012901	0.000975	28976.9	0.045499	0.046366	0.001576	45831.5				
0.038	37999.7	0.013428	0.013977	0.000997	29685.5	0.049271	0.050175	0.001643	47886.2				
0.039	38999.69	0.01458	0.01514	0.001019	30382.2	0.053954	0.055109	0.0021	51400.9				
0.04	39999.68	0.015815	0.016387	0.00104	31068.3	0.05886	0.060521	0.00302	54009.9				
0.041	40999.67	0.017171	0.017756	0.001064	31770	0.063805	0.066003	0.003997	55035.2				
0.042	41999.66	0.018758	0.01936	0.001093	32561.6	0.068767	0.07152	0.005005	55920.1				
0.043	42999.66	0.02043	0.021048	0.001124	33345.9	0.073728	0.077044	0.006028	56871.5				
0.044	43999.65	0.022169	0.022804	0.001155	34126.5	0.078683	0.082565	0.007058	58059				
0.045	44999.64	0.023957	0.02461	0.001186	34905.8	0.083629	0.088079	0.00809	59147.6				
0.046	45999.63	0.025798	0.026468	0.001219	35692.4	0.088562	0.093579	0.009121	60257.5				
0.047	46999.62	0.027693	0.028382	0.001253	36505.6	0.093478	0.099062	0.010151	61383				
0.048	47999.62	0.029642	0.030351	0.001289	37384.9	0.098382	0.10453	0.011178	62520.7				
0.049	48999.61	0.031627	0.032357	0.001327	38359.9	0.10327	0.109982	0.012204	63668.4				
0.05	49999.6	0.033653	0.034405	0.001366	39404.6	0.108143	0.115418	0.013227	64824.7				
0.051	50999.59	0.035722	0.036496	0.001406	40547.8	0.112999	0.120835	0.014247	65988.8				
0.052	51999.58	0.037826	0.038621	0.001446	41716.6	0.117839	0.126236	0.015267	67160.4				
0.053	52999.58	0.039962	0.040779	0.001485	42936.6	0.122661	0.131618	0.016285	68339.6				
0.054	53999.57	0.042129	0.042967	0.001523	44205.2	0.127467	0.136983	0.017302	69526.2				
0.055	54999.56	0.044346	0.045204	0.00156	45335.7	0.132255	0.142328	0.018315	70720				
0.056	55999.55	0.046699	0.047575	0.001593	46356.9	0.137023	0.147654	0.019329	71921.1				
0.057	56999.54	0.049269	0.050172	0.001642	47855.8	0.141771	0.152961	0.020345	73129.4				
0.058	57999.54	0.052336	0.053336	0.001818	50314.7	0.146501	0.158248	0.021358	74345				

0.059	58999.53	0.055587	0.056906	0.002398	53479.5	0.151209	0.163514	0.022373	75567.8
0.06	59999.52	0.058862	0.060523	0.00302	54086.9	0.155899	0.168761	0.023385	76797.6
0.061	60999.51	0.062154	0.064171	0.003667	54582.5				
0.062	61999.5	0.06546	0.067842	0.004331	55195.6				
0.063	62999.5	0.068768	0.071521	0.005005	55845.4				
0.064	63999.49	0.072076	0.075204	0.005686	56660.1				
0.065	64999.48	0.075382	0.078887	0.006371	57499.3				
0.066	65999.47	0.078685	0.082568	0.007059	58058				
0.067	66999.46	0.081984	0.086244	0.007746	58781.9				
0.068	67999.46	0.085277	0.089915	0.008434	59515.7				
0.069	68999.45	0.088565	0.093582	0.009122	60257.7				
0.07	69999.44	0.091843	0.097237	0.009809	61006.6				
0.071	70999.43	0.095117	0.100889	0.010495	61761.5				
0.072	71999.42	0.098384	0.104532	0.011179	62521.2				
0.073	72999.42	0.101644	0.108169	0.011864	63285.3				
0.074	73999.41	0.104898	0.111798	0.012545	64053.4				
0.075	74999.4	0.108145	0.11542	0.013227	64810.5				
0.076	75999.39	0.111388	0.119038	0.013909	65706.4				
0.077	76999.38	0.114616	0.12264	0.014589	66378.9				
0.078	77999.38	0.117841	0.126238	0.015267	67160.7				
0.079	78999.37	0.121058	0.129828	0.015945	67946				
0.08	79999.36	0.124267	0.13341	0.016624	68734.7				
0.081	80999.35	0.12747	0.136985	0.0173	69526.6				
0.082	81999.34	0.130663	0.140551	0.017978	70321.7				
0.083	82999.34	0.133848	0.144108	0.018655	71120				
0.084	83999.33	0.137025	0.147657	0.019331	71921.5				
0.085	84999.32	0.140192	0.151196	0.020007	72726.3				
0.086	85999.31	0.143352	0.154727	0.020682	73534.3				
0.087	86999.3	0.146503	0.15825	0.021358	74345.5				
0.088	87999.3	0.149644	0.161763	0.022035	75159.9				
0.089	88999.29	0.152777	0.165268	0.022711	75977.4				
0.09	89999.28	0.155902	0.168764	0.023385	76854.6				

Free Field - Double Bolt, Normal Temperature Condition

		3/8" Plate				1/4" Plate				1/8" Plate			
Time (sec)	Load (lbs)	Disp. Node 294 (in)	Disp. Node 295 (in)	Strain,ε = ΔL/L (in/in)	Stress (psi)	Disp. Node 294 (in)	Disp. Node 295 (in)	Strain,ε = ΔL/L (in/in)	Stress (psi)	Disp. Node 294 (in)	Disp. Node 295 (in)	Strain,ε = ΔL/L (in/in)	Stress (psi)
0	0	0	0	0	0	0	0	0	0	0	0	0	0
0.001	1999.984	0.000129	0.000144	2.86E-05	818.977	0.000193	0.000216	4.29E-05	1228.48	0.000386	0.000433	8.58E-05	2457.02
0.002	3999.968	0.000257	0.000289	5.72E-05	1637.99	0.000386	0.000433	8.58E-05	2457.02	0.000773	0.000867	0.000172	4914.09
0.003	5999.952	0.000386	0.000433	8.58E-05	2457.02	0.000579	0.000649	0.000129	3685.64	0.001198	0.001339	0.000257	7365.38
0.004	7999.936	0.000514	0.000577	0.000114	3276.09	0.000773	0.000867	0.000172	4914.09	0.001671	0.001859	0.000342	9809.34
0.005	9999.92	0.000643	0.000722	0.000143	4095.18	0.000977	0.001095	0.000214	6141.13	0.00219	0.002425	0.000426	12248.5
0.006	11999.9	0.000773	0.000867	0.000172	4914.09	0.001198	0.001339	0.000257	7365.39	0.002772	0.003053	0.00051	14679.6
0.007	13999.89	0.000908	0.001018	0.0002	5732.32	0.00143	0.001594	0.000299	8587.93	0.003419	0.003746	0.000594	17103.5
0.008	15999.87	0.001049	0.001175	0.000228	6549.46	0.001671	0.001859	0.000342	9809.45	0.00416	0.004533	0.000678	19526.2
0.009	17999.86	0.001198	0.001339	0.000257	7365.4	0.001923	0.002135	0.000384	11029.9	0.00531	0.005728	0.000761	21939.3
0.01	19999.84	0.001351	0.001508	0.000285	8180.53	0.00219	0.002425	0.000426	12248.8	0.00688	0.007344	0.000843	24344.8
0.011	21999.82	0.001509	0.001681	0.000313	8995.22	0.002473	0.00273	0.000469	13465.9	0.008747	0.009256	0.000925	26736.3
0.012	23999.81	0.001671	0.001859	0.000342	9809.5	0.002769	0.00305	0.000511	14681.5	0.010939	0.011492	0.001005	29107
0.013	25999.79	0.001838	0.002042	0.00037	10623.3	0.003082	0.003386	0.000553	15895.5	0.013583	0.01418	0.001085	31440.7
0.014	27999.78	0.00201	0.002229	0.000398	11436.6	0.003414	0.003741	0.000594	17107.2	0.016792	0.017433	0.001165	33737
0.015	29999.76	0.00219	0.002424	0.000426	12249	0.003773	0.004123	0.000636	18316.3	0.02059	0.021285	0.001263	36213.8
0.016	31999.74	0.002376	0.002626	0.000455	13060.7	0.004166	0.004539	0.000678	19523.1	0.025147	0.025912	0.001391	39102.2
0.017	33999.73	0.002569	0.002834	0.000483	13871.6	0.004677	0.005072	0.000719	20725.3	0.030245	0.031094	0.001543	42675.8
0.018	35999.71	0.002768	0.003049	0.000511	14682	0.005325	0.005743	0.00076	21933	0.036537	0.037623	0.001973	47274.2
0.019	37999.7	0.002973	0.00327	0.000539	15491.9	0.006058	0.006499	0.000802	23142.6	0.044686	0.046656	0.003581	50455.7
0.02	39999.68	0.003189	0.003501	0.000567	16300.5	0.00688	0.007344	0.000843	24344.6	0.0537	0.056719	0.005489	52802.7
0.021	41999.66	0.003412	0.003739	0.000594	17108.4	0.007776	0.008262	0.000884	25542.8	0.062981	0.067123	0.007531	55943.9
0.022	43999.65	0.003647	0.003989	0.000622	17915.1	0.008746	0.009254	0.000925	26736.8	0.072347	0.077638	0.00962	58435.1
0.023	45999.63	0.003897	0.004255	0.00065	18720.6	0.009796	0.010327	0.000965	27925.6	0.081721	0.088169	0.011724	60906.1
0.024	47999.62	0.004162	0.004534	0.000678	19525.2	0.010937	0.01149	0.001005	29107.3	0.091066	0.098674	0.013833	63369.8
0.025	49999.6	0.00448	0.004868	0.000705	20327.5	0.012188	0.012763	0.001045	30277.5	0.100369	0.109137	0.015942	65840.5
0.026	51999.58	0.004881	0.005284	0.000733	21128.4	0.013582	0.014179	0.001085	31440.9	0.109619	0.119545	0.018047	68326.8

0.027	53999.57	0.00531	0.005728	0.000761	21938.3	0.015128	0.015746	0.001124	32592.1	0.118811	0.129894	0.020151	70833.1
0.028	55999.55	0.005799	0.006233	0.000788	22741.8	0.016791	0.017432	0.001165	33737.2	0.127941	0.140179	0.022251	73361.2
0.029	57999.54	0.006323	0.006772	0.000816	23543.7	0.018605	0.019271	0.001211	34930.9	0.137003	0.150396	0.024351	75911.4
0.03	59999.52	0.006879	0.007343	0.000843	24344.6	0.02059	0.021285	0.001264	36214				
0.031	61999.5	0.007468	0.007947	0.000871	25143.7	0.02279	0.023518	0.001323	37598.9				
0.032	63999.49	0.008091	0.008585	0.000898	25940.9	0.025147	0.025912	0.001391	39102.1				
0.033	65999.47	0.008746	0.009255	0.000925	26736.4	0.027618	0.028423	0.001463	40776.2				
0.034	67999.46	0.009435	0.009959	0.000952	27529.9	0.030245	0.031094	0.001543	42675.6				
0.035	69999.44	0.010165	0.010703	0.000979	28320.3	0.033092	0.033983	0.00162	44656.5				
0.036	71999.42	0.010937	0.01149	0.001005	29106.9	0.036537	0.037622	0.001973	47273.8				
0.037	73999.41	0.011756	0.012324	0.001032	29888.6	0.040422	0.041914	0.002713	49280.7				
0.038	75999.39	0.012632	0.013215	0.001058	30666.4	0.044686	0.046656	0.003581	50582.3				
0.039	77999.38	0.013582	0.014178	0.001085	31441.1	0.049144	0.051624	0.004509	51933.3				
0.04	79999.36	0.014598	0.01521	0.001111	32210.6	0.0537	0.056719	0.005489	53453.4				
0.041	81999.34	0.01567	0.016296	0.001138	32974	0.058321	0.061896	0.006501	54493.4				
0.042	83999.33	0.016793	0.017433	0.001165	33736.8	0.062981	0.067123	0.007531	55943.9				
0.043	85999.31	0.017972	0.018629	0.001194	34515.2	0.067659	0.072373	0.008572	56916.9				
0.044	87999.3	0.019251	0.019927	0.001228	35354.3	0.072347	0.077638	0.00962	58435				
0.045	89999.28	0.020591	0.021286	0.001264	36213.7	0.077036	0.082905	0.010671	59672.5				
0.046	91999.26	0.022031	0.022748	0.001302	37117.4	0.081721	0.088169	0.011724	60906.1				
0.047	93999.25	0.023564	0.024304	0.001345	38095.3	0.086398	0.093427	0.012779	62137.9				
0.048	95999.23	0.025147	0.025912	0.001391	39102.2	0.091067	0.098675	0.013833	63369.9				
0.049	97999.22	0.02678	0.02757	0.001438	40193.2	0.095723	0.103911	0.014888	64603.7				
0.05	99999.2	0.028478	0.029297	0.001489	41393	0.100368	0.109136	0.015942	65840.5				
0.051	101999.2	0.030245	0.031094	0.001543	42675.8	0.105001	0.114348	0.016995	67081.3				
0.052	103999.2	0.032092	0.03297	0.001597	43985.5	0.109619	0.119545	0.018047	68326.8				
0.053	105999.2	0.034187	0.035101	0.001661	45657.6	0.114223	0.124728	0.0191	69577.3				
0.054	107999.1	0.036537	0.037622	0.001973	47496.1	0.118812	0.129894	0.020149	70833.1				
0.055	109999.1	0.039073	0.040416	0.002441	48225.1	0.123385	0.135046	0.021202	72094.5				
0.056	111999.1	0.04181	0.04346	0.003	49563.6	0.127941	0.140179	0.022251	73361.2				
0.057	113999.1	0.044686	0.046655	0.003581	51103.1	0.132481	0.145297	0.023302	74633.6				
0.058	115999.1	0.047644	0.04995	0.004193	51854.3	0.137003	0.150396	0.024351	75911.4				

0.059	117999.1	0.050655	0.053312	0.004832	51934.7	0.141509	0.155478	0.025398	77194.8	
0.06	119999	0.053699	0.056718	0.005489	53453.5					
0.061	121999	0.056775	0.060163	0.006161	53690.7					
0.062	123999	0.05987	0.063634	0.006842	54578.5					
0.063	125999	0.06298	0.067122	0.007531	55943.8					
0.064	127999	0.066098	0.070621	0.008224	56489.2					
0.065	129999	0.069221	0.074128	0.008921	57607					
0.066	131998.9	0.072347	0.077637	0.00962	58435					
0.067	133998.9	0.075473	0.081149	0.01032	59260.5					
0.068	135998.9	0.078598	0.08466	0.011022	60084					
0.069	137998.9	0.081721	0.08817	0.011725	60693.5					
0.07	139998.9	0.084841	0.091676	0.012427	61727.3					
0.071	141998.9	0.087956	0.095177	0.01313	62548.4					
0.072	143998.8	0.091067	0.098675	0.013833	63369.9					
0.073	145998.8	0.094172	0.102166	0.014535	64192.2					
0.074	147998.8	0.097274	0.105655	0.015239	65015.6					
0.075	149998.8	0.100376	0.109144	0.015942	65840.4					
0.076	151998.8	0.103459	0.112613	0.016644	66667.5					
0.077	153998.8	0.106542	0.116082	0.017345	67496.2					
0.078	155998.8	0.10962	0.119545	0.018045	68326.9					
0.079	157998.7	0.11269	0.123001	0.018747	69160					
0.08	159998.7	0.115753	0.126451	0.019451	69995.4					
0.081	161998.7	0.118811	0.129894	0.020151	70833.2					
0.082	163998.7	0.121861	0.13333	0.020853	71673.4					
0.083	165998.7	0.124905	0.136759	0.021553	72516.1					
0.084	167998.7	0.127941	0.14018	0.022253	73361.3					
0.085	169998.6	0.130969	0.143593	0.022953	74208.9					
0.086	171998.6	0.133991	0.146999	0.023651	75059					
0.087	173998.6	0.137004	0.150396	0.024349	75911.5					
0.088	175998.6	0.14001	0.153787	0.025049	76766.4					
0.089	177998.6	0.143008	0.157169	0.025747	77623.8					

APPENDIX C. STRESSES AND STRAINS FOR SHEAR CONNECTIONS AT ELEVATED TEMPERATURES

Bearing at Bolt - Single Bolt, Elevated Temperature Condition

	3/8" Plate					1/4" Plate				
	Load/step:	445.8182	Total Load = 122600#			Load/step:	445.9016	Total Load = 81600#		
Time (s)	Load (lbs)	Disp. Node 272 (in)	Strain,ε = ΔL/L (in/in)	Stress (psi)	Temp (F)	Load (lbs)	Disp. Node 272 (in)	Strain,ε = ΔL/L (in/in)	Stress (psi)	Temp (F)
0	0	0	0	0	0.0	0	0	0	0	0.0
2	445.8182	0.000114	0.000141	81.0986	79.9	445.9016	0.000153	0.00019	123.42	81.6
3	891.6364	5.28E-05	6.55E-05	343.691	57.1	891.8033	0.00011	0.000136	401.886	59.1
4	1337.455	4.73E-05	5.86E-05	591.336	47.6	1337.705	0.000122	0.000151	624.264	49.9
5	1783.273	0.000212	0.000263	238.178	79.9	1783.607	0.000307	0.00038	378.581	83.1
6	2229.091	0.000254	0.000315	285.627	82.2	2229.508	0.000368	0.000457	453.685	86.2
7	2674.909	0.000207	0.000257	525.265	62.9	2675.41	0.000339	0.00042	721.013	67.1
8	3120.727	0.000285	0.000354	488.937	73.9	3121.311	0.000437	0.000543	716.462	78.8
9	3566.545	0.000378	0.000469	435.327	88.5	3567.213	0.000559	0.000694	682.19	94.2
10	4012.364	0.000367	0.000455	589.584	77.9	4013.115	0.000569	0.000706	864.461	84.1
11	4458.182	0.000385	0.000478	688.046	74.3	4459.016	0.000617	0.000766	977.531	81.1
12	4904	0.000473	0.000587	644.894	87.0	4904.918	0.000748	0.000928	929.441	94.5
13	5349.818	0.000511	0.000634	705.312	87.5	5350.82	0.000822	0.00102	995.494	95.7
14	5795.636	0.000517	0.000641	831.287	80.5	5796.721	0.000859	0.001066	1130.96	89.1
15	6241.455	0.000577	0.000715	848.869	85.7	6242.623	0.000961	0.001192	1146.43	95.0
16	6687.273	0.000646	0.000802	850.959	91.8	6688.525	0.001069	0.001326	1155.22	101.7
17	7133.091	0.00067	0.000831	940.863	88.1	7134.426	0.001129	0.0014	1253.67	98.6
18	7578.909	0.00071	0.000881	999.581	87.7	7580.328	0.001209	0.001499	1318.5	98.8
19	8024.727	0.000784	0.000972	996.677	93.4	8026.23	0.001324	0.001642	1322.14	105.2
20	8470.545	0.000833	0.001033	1040.73	94.1	8472.131	0.001416	0.001756	1369.95	106.5
21	8916.364	0.000869	0.001078	1108.9	92.2	8918.033	0.001497	0.001857	1440.22	105.2
22	9362.182	0.000931	0.001155	1130.11	95.1	9363.934	0.00161	0.001996	1455.92	108.7
23	9808	0.000994	0.001233	1150.18	98.1	9809.836	0.001727	0.002142	1469.48	112.4

24	10253.82	0.00104	0.001289	1203.92	97.3	10255.74	0.001824	0.002262	1517.22	112.2
25	10699.64	0.001093	0.001355	1243.96	98.0	10701.64	0.001931	0.002395	1549.41	113.5
26	11145.45	0.00116	0.001439	1261.49	101.0	11147.54	0.002057	0.002551	1555.91	117.1
27	11591.27	0.001217	0.00151	1297.68	102.0	11593.44	0.002173	0.002696	1579.21	118.7
28	12037.09	0.001271	0.001576	1340.62	102.0	12039.34	0.002293	0.002844	1602.41	119.3
29	12482.91	0.001336	0.001656	1364.79	103.9	12485.25	0.002426	0.003009	1604.41	121.9
30	12928.73	0.001402	0.001739	1388.39	105.8	12931.15	0.002561	0.003176	1611.79	124.4
31	13374.55	0.001462	0.001813	1423.91	106.3	13377.05	0.002694	0.003341	1650	125.5
32	13820.36	0.001526	0.001893	1452.22	107.3	13822.95	0.00284	0.003522	1685.57	127.2
33	14266.18	0.001598	0.001982	1468.91	109.3	14268.85	0.002997	0.003717	1718.97	129.7
34	14712	0.001667	0.002068	1491.39	110.3	14714.75	0.003154	0.003911	1752.07	131.4
35	15157.82	0.001737	0.002154	1515.3	111.1	15160.66	0.003318	0.004115	1784.72	132.8
36	15603.64	0.001811	0.002246	1531.87	112.7	15606.56	0.003502	0.004344	1815.3	135.0
37	16049.45	0.001885	0.002338	1548.85	114.1	16052.46	0.003725	0.00462	1845.01	137.1
38	16495.27	0.001958	0.002428	1570.12	115.1	16498.36	0.003974	0.004929	1875.53	138.6
39	16941.09	0.002034	0.002522	1587.12	116.3	16944.26	0.00425	0.005271	1906.7	140.4
40	17386.91	0.002113	0.002621	1599.52	117.8	17390.16	0.004547	0.005639	1939.52	142.6
41	17832.73	0.002192	0.002718	1613.81	118.9	17836.07	0.004857	0.006024	1973.28	144.4
42	18278.55	0.002274	0.00282	1625.17	120.0	18281.97	0.005187	0.006433	2007.41	146.0
43	18724.36	0.00236	0.002927	1631.21	121.4	18727.87	0.005532	0.006861	2041.46	148.0
44	19170.18	0.002446	0.003034	1636.52	122.7	19173.77	0.005891	0.007307	2075.76	150.0
45	19616	0.002533	0.003142	1643.11	123.8	19619.67	0.006269	0.007776	2109.69	151.7
46	20061.82	0.002622	0.003252	1645.77	125.0	20065.57	0.006662	0.008262	2142.61	153.5
47	20507.64	0.002715	0.003367	1670.19	126.4	20511.48	0.007073	0.008773	2174.71	155.5
48	20953.45	0.002811	0.003486	1694.28	127.6	20957.38	0.007506	0.009309	2205.65	157.3
49	21399.27	0.00291	0.003609	1717.37	128.8	21403.28	0.007957	0.00987	2225.85	159.1
50	21845.09	0.003013	0.003737	1740.13	130.0	21849.18	0.008435	0.010462	2241.51	161.0
51	22290.91	0.003118	0.003867	1762.06	131.3					
52	22736.73	0.003224	0.003999	1784.01	132.5					
53	23182.55	0.003336	0.004138	1805.35	133.7					
54	23628.36	0.003454	0.004285	1826.15	135.0					
55	24074.18	0.003591	0.004454	1846.35	136.2					

56	24520	0.003743	0.004643	1866.12	137.5
57	24965.82	0.003908	0.004847	1886.31	138.7
58	25411.64	0.004084	0.005065	1907.01	140.0
59	25857.45	0.004273	0.005299	1927.92	141.2
60	26303.27	0.004469	0.005543	1949.77	142.4
61	26749.09	0.004671	0.005793	1971.8	143.7
62	27194.91	0.004881	0.006054	1994.5	144.9
63	27640.73	0.005101	0.006327	2017.2	146.2
64	28086.55	0.005328	0.006608	2039.95	147.4
65	28532.36	0.00556	0.006896	2062.85	148.7
66	28978.18	0.005799	0.007193	2085.61	149.9
67	29424	0.006047	0.0075	2108.36	151.1
68	29869.82	0.006302	0.007816	2130.61	152.4
69	30315.64	0.006563	0.008141	2152.33	153.6
70	30761.45	0.006831	0.008472	2173.76	154.9
71	31207.27	0.007109	0.008817	2194.63	156.1
72	31653.09	0.007396	0.009173	2215.11	157.3
73	32098.91	0.00769	0.009538	2235.04	158.6
74	32544.73	0.007995	0.009916	2246.41	159.8
75	32990.55	0.00831	0.010306	2257.43	161.1

Bearing at Bolt - Single Bolt, Elevated Temperature Condition

1/8" Plate

Load/step: 448.3516 Total Load = 40800#

Load (lbs)	Disp. Node 272 (in)	Strain,$\varepsilon = \Delta L/L$ (in/in)	Stress (psi)	Temp (F)
0	0	0	0	0.0
448.3516	0.000272	0.000337	253.663	86.7
896.7033	0.000282	0.00035	642.73	65.0
1345.055	0.000348	0.000432	932.045	56.7

1793.407	0.000625	0.000775	775.043	92.8
2241.758	0.000786	0.000975	885.658	97.9
2690.11	0.000839	0.00104	1205.51	79.8
3138.462	0.001057	0.001311	1208.64	93.5
3586.813	0.00131	0.001625	1178.54	111.3
4035.165	0.001437	0.001782	1383.57	102.7
4483.516	0.001621	0.002011	1491.76	101.2
4931.868	0.001906	0.002364	1439.08	116.9
5380.22	0.002137	0.00265	1496.29	120.0
5828.571	0.002345	0.002909	1597.34	115.0
6276.923	0.002638	0.003272	1602.68	122.8
6725.275	0.002964	0.003676	1667.8	131.7
7173.626	0.003261	0.004045	1741.16	130.2
7621.978	0.003672	0.004555	1804.24	132.2
8070.33	0.004218	0.005232	1862.73	140.6
8518.681	0.004812	0.005969	1930.56	143.8
8967.033	0.005461	0.006773	2001.31	144.2
9415.385	0.006196	0.007685	2069.64	149.6
9863.736	0.006998	0.008679	2134.3	155.2
10312.09	0.007864	0.009754	2192.77	156.8
10760.44	0.008843	0.010969	2222.18	160.0
11208.79	0.009975	0.012372	2316.73	165.5
11657.14	0.011297	0.014011	2403.83	169.0
12105.49	0.012865	0.015957	2511.55	171.4
12553.85	0.0148	0.018356	2750.18	175.9

Bearing at Bolt - Double Bolt, Elevated Temperature Condition

	3/8" Plate					1/4" Plate				
	Load/step: 1154.171		Total Load = 229680#			Load/step: 1160		Total Load = 153120#		
Time (sec)	Load (lbs)	Disp. Node 272 (in)	Strain,ε = ΔL/L (in/in)	Stress (psi)	Temp (F)	Load (lbs)	Disp. Node 272 (in)	Strain,ε = ΔL/L (in/in)	Stress (psi)	Temp (F)
0	0	0	0	0	0	0	0	0	0	0
2	2308.342	0.000222	0.000276	265.2	79.9011	2320	0.000315	0.000391	408.486	81.6059
3	3462.513	0.0002	0.000248	981.618	57.102	3480	0.000338	0.00042	1185.04	59.0787
4	4616.683	0.00024	0.000298	1612.81	47.5835	4640	0.000433	0.000537	1797.49	49.8603
5	5770.854	0.000488	0.000606	779.946	79.8652	5800	0.000785	0.000974	1135.55	83.0882
6	6925.025	0.000605	0.00075	915.62	82.2481	6960	0.000992	0.001231	1307.99	86.1592
7	8079.196	0.000612	0.000759	1499.11	62.87	8120	0.001087	0.001348	1913.35	67.0951
8	9233.367	0.000788	0.000977	1384.23	73.8902	9280	0.001376	0.001707	1847.45	78.7875
9	10387.54	0.000996	0.001235	1264.31	88.4657	10440	0.001717	0.002129	1740.34	94.1833
10	11541.71	0.001067	0.001324	1599.45	77.8488	11600	0.00192	0.002381	2082.85	84.0576
11	12695.88	0.001185	0.00147	1809.67	74.337	12760	0.002197	0.002725	2264.26	81.0595
12	13850.05	0.001408	0.001746	1692.99	86.984	13920	0.002605	0.003232	2133.04	94.4644
13	15004.22	0.001572	0.00195	1798.86	87.5323	15080	0.00299	0.003709	2189.62	95.6562
14	16158.39	0.001699	0.002107	2037.61	80.5184	16240	0.003525	0.004372	2339	89.1461
15	17312.56	0.001904	0.002362	2044.71	85.739	17400	0.004247	0.005268	2273.43	95.0147
16	18466.73	0.002128	0.002639	2036.29	91.7596	18560	0.005073	0.006292	2239.76	101.732
17	19620.9	0.002305	0.002858	2185.03	88.0809	19720	0.005932	0.007357	2344.2	98.6208
18	20775.08	0.002517	0.003122	2265.83	87.6875	20880	0.00691	0.00857	2417.37	98.8098
19	21929.25	0.002784	0.003453	2232.72	93.3688	22040	0.008032	0.009963	2465	105.167
20	23083.42	0.003064	0.0038	2266.49	94.0803	23200	0.00926	0.011485	2594.81	106.505
21	24237.59	0.003417	0.004238	2325.5	92.1503					
22	25391.76	0.003858	0.004785	2298.6	95.0811					
23	26545.93	0.004348	0.005393	2279.48	98.0666					
24	27700.1	0.004864	0.006032	2318.78	97.3141					
25	28854.27	0.005424	0.006728	2349.08	98.0274					
26	30008.44	0.006041	0.007492	2359.48	101.005					

27	31162.61	0.006689	0.008297	2405.23	101.948
28	32316.78	0.00738	0.009153	2463.63	101.982

Bearing at Bolt - Double Bolt, Elevated Temperature Condition

1/8" Plate

Load/step: 1177.846 | Total Load = 76560#

Load (lbs)	Disp. Node 272 (in)	Strain,ε = ΔL/L (in/in)	Stress (psi)	Temp (F)
0	0	0	0	0
2355.692	0.000647	0.001115	821.25	86.7201
3533.538	0.000899	0.001611	1719.06	65.0091
4711.385	0.001299	0.002526	2269.36	56.6904
5889.231	0.002036	0.003367	1808.16	92.7572
7067.077	0.002714	0.004719	1971.76	97.8925
8244.923	0.003805	0.006603	2376.03	79.7702
9422.769	0.005323	0.009072	2239.21	93.4795
10600.62	0.007314	0.01146	2247.53	111.336
11778.46	0.00924	0.015003	2554.07	102.684
12956.31	0.012096	0.019919	2979.6	101.227
14134.15	0.016059	0.025749	4040.16	116.906
15312	0.02076	0	5660.76	120.028

Free Field - Single Bolt, Elevated Temperature Condition

	3/8" Plate						1/4" Plate					
	Load per timestep:		445.8182	Total Load = 122600#			Load per timestep:		445.9016	Total Load = 81600#		
Time (sec)	Load (lbs)	Disp. Node 294 (in)	Disp. Node 295 (in)	Strain,ε = ΔL/L (in/in)	Stress Node 295 (psi)	Temp (F)	Load (lbs)	Disp. Node 294 (in)	Disp. Node 295 (in)	Strain,ε = ΔL/L (in/in)	Stress Node 295 (psi)	Temp (F)
0	0	0	0	0	0	0	0	0	0	0	0	0
1	445.8182	-0.00048	-0.00057	-0.00018	383.611	36.4896	445.9016	-0.00044	-0.00053	-0.00016	561.107	37.7442
2	891.6364	0.000329	0.000392	0.000115	700.257	83.3884	891.8033	0.000423	0.000504	0.000147	1054.1	86.8394
3	1337.455	9.11E-06	5.45E-06	-6.7E-06	1076.27	61.1633	1337.705	0.000137	0.000156	3.43E-05	1608.5	65.1648
4	1783.273	-8.74E-05	-0.00011	-4.8E-05	1441.24	52.246	1783.607	7.58E-05	7.73E-05	2.67E-06	2151.74	56.8548
5	2229.091	0.000516	0.000608	0.000168	1768.3	86.4525	2229.508	0.000729	0.000859	0.000236	2655.42	92.9771
6	2674.909	0.00062	0.000731	0.000203	2121.71	90.2683	2675.41	0.000876	0.001033	0.000285	3186.05	98.1855
7	3120.727	0.000356	0.000412	0.000102	2495.38	71.5369	3121.311	0.000647	0.000753	0.000193	3738.22	80.0895
8	3566.545	0.000604	0.000707	0.000187	2841.66	83.9091	3567.213	0.00094	0.001101	0.000293	4261.3	93.8229
9	4012.364	0.000914	0.001077	0.000297	3183.92	100.174	4013.115	0.001306	0.001537	0.00042	4779.75	111.748
10	4458.182	0.000797	0.000935	0.000251	3549.22	90.5833	4459.016	0.001231	0.001442	0.000384	5323.02	103.152
11	4904	0.000801	0.000937	0.000247	3908.6	88.1067	4904.918	0.001283	0.001499	0.000393	5858.13	101.715
12	5349.818	0.001081	0.001271	0.000345	4252.78	102.295	5350.82	0.00163	0.001908	0.000506	6375.29	117.438
13	5795.636	0.001157	0.001359	0.000368	4607.96	104.182	5796.721	0.001763	0.002061	0.000542	6904.87	120.627
14	6241.455	0.001102	0.00129	0.000343	4969.6	98.2013	6242.623	0.001759	0.00205	0.000529	7442.98	115.666
15	6687.273	0.001258	0.001475	0.000394	5320.82	104.731	6688.525	0.001979	0.002306	0.000594	7967.27	123.508
16	7133.091	0.001435	0.001683	0.000451	5668.78	112.187	7134.426	0.002218	0.002584	0.000666	8490.02	132.375
17	7578.909	0.001441	0.001687	0.000447	6027.04	109.683	7580.328	0.00228	0.002651	0.000674	9023.76	131.019
18	8024.727	0.001506	0.00176	0.000463	6382.06	110.471	8026.23	0.002405	0.002792	0.000704	9553.73	132.986
19	8470.545	0.001681	0.001965	0.000518	6729.94	117.53	8472.131	0.002645	0.00307	0.000773	10076	141.412
20	8916.364	0.001768	0.002066	0.000541	7083	119.537	8918.033	0.002797	0.003243	0.00081	10603.6	144.688
21	9362.182	0.001808	0.00211	0.000548	7439.03	118.785	9363.934	0.002902	0.003358	0.00083	11134.2	145.099
22	9808	0.001936	0.002258	0.000585	7789.72	123.003	9809.836	0.003102	0.003587	0.000881	11658.1	150.599

23	10253.82	0.002067	0.00241	0.000623	8139.97	127.323	10255.74	0.003308	0.003821	0.000933	12181.5	156.233
24	10699.64	0.002132	0.002482	0.000638	8494.27	127.802	10701.64	0.003445	0.003973	0.00096	12709.3	157.924
25	11145.45	0.002223	0.002586	0.000661	8847.07	129.752	11147.54	0.00361	0.004159	0.000997	13235.3	161.101
26	11591.27	0.002357	0.002741	0.000699	9197.1	134.042	11593.44	0.003824	0.004401	0.001049	13757.9	166.692
27	12037.09	0.002455	0.002853	0.000724	9549.28	136.265	12039.34	0.004002	0.0046	0.001088	14282.7	170.172
28	12482.91	0.002537	0.002946	0.000743	9902.38	137.533	12485.25	0.00417	0.004786	0.00112	14807.5	172.66
29	12928.73	0.002655	0.003081	0.000774	10253.2	140.766	12931.15	0.004377	0.005018	0.001165	15329.6	177.16
30	13374.55	0.002774	0.003217	0.000805	10603.9	143.936	13377.05	0.004584	0.00525	0.00121	15851.6	181.607
31	13820.36	0.002868	0.003323	0.000827	10956.1	145.629	13822.95	0.00477	0.005455	0.001246	16374.4	184.538
32	14266.18	0.002975	0.003444	0.000853	11307.5	147.966	14268.85	0.004977	0.005684	0.001285	16895.3	188.121
33	14712	0.003099	0.003585	0.000884	11657.4	151.172	14714.75	0.005206	0.005938	0.00133	17414.6	192.599
34	15157.82	0.00321	0.003711	0.00091	12008	153.536	15160.66	0.005423	0.006177	0.00137	17934.1	196.218
35	15603.64	0.003317	0.003831	0.000934	12358.9	155.575	15606.56	0.005644	0.006418	0.001407	18453.3	199.499
36	16049.45	0.003439	0.003968	0.000963	12708.8	158.389	16052.46	0.005893	0.006691	0.00145	18970.4	203.573
37	16495.27	0.00356	0.004105	0.000992	13058.7	161.138	16498.36	0.006181	0.007001	0.001492	19486.8	207.586
38	16941.09	0.003672	0.004231	0.001017	13409.2	163.321	16944.26	0.006486	0.007328	0.00153	20003.2	211.017
39	17386.91	0.003791	0.004365	0.001043	13759.2	165.782	17390.16	0.006822	0.007686	0.00157	20518.3	214.73
40	17832.73	0.003917	0.004507	0.001072	14108.6	168.563	17836.07	0.007184	0.008071	0.001613	21032.6	218.774
41	18278.55	0.004038	0.004643	0.001099	14458.3	171.003	18281.97	0.007554	0.008463	0.001653	21546.6	222.469
42	18724.36	0.004161	0.00478	0.001125	14807.6	173.336	18727.87	0.007944	0.008875	0.001692	22060.1	226.052
43	19170.18	0.004292	0.004926	0.001152	15156.1	175.973	19173.77	0.008352	0.009306	0.001734	22572.1	229.946
44	19616	0.004422	0.005071	0.00118	15504.6	178.569	19619.67	0.008775	0.009751	0.001775	23083.4	233.8
45	20061.82	0.00455	0.005213	0.001206	15853.2	180.95	20065.57	0.009213	0.010211	0.001815	23593.5	237.433
46	20507.64	0.004681	0.00536	0.001233	16201.4	183.448	20511.48	0.009667	0.010687	0.001855	24101.2	241.185
47	20953.45	0.004818	0.005512	0.001261	16549.1	186.064	20957.38	0.010142	0.011185	0.001896	24606.5	245.059
48	21399.27	0.004956	0.005664	0.001288	16896.5	188.542	21403.28	0.010636	0.011701	0.001936	25108.3	248.792
49	21845.09	0.005096	0.005819	0.001314	17243.6	190.986	21849.18	0.01115	0.012237	0.001976	25602.2	252.489
50	22290.91	0.005242	0.00598	0.001342	17590.2	193.549	22295.08	0.011691	0.012799	0.002016	26093.6	256.308
51	22736.73	0.005389	0.006142	0.001369	17936.4	196.09	22740.98	0.012258	0.013389	0.002056	26581.6	260.106
52	23182.55	0.005536	0.006304	0.001396	18282.6	198.549	23186.89	0.012859	0.014012	0.002096	27064.6	263.819
53	23628.36	0.005689	0.006472	0.001423	18628.2	201.058	23632.79	0.013497	0.014672	0.002136	27541.9	267.582
54	24074.18	0.005849	0.006647	0.00145	18973.3	203.609	24078.69	0.014186	0.015383	0.002177	28010.4	271.39

55	24520	0.006027	0.006839	0.001477	19317.9	206.105	24524.59	0.014936	0.016155	0.002217	28470.7	275.141
56	24965.82	0.006219	0.007047	0.001504	19661.9	208.591	24970.49	0.015744	0.016986	0.002258	28929.1	278.882
57	25411.64	0.006425	0.007267	0.001531	20005.9	211.123	25416.39	0.016618	0.017883	0.0023	29404.4	282.669
58	25857.45	0.006641	0.007498	0.001558	20349.5	213.645	25862.3	0.017633	0.018924	0.002347	29942.1	286.446
59	26303.27	0.006871	0.007743	0.001585	20692.9	216.135	26308.2	0.018685	0.020001	0.002393	30466.6	290.192
60	26749.09	0.007108	0.007995	0.001612	21035.9	218.646	26754.1	0.019773	0.021115	0.002439	30987.2	293.958
61	27194.91	0.007351	0.008253	0.001639	21378.9	221.173	27200	0.020903	0.02227	0.002485	31510.6	297.74
62	27640.73	0.007602	0.008519	0.001667	21721.6	223.677	27645.9	0.02206	0.023453	0.002533	32073.2	301.499
63	28086.55	0.007864	0.008795	0.001694	22063.8	226.179	28091.8	0.023223	0.024642	0.00258	32671.9	305.256
64	28532.36	0.008131	0.009077	0.001721	22405.6	228.699	28537.7	0.0244	0.025845	0.002628	33272.5	309.031
65	28978.18	0.008404	0.009366	0.001748	22747	231.213	28983.61	0.025651	0.027124	0.002679	34035.8	312.801
66	29424	0.008685	0.009661	0.001775	23087.9	233.716	29429.51	0.026926	0.028428	0.002732	34866.6	316.559
67	29869.82	0.008974	0.009966	0.001802	23428.4	236.227	29875.41	0.028223	0.029754	0.002785	35695.7	320.325
68	30315.64	0.00927	0.010276	0.001829	23767.9	238.744	30321.31	0.029544	0.031104	0.002835	36585.2	324.097

Free Field - Single Bolt, Elevated Temperature Condition

1/8" Plate

Load per timestep:	448.3516	Total Load = 40800#			
Load (lbs)	Disp. Node 294 (in)	Disp. Node 295 (in)	Strain,ε = ΔL/L (in/in)	Stress Node 295 (psi)	Temp (F)
0	0	0	0	0	0
448.3516	-0.00031	-0.00038	-0.00012	1099.36	41.5079
896.7033	0.000706	0.00084	0.000244	2127.32	97.1924
1345.055	0.000524	0.000611	0.000158	3222.46	77.1692
1793.407	0.00057	0.000655	0.000155	4306.19	70.6811
2241.758	0.0014	0.001643	0.000442	5340.96	112.551
2690.11	0.001717	0.00201	0.000534	6403.14	121.937
3138.462	0.001618	0.001876	0.00047	7492.05	105.747

3586.813	0.002098	0.002435	0.000613	8543.08	123.564
4035.165	0.002672	0.003106	0.000789	9587.43	146.471
4483.516	0.00277	0.003203	0.000788	10662.5	140.857
4931.868	0.003016	0.003474	0.000833	11726.4	142.54
5380.22	0.003589	0.004135	0.000993	12768.2	162.866
5828.571	0.003944	0.004534	0.001072	13824.2	169.963
6276.923	0.004166	0.004767	0.001094	14887.6	168.061
6725.275	0.00464	0.005301	0.001202	15932.8	179.839
7173.626	0.005161	0.005886	0.001318	16973.3	192.938
7621.978	0.005515	0.006266	0.001365	18024.5	195.026
8070.33	0.006025	0.006813	0.001433	19067.2	200.53
8518.681	0.006755	0.007606	0.001546	20097	213.059
8967.033	0.007466	0.00836	0.001625	21131.9	220.138
9415.385	0.008192	0.009118	0.001682	22167.1	224.042
9863.736	0.009075	0.010052	0.001775	23191	233.389
10312.09	0.010028	0.011056	0.00187	24205.8	242.964
10760.44	0.010991	0.012055	0.001936	25213.2	248.287
11208.79	0.012087	0.013194	0.002011	26194	255.15
11657.14	0.013374	0.014532	0.002106	27143.2	264.64
12105.49	0.014823	0.016024	0.002184	28074	271.894
12553.85	0.016512	0.017755	0.00226	29021.8	278.042
13002.2	0.018613	0.01991	0.002359	30088.8	286.344
13450.55	0.020853	0.022206	0.00246	31225	294.623
13898.9	0.023184	0.024589	0.002553	32467.6	301.264
14347.25	0.025679	0.02714	0.002657	34185	308.584
14795.6	0.028273	0.029793	0.002763	36017.2	316.881
15243.96	0.030959	0.032525	0.002847	37059.4	324.266
15692.31	0.033748	0.035369	0.002947	38578.9	331.272
16140.66	0.03669	0.038386	0.003083	43736.6	339.128
16589.01	0.040978	0.04333	0.004275	41839	346.931
17037.36	0.045157	0.048026	0.005217	42652.6	354.106
17485.71	0.0494	0.052798	0.006178	43528.2	361.574

17934.07	0.053682	0.057615	0.00715	44449.7	369.404
18382.42	0.057974	0.062439	0.008119	45403.4	376.864
18830.77	0.062277	0.067274	0.009086	46384	384.197
19279.12	0.066592	0.072121	0.010052	47377.3	391.864
19727.47	0.070912	0.07697	0.011014	48381.4	399.493
20175.82	0.075229	0.081813	0.01197	49395.9	406.882
20624.18	0.079546	0.086653	0.012923	50411.4	414.397
21072.53	0.083864	0.091494	0.013874	51431.6	422.044
21520.88	0.088172	0.096324	0.01482	52456.3	429.542
21969.23	0.092472	0.101142	0.015764	53481.1	436.999
22417.58	0.096765	0.105953	0.016706	54510.3	444.587
22865.93	0.101049	0.110755	0.017647	55543.9	452.153
23314.29	0.105322	0.115543	0.018584	56579	459.628
23762.64	0.109584	0.12032	0.01952	57614.2	467.156
24210.99	0.113834	0.125085	0.020456	58653	474.733
24659.34	0.118069	0.129834	0.021391	59694.3	482.249
25107.69	0.122291	0.134569	0.022324	60737.2	489.753
25556.04	0.126501	0.139292	0.023256	61783.1	497.307
26004.4	0.130695	0.143999	0.024189	62828.9	504.851
26452.75	0.134875	0.148691	0.02512	63878.2	512.36
26901.1	0.139039	0.153368	0.026053	64931	519.892
27349.45	0.143191	0.158031	0.026982	65984.9	527.441
27797.8	0.147326	0.162679	0.027915	67041.7	534.966
28246.15	0.151447	0.167311	0.028844	68102.5	542.487
28694.51	0.155553	0.171928	0.029773	69164.3	550.028
29142.86	0.159644	0.17653	0.030702	70230.6	557.564
29591.21	0.163719	0.181117	0.031633	71297	565.087
30039.56	0.16778	0.185689	0.032562	72364.6	572.619
30487.91	0.171826	0.190246	0.033491	73435.1	580.157

Free Field - Double Bolt, Elevated Temperature Condition

	3/8" Plate						1/4" Plate					
	Load per timestep:		1154.171	Total Load = 229680#			Load per timestep:		1160	Total Load = 153120#		
Time (sec)	Load (lbs)	Disp. Node 294 (in)	Disp. Node 295 (in)	Strain,ε = ΔL/L (in/in)	Stress Node 295 (psi)	Temp (F)	Load (lbs)	Disp. Node 294 (in)	Disp. Node 295 (in)	Strain,ε = ΔL/L (in/in)	Stress Node 295 (psi)	Temp (F)
0	0	0	0	0	0	0	0	0	0	0	0	0
1	1154.171	-0.00041	-0.0005	-0.00015	1045.95	36.4507	1160	-0.00033	-0.0004	-0.00013	1524.01	37.6858
2	2308.342	0.000519	0.000605	0.000156	1878.54	83.2813	2320	0.000708	0.000823	0.00021	2848.02	86.6788
3	3462.513	0.000271	0.000302	5.6E-05	2879.85	61.0392	3480	0.000542	0.000613	0.000129	4334.85	64.9786
4	4616.683	0.000257	0.000277	3.6E-05	3853.51	52.103	4640	0.000619	0.00069	0.000129	5792.08	56.6403
5	5770.854	0.000989	0.001139	0.000272	4729.68	86.2501	5800	0.001499	0.001715	0.000393	7145.19	92.6735
6	6925.025	0.001205	0.001384	0.000327	5673.27	90.0227	6960	0.001845	0.002105	0.000473	8568.48	97.8171
7	8079.196	0.001028	0.001164	0.000247	6665.67	71.2717	8120	0.00179	0.002017	0.000412	10042.1	79.6916
8	9233.367	0.00141	0.001604	0.000353	7586.46	83.6015	9280	0.002326	0.002624	0.000543	11440.6	93.3615
9	10387.54	0.001873	0.002138	0.000483	8498.78	99.8145	10440	0.002962	0.003346	0.000699	12829.5	111.209
10	11541.71	0.001872	0.002123	0.000457	9469.17	90.1935	11600	0.003127	0.00351	0.000695	14277.7	102.567
11	12695.88	0.002008	0.002269	0.000474	10422.5	87.6846	12760	0.003457	0.003861	0.000734	15704.7	101.082
12	13850.05	0.002458	0.002783	0.000591	11336.9	101.825	13920	0.004131	0.004613	0.000877	17090.8	116.733
13	15004.22	0.002693	0.003042	0.000634	12279	103.672	15080	0.00462	0.005139	0.000944	18503.5	119.862
14	16158.39	0.002791	0.003137	0.00063	13237.3	97.6596	16240	0.005158	0.005687	0.000961	19932.8	114.854
15	17312.56	0.003126	0.003512	0.000701	14167.4	104.149	17400	0.006043	0.006624	0.001056	21329.9	122.634
16	18466.73	0.00349	0.003918	0.000778	15093.7	111.561	18560	0.007043	0.00768	0.001158	22721.4	131.435
17	19620.9	0.00368	0.004117	0.000794	16042.3	109.021	19720	0.007947	0.008604	0.001196	24132.7	130.026
18	20775.08	0.003948	0.004405	0.000831	16981.8	109.772	20880	0.009012	0.009702	0.001254	25529.9	131.938
19	21929.25	0.004348	0.004846	0.000905	17905.7	116.789	22040	0.010305	0.011049	0.001352	26904.8	140.301
20	23083.42	0.004696	0.005218	0.000949	18839.8	118.757	23200	0.011638	0.012418	0.001418	28277.8	143.517
21	24237.59	0.005082	0.005619	0.000975	19779.3	117.969	24360	0.013069	0.013876	0.001466	29650.5	143.875
22	25391.76	0.005619	0.006187	0.001032	20706.8	122.147	25520	0.014823	0.015676	0.001551	31027	149.315
23	26545.93	0.006206	0.006805	0.00109	21633.4	126.426	26680	0.016747	0.017649	0.001639	32409.4	154.888
24	27700.1	0.006768	0.007387	0.001124	22567.5	126.868	27840	0.018863	0.019805	0.001714	33943.9	156.522

25	28854.27	0.007395	0.008037	0.001167	23496.3	128.779	29000	0.021328	0.022322	0.001808	35648.7	159.643
26	30008.44	0.008107	0.008781	0.001224	24417.1	133.03	30160	0.024007	0.025065	0.001925	37578	165.173
27	31162.61	0.008825	0.009523	0.001269	25340.6	135.214	31320	0.02685	0.027973	0.002042	39916.1	168.595
28	32316.78	0.009573	0.010292	0.001307	26263.7	136.443	32480	0.030097	0.031268	0.002129	42010.2	171.026
29	33470.95	0.010404	0.011151	0.001357	27178	139.637	33640	0.034457	0.03611	0.003004	45413.4	175.467
30	34625.13	0.011291	0.012065	0.001407	28085.4	142.767	34800	0.039245	0.041401	0.003919	46079.1	179.855
31	35779.3	0.012213	0.013009	0.001448	28995.9	144.423	35960	0.044184	0.046887	0.004914	47323.2	182.728
32	36933.47	0.013218	0.014039	0.001493	29898.1	146.721	37120	0.049246	0.052529	0.005967	48616.9	186.252
33	38087.64	0.014344	0.015194	0.001546	30813.9	149.887	38280	0.054411	0.058296	0.007063	49933.2	190.672
34	39241.81	0.015532	0.016409	0.001593	31719.4	152.212	39440	0.0596	0.064097	0.008177	51265	194.232
35	40395.98	0.016789	0.017691	0.001641	32636	154.213	40600	0.064805	0.069923	0.009306	52602.4	197.456
36	41550.15	0.018202	0.019137	0.001701	33647.5	156.987	41760	0.070038	0.075787	0.010452	53943.4	201.471
37	42704.32	0.019704	0.020673	0.001761	34679.6	159.697	42920	0.075274	0.081658	0.011608	55289.5	205.425
38	43858.49	0.021356	0.022359	0.001825	35812.1	161.842	44080	0.080493	0.087514	0.012766	56642.9	208.798
39	45012.66	0.023081	0.024123	0.001893	37063	164.264	45240	0.085711	0.093373	0.013932	58001.3	212.453
40	46166.83	0.024893	0.025974	0.001966	38426.3	167.006						
41	47321.01	0.026794	0.027919	0.002045	39985.8	169.407						
42	48475.18	0.028808	0.029978	0.002127	41732.5	171.701						
43	49629.35	0.031245	0.032518	0.002314	44630.8	174.299						
44	50783.52	0.033989	0.035563	0.002861	46720	176.856						
45	51937.69	0.037023	0.038923	0.003455	47302.1	179.198						
46	53091.86	0.040221	0.042472	0.004092	48109.1	181.657						
47	54246.03	0.04351	0.046131	0.004767	48954.9	184.234						
48	55400.2	0.046856	0.049862	0.005467	49824	186.673						
49	56554.37	0.050243	0.053645	0.006186	50706.4	189.078						
50	57708.54	0.053666	0.057472	0.006919	51597	191.602						
51	58862.71	0.057118	0.061333	0.007663	52492.2	194.104						
52	60016.88	0.060583	0.06521	0.008413	53391.1	196.524						
53	61171.06	0.064058	0.069101	0.009169	54291.7	198.994						
54	62325.23	0.067541	0.073003	0.00993	55194.2	201.507						
55	63479.4	0.071024	0.076906	0.010695	56098.4	203.964						
56	64633.57	0.074507	0.080812	0.011462	57004.7	206.411						

Free Field - Double Bolt, Elevated Temperature Condition					
1/8" Plate					
Load per timestep:		1160	Total Load = 75650#		
Load (lbs)	Disp. Node 294 (in)	Disp. Node 295 (in)	Strain,ε = ΔL/L (in/in)	Stress Node 295 (psi)	Temp (F)
0	0	0	0	0	0
1160	-6.50E-05	-9.78E-05	-6E-05	2789.09	41.3911
2320	0.001314	0.001515	0.000367	5661.7	96.8712
3480	0.001475	0.001664	0.000343	8548.94	76.7969
4640	0.001953	0.002173	0.000401	11396.3	70.2522
5800	0.003346	0.003757	0.000747	14135.2	111.944
6960	0.004274	0.004768	0.000899	16942.2	121.2
8120	0.005302	0.005794	0.000896	19795.9	104.951
9280	0.00717	0.007774	0.001097	22560.8	122.642
10440	0.009569	0.010301	0.00133	25298	145.394
11600	0.011553	0.012316	0.001387	28077.3	139.687
12760	0.014579	0.015403	0.001499	30842.1	141.273
13920	0.019009	0.019977	0.001759	33984	161.457
15080	0.024073	0.025155	0.001967	37899.3	168.433
16240	0.030544	0.031909	0.002481	43286.4	166.435
17400	0.039902	0.042215	0.004204	45610	178.092
18560	0.04978	0.053166	0.006157	48165.6	191.06
19720	0.059659	0.064145	0.008157	50830.1	193.041
20880	0.069708	0.075348	0.010253	53539.8	198.435
22040	0.079941	0.086786	0.012446	56282.2	210.837
23200	0.090058	0.098111	0.014641	59064.2	217.798
24360	0.100082	0.109345	0.016842	61873.2	221.594
25520	0.110176	0.120682	0.019102	64695.8	230.821

26680	0.120218	0.131975	0.021376	67535.8	240.274
27840	0.130102	0.143101	0.023635	70395	245.485
29000	0.139946	0.154197	0.025911	73268.9	252.232